SPIRE Photometer Flux Density Calibration

Document Number: SPIRE-UCF-DOC-3168

Matt Griffin (with inputs from the SPIRE ICC)

Issue 6

November 4 2010

Contents

1. Introduction

The SPIRE flux calibration scheme is described, based on the scheme presented in [1], and data for the corresponding calibration files are presented.

Section 2 contains a list of the symbols used and their meanings. Information on the SPIRE photometer passbands is given in Section 3. In Section 4 we outline the calibration scheme and the main equations to be implemented, and the results of calculations of the relevant parameters are given in Section 5. Section 6 outlines the procedure for correcting the point source calibration of the pipeline to that corresponding to extended emission. Some aspects of point source extraction from SPIRE maps and Level-1 products are discussed in Section 7. The currently adopted models for Neptune and Uranus and Mars are described in Section 8. Predicted flux densities for some of the larger asteroids, based on the Standard Thermal Model, are given in Section 9 and an outline of the status of stellar calibration sources is presented in Section 10. Section 11 discusses the currently estimated calibration accuracy for the SPIRE photometer and Section 12 outlines some possible future developments. Details of all calculations are given in the annex.

2. List of symbols

Symbol	Definition
A_{Beam}	Beam area
$B(\theta, \phi)$	Normalised beam profile as a function of radial offset angle θ and azimuthal offset angle ϕ
D_H	Herschel-planet distance
e	Eccentricity of planetary disk
$I_\nu(\theta, \phi)$	Sky intensity profile as a function of radial offset angle θ and azimuthal offset angle ϕ
K_1, K_2, K_3	Parameters defining function fitted to variation of overall system responsivity with operating point voltage
K_4	Constant of proportionality relating RSRF-weighted flux density to monochromatic flux density
K_{Beam}	Beam correction factor for a uniform disk source
K_C	Spectral index (colour) correction factor to convert measured flux density to a different assumed source spectral index
P	Map pixel correction factor
r_{eq}	Equatorial radius of planet
r_{gm}	Geometric mean radius of planet
R_p	Polar radius of planet
$R(\nu)$	Relative Spectral Response Function of a photometer band
$\bar{S}_{Calib}$	RSRF-weighted flux density for calibration source
$\bar{S}_S$	RSRF-weighted flux density for source
$S(\nu)$	Astronomical source in-beam flux density at frequency ν
U	Uncertainty in map pixelisation correction
α_C	Astronomical calibration source power law spectral index
α_S	Astronomical source power law spectral index
α_{So}	Nominal source spectral index for which SPIRE flux densities will be quoted
ϕ	Latitude of planet's sub-Earth point
ν	Radiation frequency
ν_o	Frequency at which measured flux density is to be quoted
θ_p	Angular radius of observed planetary disk
θ_{Beam}	Beam FWHM
θ_P	Radius of planetary disk
θ_{Pix}	Square map pixel side
Ω	Solid angle
Ω_P	Solid angle of observed planetary disk

3. The SPIRE photometer bands

As noted in [1], for a SPIRE observation, the property of the source that is directly proportional to source power absorbed by the bolometer is the integral over the passband of the flux density weighted by the instrument Relative Spectral Response Function (RSRF):

$$\bar{S}_S = \frac{\int_{Passband} S_S(\nu) R(\nu)\, d\nu}{\int_{Passband} R(\nu)\, d\nu} , \qquad (1)$$

where $S_S(\nu)$ represents the in-beam source flux density at the telescope aperture and $R(\nu)$ is the RSRF.

The three photometer filter profiles are taken from [2] and are shown in Figure 1. These plots give the RSRFs for the case of a point source and for an extended source (defined here as a source that fills the entire beam solid angle with a uniform surface brightness). For the latter the profiles are weighted by λ^2 to take into account the single-mode coupling via the feedhorns. Note that the vertical scale is irrelevant to the computations in this note as all relevant parameters involve ratios of RSRF integrals.

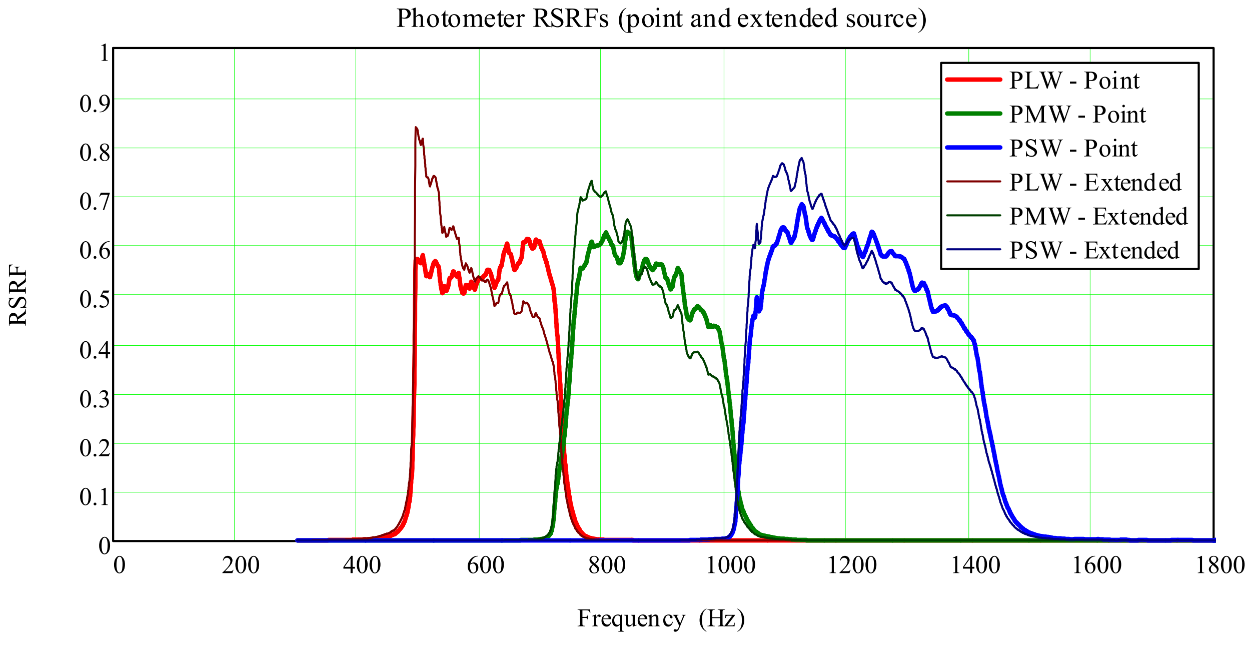

Figure 1: Photometer RSRFs for point source observations (no weighting of filter transmission profiles) and extended source (λ^2 weighting).

4. SPIRE calibration scheme

The photometer pipeline produces monochromatic in-beam flux densities at standard frequencies corresponding to 250, 350 and 500 μm, and calculated under the assumptions of (i) a point source observation and (ii) a flat $\nu S(\nu)$ spectrum. The detailed computations, and the appropriate corrections for an extended source or to convert to a different assumed source spectrum, are described in this section.

4.1 Calibration flux densities

Let the RSRF for a point source observation be $R_P(\nu)$ (as shown in Figure 1) and that for an extended source be $R_E(\nu)$ (as shown in). All standard calibration sources for SPIRE are effectively point sources, for which $R_P(\nu)$ is the appropriate RSRF. The flux calibration in the SPIRE pipeline is also based on the point source case: i.e., the pipeline always outputs an in-beam flux density (Jy/beam) computed under the assumption that a point source is being observed.

When observing a calibration source, the property that is directly proportional to absorbed detector power is

$$\bar{S}_{\rm Calib} = K_{\rm Beam}\left[\frac{\int_{Passband} S_{\rm C}(\nu)R_{\rm P}(\nu)\,{\rm d}\nu}{\int_{Passband} R_{\rm P}(\nu)\,{\rm d}\nu}\right], \qquad (2)$$

where $S_C(\nu)$ is the calibrator flux density at the telescope aperture and K_{Beam} is a correction factor for partial resolution of the calibrator by the telescope beam. For a Gaussian beam profile coupling to a uniformly bright disk (planet or asteroid), the beam correction factor is given by [3]:

$$K_{\rm Beam}(r_{\rm C},\theta_{\rm Beam}) = \frac{1-\exp\left(-\dfrac{4\ln(2)\theta_{\rm p}^{2}}{\theta_{\rm Beam}^{2}}\right)}{\dfrac{4\ln(2)\theta_{\rm p}^{2}}{\theta_{\rm Beam}^{2}}}, \qquad (3)$$

where θ_p is the angular radius of the disk, and θ_{Beam} is the beam FWHM.

$\bar{S}_{\rm Calib}$ is used, as described in [1], in the derivation of the flux density conversion module parameters, K_1, K_2 and K_3, which are in turn used to derive the RSRF-weighted source flux density $\bar{S}_{\rm S}$.

4.2 Conversion of RSRF-weighted flux density to monochromatic flux density

Definition of a monochromatic flux density requires the adoption of a standard frequency for the band and some assumption about the shape of the source spectrum. The approach adopted for SPIRE and PACS is to assume that the spectrum is a power law across the band defined by the flux density at a standard frequency ν_o, and a spectral index α_S:

$$S_{\rm S}(\nu) = S_{\rm S}(\nu_{\rm o})\left(\frac{\nu}{\nu_{\rm o}}\right)^{\alpha_{\rm S}}. \qquad (4)$$

The convention adopted for Herschel is to adopt $\alpha_S = \alpha_{So} = -1$ (corresponding to νS_ν flat across the band). For SPIRE, we choose values of ν_o to correspond to wavelengths of 250, 350 and 500 μm for the three bands, and flux densities at those frequencies are quoted to the observer.

The measured RSRF-weighted flux density (to which the output voltage due to the source is proportional in the linear regime) is

$$\bar{S}_S = \frac{S_S(\nu_o)}{\nu_o^{\alpha_S}} \left[\frac{\int_{Passband} \nu^{\alpha_S} R(\nu)\, d\nu}{\int_{Passband} R(\nu)\, d\nu} \right], \tag{5}$$

where $R(\nu) = R_P(\nu)$ for a point source or $R_E(\nu)$ for an extended source.

The flux density at frequency ν_o, which is quoted to the observer, is therefore given by:

$$S_S(\nu_o) = \bar{S}_S \left[\frac{\nu_o^{\alpha_S} \int_{Passband} R(\nu)\, d\nu}{\int_{Passband} \nu^{\alpha_S} R(\nu)\, d\nu} \right] = K_4\, \bar{S}_S\,. \tag{6}$$

The measured RSRF-weighted flux density must therefore be multiplied by K_4 to derive the monochromatic flux density at the standard wavelength to be quoted to the user.

Putting $\alpha_S = -1$ gives

$$K_4 = \frac{\int_{Passband} R(\nu)\, d\nu}{\nu_o \int_{Passband} \frac{R(\nu)}{\nu} d\nu}\,. \tag{7}$$

Note that the values of K_4 are different for point and extended sources:

$$K_{4P} = \frac{\int_{Passband} R_P(\nu)\, d\nu}{\nu_o \int_{Passband} \frac{R_P(\nu)}{\nu} d\nu} \qquad K_{4E} = \frac{\int_{Passband} R_E(\nu)\, d\nu}{\nu_o \int_{Passband} \frac{R_E(\nu)}{\nu} d\nu} \tag{8}$$

The SPIRE pipeline is based on K_4 for the point source case. To derive the flux density for an extended source, the pipeline output must be multiplied by K_{4E}/K_{4P}.

The parameter K_4 is taken into account in the photometer pipeline by incorporating it as a multiplicative factor in the voltage-to-flux density conversion parameters K_1 and K_2.

4.3 Conversion from point source to extended source calibration

To convert from the point source-based calibration adopted in the pipeline to an extended source calibration, two conversions are needed: (i) a correction must be made for the different RSRF that is adopted for extended sources, as embodied by the K_4 parameter; (ii) the in-beam flux density must be converted to surface brightness using knowledge of the beam.

4.3.1 RSRF (K_4) correction

The factor K_{4P} is included in the pipeline products. To convert to extended source calibration the data should therefore be multiplied by K_{4E}/K_{4P}.

4.3.2 Conversion of in-beam flux density to surface brightness

The in-beam astronomical flux density at a given frequency, ν, is defined as:

$$S(\nu) = \oint_{4\pi} B(\theta, \phi) I_\nu(\theta, \phi) \, \mathrm{d}\Omega \quad , \tag{9}$$

where θ (= 0 – π) is a radial angular offset from the beam centre, ϕ (= 0 – 2π) is an azimuthal angular offset, $B(\theta,\phi)$ is the beam profile (normalised to unity at the peak), $I_\nu(\theta, \phi)$ is the sky intensity (surface brightness) profile, and $\mathrm{d}\Omega$ is a solid angle element in the direction defined by (θ, ϕ). Note that we assume here that the beam profile can be regarded as uniform across the spectral passband.

The surface brightness is obtained from the flux density (Jy in beam) by dividing it by the beam area,

$$A_{\mathrm{Beam}} = \oint_{4\pi} B(\theta,\phi) \, \mathrm{d}\Omega \ . \tag{10}$$

For a Gaussian beam profile with FWHM θ_{Beam} , the beam area is given by

$$A_{\mathrm{Beam}} = \frac{\pi \, \theta_{\mathrm{Beam}}{}^2}{4\ln(2)} \ , \tag{11}$$

However, as noted below in Section 6 , it is recommended that the explicitly measured beam areas be used.

4.4 Colour correction

No colour correction is carried out in the generation of Level-1 or Level-2 data products. The assumption that the source has a spectrum with νS_ν flat across the band ($\alpha_{\mathrm{So}} = -1$) will not be the case for most observations, and for the highest calibration accuracy a colour correction should be applied by the astronomer based on other information (for instance, measurements in other SPIRE or PACS bands and/or data from other telescopes).

Given the width of the SPIRE bands and the nature of the observed source SEDs, in most cases it will be appropriate to assume that the source spectrum follows a power law across the band, but with a different spectral index, α_{Snew}. Let $S'_{\mathrm{S}}(\nu_{\mathrm{o}})$ be the source flux density at ν_{o} for that spectral shape. We then have from equation (5),

$$S'_{\mathrm{S}}(\nu_{\mathrm{o}}) = \nu_{\mathrm{o}}^{(\alpha_{\mathrm{Snew}} - \alpha_{\mathrm{So}})} \left[\frac{\int_{Passband} R(\nu)\nu^{\alpha_{\mathrm{So}}}\, \mathrm{d}\nu}{\int_{Passband} R(\nu)\,\nu^{\alpha_{\mathrm{Snew}}}\, \mathrm{d}\nu} \right] S_{\mathrm{S}}(\nu_{\mathrm{o}}) = K_{\mathrm{C}}(\alpha_{\mathrm{Snew}}) S_{\mathrm{S}}(\nu_{\mathrm{o}}) . \tag{12}$$

Putting $\alpha_{\mathrm{So}} = -1$ gives

$$K_{\mathrm{C}}(\alpha_{\mathrm{Snew}}) = \nu_{\mathrm{o}}^{(\alpha_{\mathrm{Snew}} + 1)} \left[\frac{\int_{Passband} R(\nu)\nu^{-1}\, \mathrm{d}\nu}{\int_{Passband} R(\nu)\,\nu^{\alpha_{\mathrm{Snew}}}\, \mathrm{d}\nu} \right] . \tag{13}$$

Once again, K_{C} is different for point and extended sources due to the different RSRFs. As shown below in Section 5.2, the differences are significant.

5. Computation of the RSRF and colour correction factors for SPIRE

5.1 Factor K_4 to convert RSRF-weighted flux density to monochromatic flux density

For the standard spectral index of -1 adopted for Herschel, the values of K_4, given by equations (8), for the three bands are:

Point source (no RSRF weighting): $K_{4\mathrm{P}}$ (PSW, PMW, PLW) = (1.0113, 1.0060, 1.0065)
Extended source (λ^2 RSRF weighting): $K_{4\mathrm{E}}$ (PSW, PMW, PLW) = (0.9939, 0.9898, 0.9773)

The conversion factors from point source calibration (pipeline convention) to extended source calibration are therefore:

$K_{4\mathrm{E}}/K_{4\mathrm{P}}$ (PSW, PMW, PLW) = (0.9828, 0.9839, 0.9710).

The Level-2 data should therefore be multiplied by these values to convert to extended source calibration.

5.2 Factor K_{C} for colour correction

The colour correction parameter K_{C} has been computed from equation (13) for various values of α_{Snew}, and the results are given in Table 2 and Figure 2. To convert the pipeline flux densities to an assumed source spectral index other than $\alpha_{\mathrm{S}} = -1$, they should be multiplied by the appropriate factors from Table 1 (which are different for point source and extended sources). Users wishing to make more refined corrections based on a more complex model of the source spectrum within the band can derive their own corrections using equation (1) and the detailed RSRF, which is also available as a calibration product.

α_S =	$KPc_1\ \alpha_S$ =	$KPc_2\ \alpha_S$ =	$KPc_3\ \alpha_S$ =	$KEc_1\ \alpha_S$ =	$KEc_2\ \alpha_S$ =	$KEc_3\ \alpha_S$ =
-4.000	0.9820	0.9700	0.9336	0.9303	0.9259	0.8562
-3.500	0.9902	0.9798	0.9530	0.9478	0.9422	0.8864
-3.000	0.9964	0.9877	0.9693	0.9626	0.9571	0.9144
-2.500	1.0005	0.9938	0.9823	0.9751	0.9704	0.9401
-2.000	1.0025	0.9978	0.9918	0.9855	0.9821	0.9631
-1.500	1.0023	0.9999	0.9978	0.9938	0.9920	0.9832
-1.000	1.0000	1.0000	1.0000	1.0000	1.0000	1.0000
-0.500	0.9955	0.9980	0.9986	1.0041	1.0061	1.0134
0.000	0.9888	0.9940	0.9935	1.0061	1.0103	1.0232
0.500	0.9801	0.9880	0.9849	1.0059	1.0124	1.0293
1.000	0.9692	0.9799	0.9729	1.0036	1.0124	1.0316
1.500	0.9564	0.9700	0.9577	0.9990	1.0104	1.0302
2.000	0.9417	0.9582	0.9395	0.9924	1.0064	1.0249
2.500	0.9252	0.9446	0.9186	0.9836	1.0003	1.0161
3.000	0.9070	0.9293	0.8952	0.9727	0.9921	1.0037
3.500	0.8873	0.9125	0.8698	0.9598	0.9821	0.9880
4.000	0.8662	0.8942	0.8424	0.9451	0.9701	0.9692

Table 1: Colour correction parameter K_C (with $\alpha_{S_0} = -1$) vs. assumed source spectral index for point source observations: (PSW, PMW, PLW values in columns 2, 3, 4 respectively) and extended source observations (PSW, PMW, PLW values in columns 5, 7, 7 respectively).

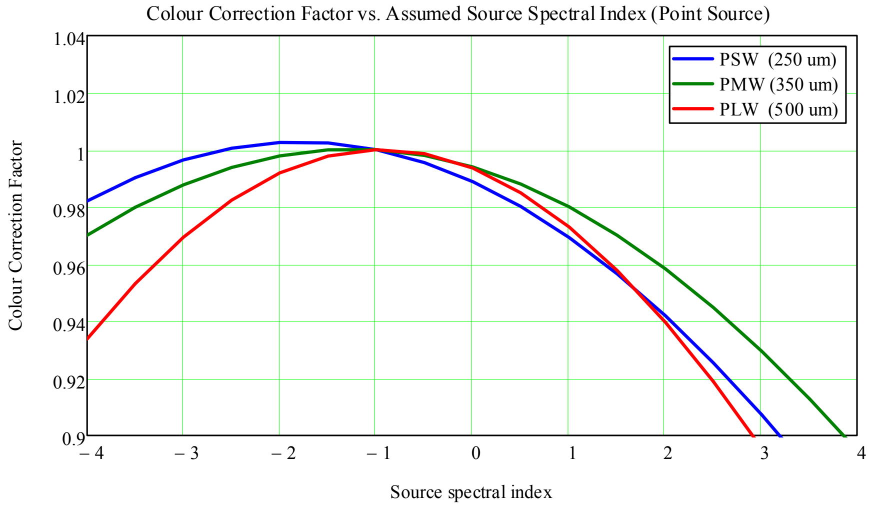

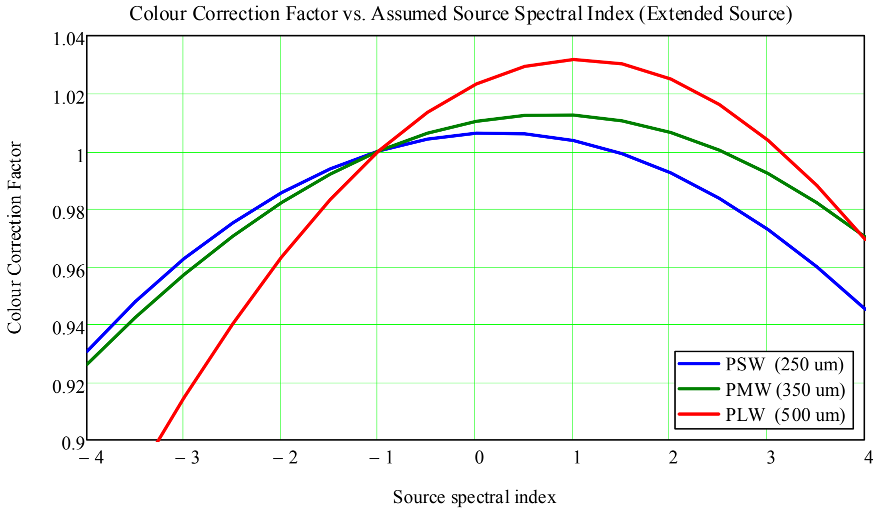

Figure 2: Colour correction parameter K_C (with $\alpha_{S_0} = -1$) vs. assumed source spectral index for point source (top) and extended source (bottom) observations.

6. Extended source calibration

The SPIRE pipeline data products are based on the assumption that the astronomical signal is from a point source. For extended sources, the surface brightness can be obtained from the flux density in Jy/beam by dividing it by the measured beam area. In addition a correction is needed because of the fact that the RSRF is different for point and extended source emission.

6.1 Photometer beam maps and areas

An interim characterisation of the beams was made available via the Herschel Science Centre website in 2009, and is described in the previous version of this document (v2.1.1, 4 Aug. 2009). As explained in Chapter 4, this has now been superseded by more accurate measurements, and the new results and accompanying detailed information are available from the HSC web site and comprise the following:

(i) new empirical beam maps based on fine-scan-map measurements of Neptune;
(ii) the raw data used for the above;
(iii) a theoretical model including coverage of the sidelobes and low-level structure due to the secondary mirror supports (unchanged from the previous issue);
(iv) a technical note providing detailed information on the beam maps and parameters and how they were derived

Empirical beam maps: The empirical beam products consist of two sets of three beam maps, one for each photometer band. The product is derived from scan-map data of Neptune, performed using a custom 'fine-scan' observing mode with the nominal source brightness setting. In these fine-scan observations, each bolometer is scanned over Neptune in four different directions. The data were reduced using the standard HIPE scan-map pipeline and the naïve map-maker. Each map constitutes an averaging in the map over all of the individual bolometers crossing the source, and represents the realistic point source response function of the system, including all scanning artefacts. It is worth noting that in a normal SPIRE scan-map, any individual source in the map will be covered by only a subset of bolometers, leading to low-level beam profile variations, from position to position in the map, about the average profile presented here.

The beam maps for all three bands are displayed in log scaling in Figure 3. Four individual maps, one from each of the four observations from which the final beam products are derived, are also available should the user want to investigate the beam stability. The beam product maps are ~10 arcmin x 30 arcmin in scale and include the same extensions and header information as the nominal maps output from HIPE. There are two versions of each map, one high resolution with a 1 arcsec pixel scale, and another with the nominal SPIRE output map pixel scale of (6, 10, 14)" per pixel for (250, 350, 500) μm.. The data have also been normalised to give a peak flux of unity in all three bands.

Note that the ellipticity seen in the maps is not a function of scanning direction, but is constant with position angle. When using these beam models it is advised that the user rotates the beam map so that it matches the position angle of the user's data. The position angle of HIPE maps can be found in the primary FITS header and is specified by the 'posangle' keyword.

Beam parameters as a function of pixel size: The basic beam parameters vary as a function of pixel scale, with the FWHM values and beam areas increasing with pixel size. This is expected since the fidelity of the surface brightness reconstruction becomes less reliable at low resolution, particularly with respect to the Airy ring pattern at higher radii from the source peak.

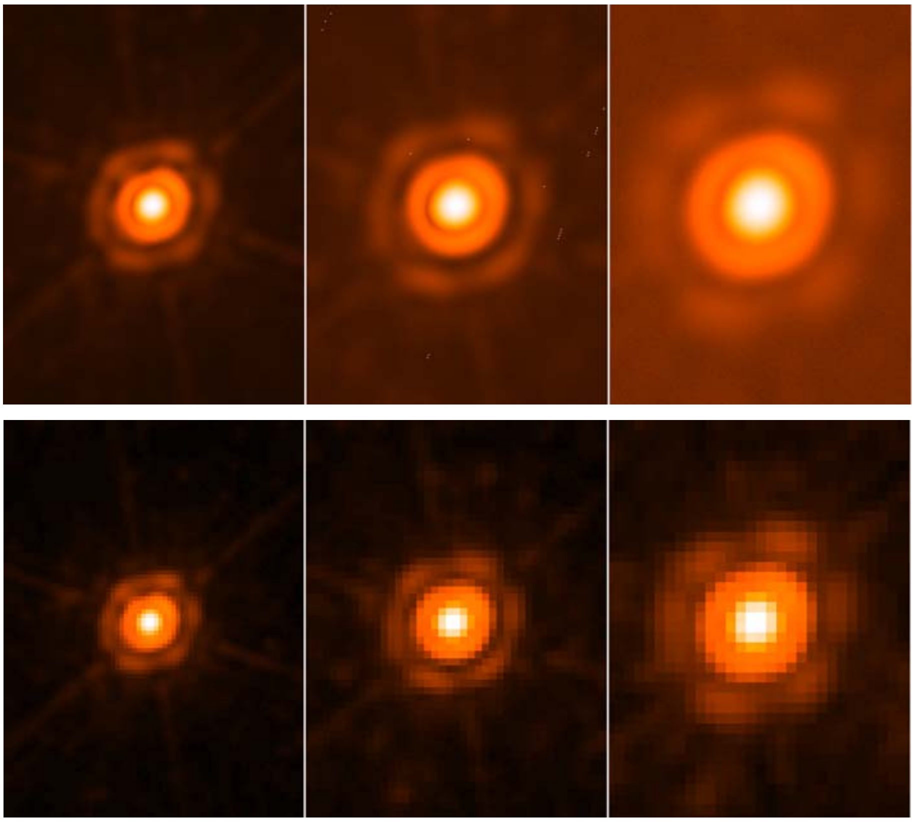

Figure 3: Log scale images for the empirical SPIRE beam model at 250, 350, and 500 μm from left to right respectively. The top row uses a 1" pixel scale for all maps, and the bottom row uses the nominal SPIRE map pixel scales of 6, 10, and 14" from left to right respectively.

Table 5.1 summarises the basic beam parameters for data binned into 1" map pixels and for the nominal SPIRE Level-2 map pixel sizes of (6, 10, 14)" at (250, 350, 500) μm. The FWHM values are determined by fitting an asymmetric 2-D Gaussian to the beam maps, and the beam areas are computed by integrating explicitly under the measured beam profiles.

Pixel side (")	Band	Major axis FWHM (")	Minor axis FWHM (")	Geometric mean FWHM (")	Ellipticity	Average beam area ($arcsec^2$)	Average beam area (sr x 10^{-8})
1	250 μm	18.3	17.0	17.6	7.8%	426	1.001
1	350 μm	24.7	23.2	23.9	6.4%	771	1.812
1	500 μm	36.9	33.4	35.1	10.2%	1626	3.822
6	250 μm	18.9	17.6	18.2	7.4%	450	1.058
10	350 μm	25.6	24.2	24.9	12%	805	1.892
14	500 μm	38.0	34.6	36.3	9.0%	1682	3.953

Table 2: Basic 2-D Gaussian parameters for measured beams with a 1 arcsec pixel size and for the nominal SPIRE Level-2 map pixel sizes (6, 10, 14)". Uncertainties in the beam FWHM values and areas are estimated at < 1%.

Figure 4 shows the variation in beam area, major, and minor FWHM parameters from top to bottom respectively, as a function of map pixel scale. The variation is given for the (250, 350, 500) μm bands from left to right. The data are fit with a second order polynomial, and the derived fit is displayed on each plot.

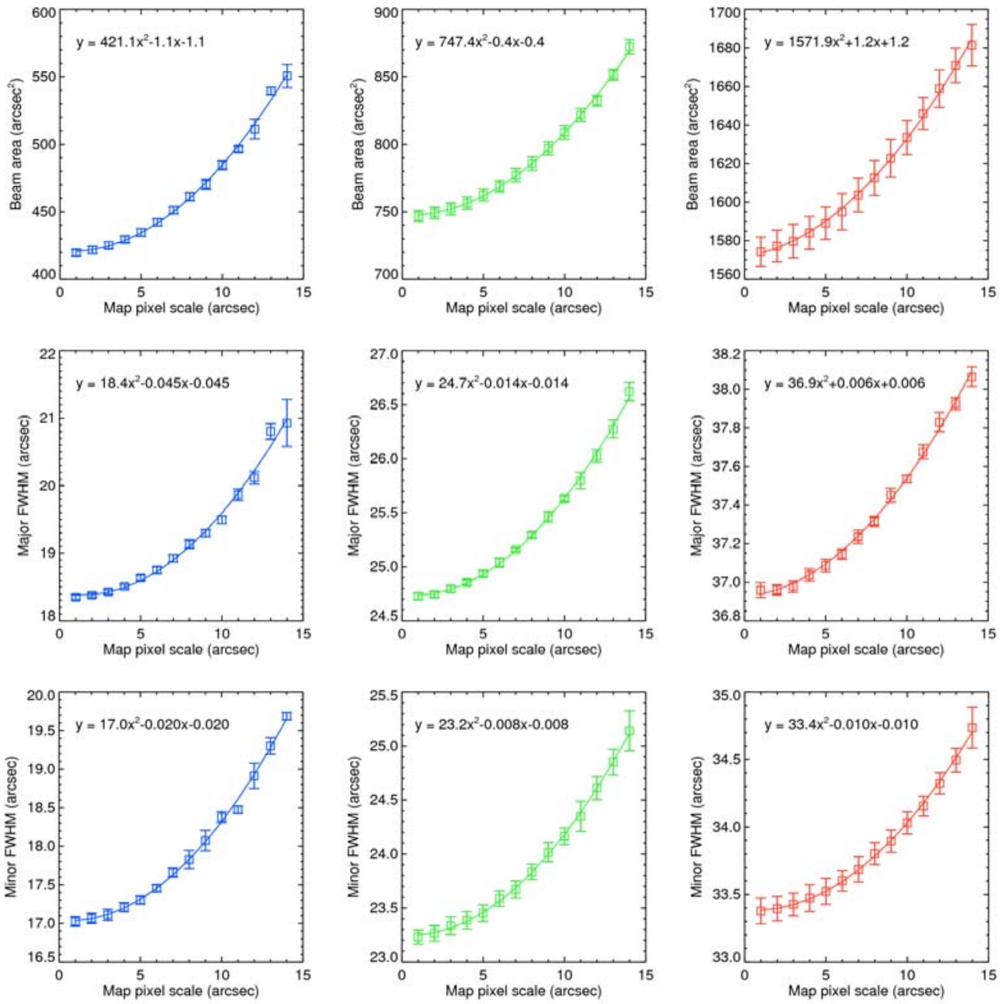

Figure 4: Variation in beam area, major and minor FWHM parameters from top to bottom respectively, as a function of map pixel scale. The variation is given for all three bands from 250 to 500 μm from left to right. Second-order polynomial fits to the data are shown by the solid lines, and the derived fits are displayed on each plot.

6.2 Extended source RSRF correction

To convert the pipeline output from point source to extended source calibration, the flux densities should be multiplied by (K_{4E}/K_{4P}) = (0.9828, 0.9839, 0.9710) for (PSW, PMW, PLW).

6.3 Example of conversion from point source to extended source calibration

The key steps in calibration of extended source emission are illustrated by the following example:

- An extended dust source has a ν^3 spectrum and a true brightness of 100 MJy/sr at 250 μm (1200 GHz).
- Its actual monochromatic intensities at (250, 350, 500) μm are therefore (100.0, 36.44, 12.50) MJy/sr
- The corresponding in-beam monochromatic flux densities are these values multiplied by the beam areas: (100.0, 36.44, 12.50) x10^6 . (1.001, 1.822, 3.822) x 10^{-8} = (1.0013, 0.6604, 0.4777) Jy/beam (this is what we are trying to measure)
- The corresponding in-beam RSRF-weighted flux densities, obtained by integrating the true source spectrum across the passbands using the extended source RSRFs, are (1.0357, 0.6725, 0.4870) Jy/beam
- But the pipeline is based on point source calibration and returns these values multiplied by K_{4P}: (1.0113, 1.0060, 1.0065).(1.0357, 0.6725, 0.4870) = (1.0474, 0.6766, 0.4902) Jy/beam
  - Note that compared to the true monochromatic flux densities, these values are **too high** by (4.6, 2.4, 2.6)%

- Knowing that the source is extended, the user multiplies the pipeline products by K_{4E}/K_{4P}:
  (1.0474, 0.6766, 0.4902).(0.9828, 0.9839, 0.9710) = (1.0294, 0.6657, 0.4760) Jy/beam
  - Note that these values are rather more accurate – high by only (2.8, 0.8, 0.0)% with respect to the true monochromatic flux densities, but are still based on an assumed ν^{-1} spectrum
- Knowing also that the source has a ν^{3} spectrum, not ν^{-1} as assumed in the pipeline, the user applies the appropriate extended source colour correction factors from Table 5.2 to obtain the true in-beam monochromatic flux densities:
  (0.9727, 0.9921, 1.0037).(1.0294, 0.6657, 0.4760) = (1.0013, 0.6604, 0.4777) Jy/beam

- What if, inappropriately, the point source calibration is left unchanged and the point source colour correction applied?
  (0.9070, 0.9293, 0.8952).(1.0474, 0.6766, 0.4902) = (0.9500, 0.6288, 0.4389) Jy/beam
  - i.e., the resulting flux densities are about 5% **too low**

7. Point source extraction from SPIRE Level-2 maps

The SPIRE flux calibration is timeline based (Jy in beam). As a result, the signal level in a map pixel depends on how the square map pixel size compares to the size of the beam. Only in the limit of infinitely small map pixels would a pixel co-aligned with a point source register the true source flux density. It is important to note that no pixel size correction factors are incorporated in the SPIRE Level-2 map-making. For a given map pixel, the flux density value represents the average in-beam flux density measured by the detectors while pointed within that area. Taking the pixel value for the flux density of an isolated co-aligned point source in an otherwise blank map would thus yield an underestimate of the true flux density.

The necessary correction factor is a function of the map pixel size and the beam size and the correction factor is a simple multiplicative factor. For a symmetrical Gaussian beam, a square pixel of side θ_{Pix} , and a co-aligned point source, the correction factor for a Gaussian beam with FWHM θ_{Beam} is:

$$P = \frac{\pi}{4\ln(2)}\left(\frac{\theta_{\mathrm{Beam}}}{\theta_{\mathrm{Pix}}}\right)^2 erf^2\left[\left(\frac{\theta_{\mathrm{Pix}}}{\theta_{\mathrm{Beam}}}\right)\left[\ln(2)\right]^{1/2}\right], \tag{14}$$

where erf is the error function $erf(x) = \frac{2}{\pi}\int_0^x e^{-t^2}\,\mathrm{d}t$.

However, in the general case the source will be randomly aligned with respect to the map pixel, resulting in a slightly different correction, and a small random uncertainty corresponding to the actual offset of the source with respect to the pixel centre for a particular observation. Empirical correction factors have been derived from scan maps of Neptune, with the map generated at various pixel scales. The data were fitted using Gaussian functions, and the median measured/model flux density ratio was fitted with an empirical quadratic function that varies with pixel scale.

The empirical pixelisation correction factor is given by

$$P = 1 - c_1\theta_{\mathrm{Pix}} - c_2\theta_{\mathrm{Pix}}^{\;2} \tag{15}$$

where θ_{Pix} is the pixel side in arcseconds and the constants (c_1, c_2) are (0.0012, 0.00143) for 250 μm, (0.00080, 0.00075) for 350 μm, and (0.0026, 0.00031) for 500 μm.

Performing this pixelisation correction involves adding an additional uncertainty, which has also been characterised empirically. The fractional uncertainty due to the pixelisation correction is given by

$$U_P = u_1 - u_1\theta_{\mathrm{Pix}} \tag{16}$$

The default HIPE pixel sizes for (250, 350, 500) μm are θ_{Pix} = (6, 10, 14)". The corresponding pixel size correction factors, given by equation (15), are *P* = (0.941, 0.917, 0.903). From equation (16), the corresponding percentage uncertainties introduced into the point source flux density estimation are (1.5, 3.2, 1.8)%. This uncertainty should be added in quadrature to the other statistical uncertainties of the measurement.

Figure 5 shows the *P*-factors vs. map pixel size for the three photometer bands.

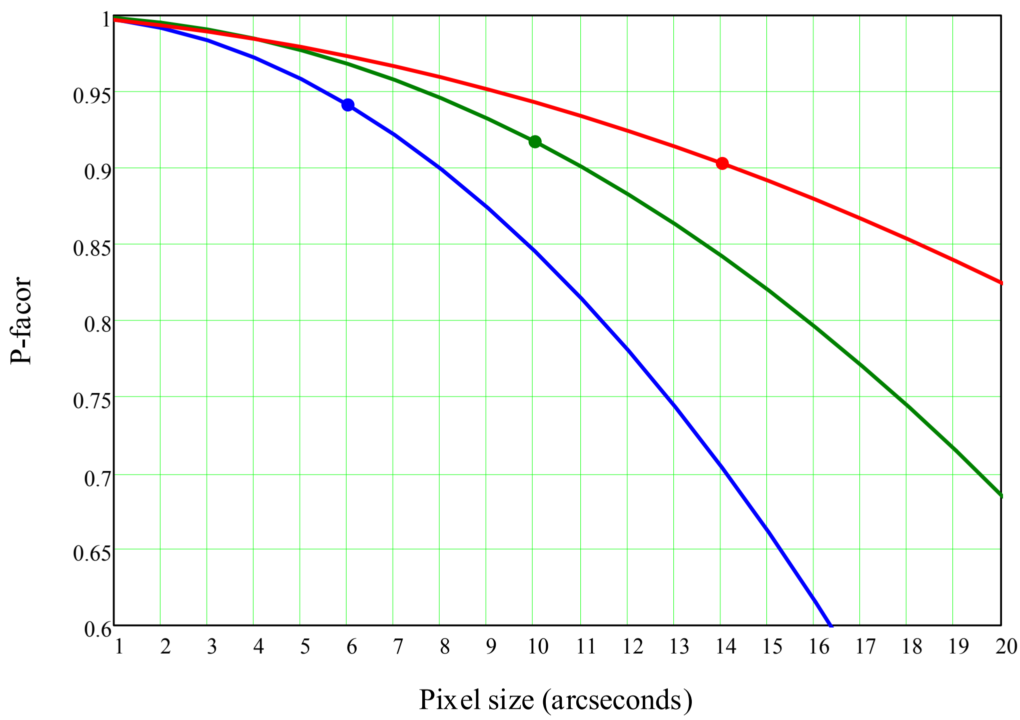

Figure 5: Pixelisation correction factor vs. map pixel size. The dots correspond to the nominal SPIRE Level-2 map pixel sizes of (6, 10, 14)" at (250, 350, 500) μm.

In principle, the following approach would yield the correct flux density of an isolated point source in an otherwise blank map in the general case in which it is not co-aligned with any map pixel:

1. Ascribe each map pixel flux density value to the central position of the pixel.
2. Derive the map pixel flux density that would have been recorded had the source been co-aligned with a pixel centre. This can be done by fitting the appropriate function to these data points and deriving the peak value. This function to be fitted is the beam profile convolved with the map pixel size. If the true beam profile were a 2-D Gaussian, the constrained parameters of this function would be (major axis, minor axis, position angle) and the free parameters would be (peak value, position of peak value).
3. Divide the resulting peak value by *P*.

This method may not be feasible or appropriate in all cases due to various effects such as limited S/N, sky background, confusion noise, astrometric errors, non-Gaussianity of the beam shape, etc. Any adopted method must take into account the definition of map pixel flux density given in boldface text above.

A method of source fitting has been developed by the SPIRE ICC which uses the timeline data directly. Essentially, a 2-D Gaussian function is fitted to the complete set of detector samples and their associated sky coordinates, thereby eliminating the use of pixel averaging in the fitting process. This method will be made available in HIPE and will be recommended to users as the most accurate.

8. Planetary models

Neptune is used as the primary calibration source for the SPIRE photometer. For completeness, in this section we summarise the models relevant for Uranus (used as primary calibrator for the SPIRE FTS), for Mars, and for a set of asteroids and stars which are being observed by PACS and/or Planck HFI, and which are therefore relevant to cross calibration.

8.1 Planetary angular sizes and solid angles

The adopted equatorial radii (1-bar level) and eccentricities for Uranus and Neptune are summarised in Table 3 and are based on the analysis of Voyager data by Lindal et al. [4] and Lindal [5]. These are similar to the values used in the ground-based observations by Griffin & Orton [9], Hildebrand et al. [6], and Orton et al. [7].

Planet	**Equatorial radius r_{eq} (km)**	**Polar radius, r_p (km)**	**Eccentricity** $e=\left[\frac{r_{eq}^2 - r_p^2}{r_p^2}\right]^{1/2}$	**Reference**
Uranus	25,559 ± 4	24,973 ± 20	0.2129	Lindal et al.
Neptune	24,766 ± 15	24,342 ± 30	0.1842	Lindal
Uranus	25,563	24,949	0.024	Griffin & Orton Hildebrand et al. Orton et al.
Neptune	24,760	24,240	0.021	

Table 3: Adopted planetary radii and eccentricities

In calculating the planetary angular sizes and solid angles, a correction is applied for the inclination of the planet's axis at the time of observation, and the apparent polar radius is given by [8]:

$$r_{\text{p-a}} = r_{eq}\left[1 - e^2\cos^2(\phi)\right]^{1/2}, \tag{17}$$

where ϕ is the latitude of the sub-Earth point, and e is the planet's eccentricity:

$$e=\left[\frac{r_{eq}^2 - r_p^2}{r_p^2}\right]^{1/2} . \tag{18}$$

The observed planetary disc is taken to have a geometric mean radius, r_{gm}, given by

$$r_{\text{gm}} = \left[r_{\text{eq}} \cdot r_{\text{p-a}}\right]^{1/2} . \tag{19}$$

For a Herschel-planet distance of D_{H}, the observed angular radius, θ, and solid angle, Ω_{P} , are thus

$$\theta_{\text{p}} = \frac{r_{\text{gm}}}{D_{\text{H}}} \quad \text{and} \quad \Omega_{\text{P}} = \pi\theta_{\text{p}}^2 . \tag{20}$$

(Note that planetary ephemerides based on Herschel as observer location can be generated in the JPL Horizons system using 500@-486 as the observer location code.) Typical angular radii for Uranus and Neptune are 1.7" and 1.1", respectively. The corresponding beam correction factors, K_{Beam}, are very close to unity: (0.988, 0.994, 0.997) for Uranus and (0.995, 0.997, 0.999) for Neptune at (250, 350, 500) μm.

8.2 Uranus and Neptune models

At the time of writing, the following planetary models are available.

8.2.1 Modified Griffin & Orton models of Uranus and Neptune

Neptune: The model of Griffin & Orton [9] with NH_3 = 9 x 10-5, with an extrapolation to 50 µm scaled from the results of Burgdorf et al. [10], which are slightly warmer. Note that this model does not yet include CO absorption lines which have a significant effect at longer wavelengths.

Uranus: The Griffin & Orton model [9], but with a uniform 4% temperature decrease. The influence of spectral lines on the Uranus spectrum is much less than for Uranus, but these may also be incorporated in the final model.

8.2.2 Glenn Orton models of Uranus and Neptune

Models of Uranus and Neptune have been computed and provided by Glenn Orton.

8.2.3 Raphael Moreno models of Uranus and Neptune

Models of Uranus and Neptune by Raphael Moreno have been agreed as the current standards by the HCALSG, and are available on the HCALSG ftp site.

The Uranus and Neptune models are quoted as accurate to ± 5%. Note that the models currently used for SPIRE are the "esa-2" tabulations. These may be subject to change as knowledge of the atmospheric properties becomes more refined, based on Herschel and other observations. Any such changes will be assessed and authorised by the HcalSG, and corresponding updates to the SPIRE and PACS flux calibration will be released accordingly. An updated model from 2010 is now available, but has not been adopted at this time. It produces 250-mm flux densities about 2.5% higher at 250 mm, less so for the other bands.

8.2.4 Uranus and Neptune: summary

The various Uranus are plotted in Figure 6, and the Neptune models in Figure 7 . The Moreno models are currently used in this document to calculate the Uranus and Neptune calibration flux densities for SPIRE. The calibration flux densities, $\bar{S}_{\text{Calib}}$, in Jy, for Uranus and Neptune, as evaluated using , are plotted in Figure 8 for the duration of the Herschel mission.

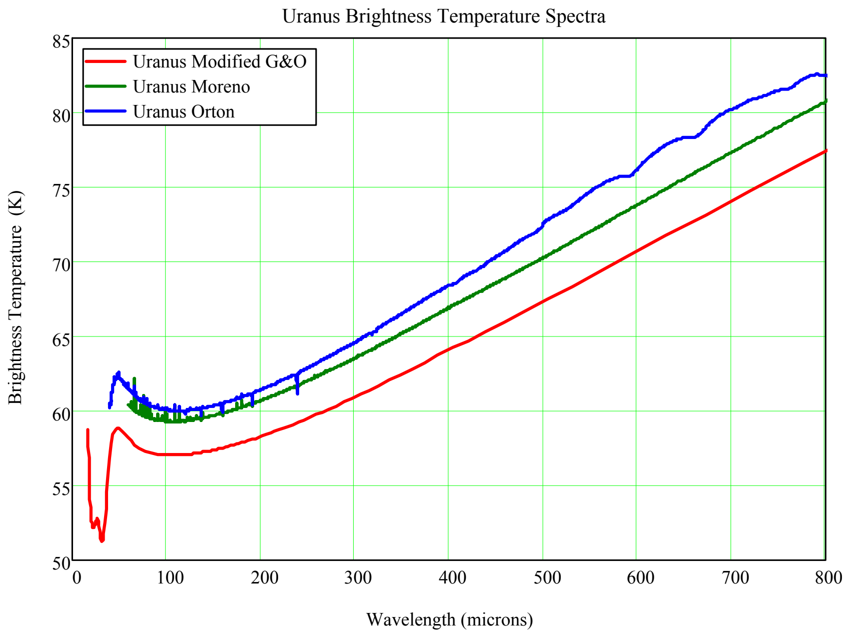

Figure 6: Models of the brightness temperature spectra of Uranus

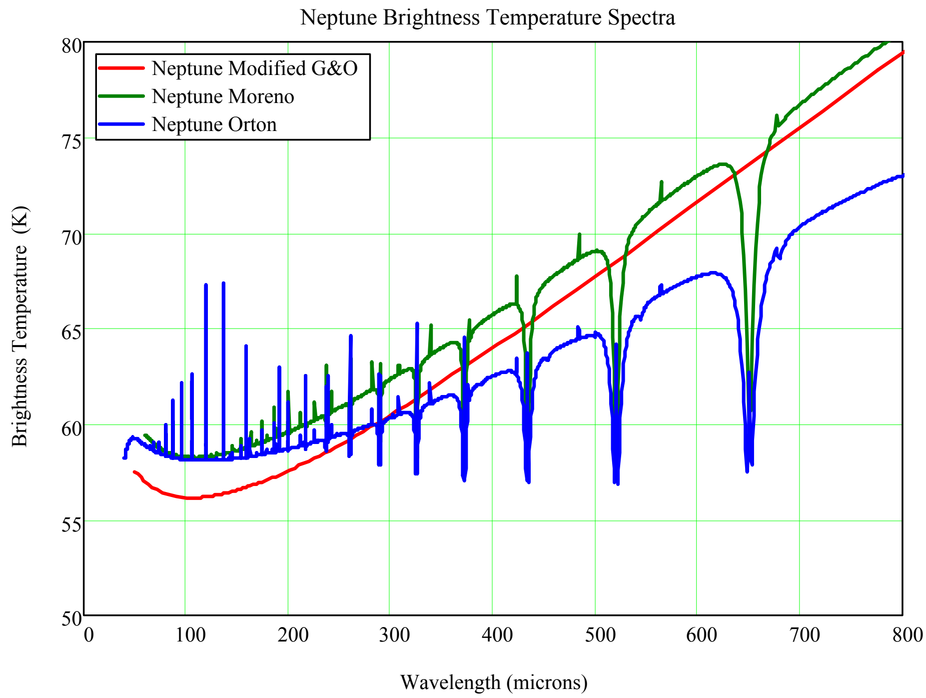

Figure 7: Models of the brightness temperature spectra of Neptune

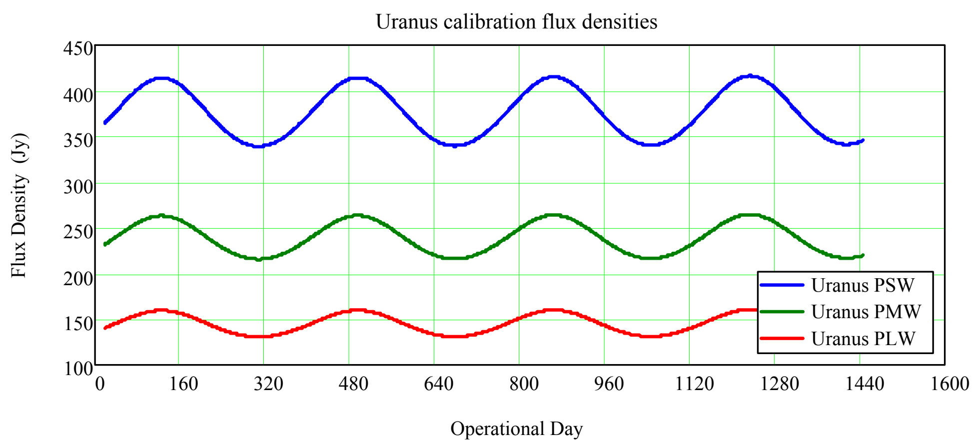

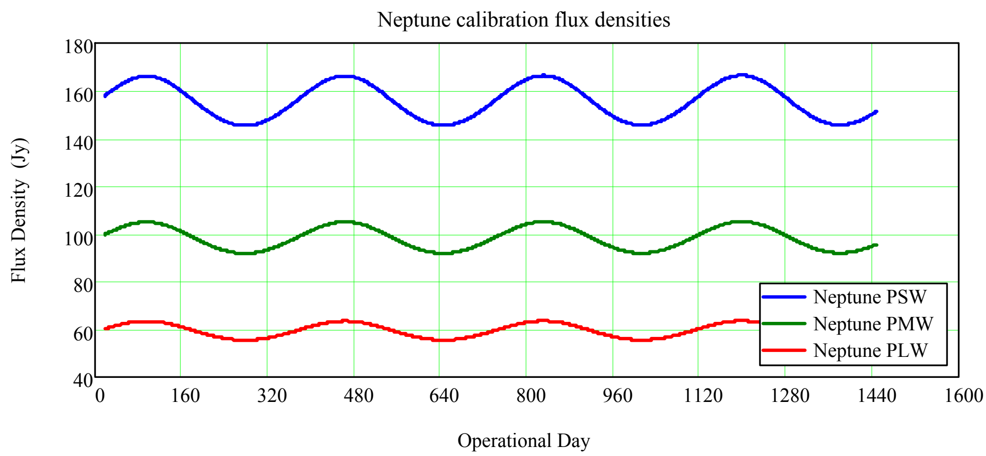

Figure 8: Uranus (top) and Neptune (bottom) calibration flux densities for the PSW, PMW, PLW bands over the duration of the Herschel mission

8.3 Mars

Web-based models of the martian continuum by Emmanuel Lellouch and Bryan Butler are available at

http://www.lesia.obspm.fr/perso/emmanuel-lellouch/mars/
and
http://www.aoc.nrao.edu/~bbutler/work/mars/model/

Mars is a very bright source for SPIRE. For example, at the time of its observation by SPIRE on OD 168 (29 Oct. 2009) it had flux densities of (9300, 5000, 2500) Jy at (250, 350, 500) μm. The nominal Herschel telescope background is equivalent to approximately (230, 250, 270) Jy, so that Mars is equivalent to (40, 20, 10) time the nominal telescope brightness. Mars thus presents a stringent test of the non-linearity correction method, particularly at 250 μm.

9. Asteroid models

The larger asteroids can also be used as SPIRE calibration sources, and have been particularly important in the early part of the mission when Uranus and Neptune were not available. The most accurate asteroid models are the thermophysical models of Thomas Müller [11], which must be computed in detail for a given observation date and time (there can be significant variations in brightness associated with the asteroid rotation period). This will be done after the observations have been made. For planning purposes, the Standard Thermal Model (STM) can be used to estimate the expected flux densities.

As an illustration, STM spectra for Dec. 9 2009 are illustrated in Figure 9 for the four largest asteroids, 1-Ceres, 2-Pallas, 3-Juno, and 4-Vesta. Note that STM asteroid spectra are all of approximately the same shape, close to that of a Rayleigh-Jeans black body: the monochromatic flux density ratios are typically 1.98 for S_{350}/S_{500} and 3.7–3.8 for S_{250}/S_{500}. The calibration accuracy of the STM as estimated by Thomas Müller [12] is approximately 5% for Ceres and 5-10% for Vesta.

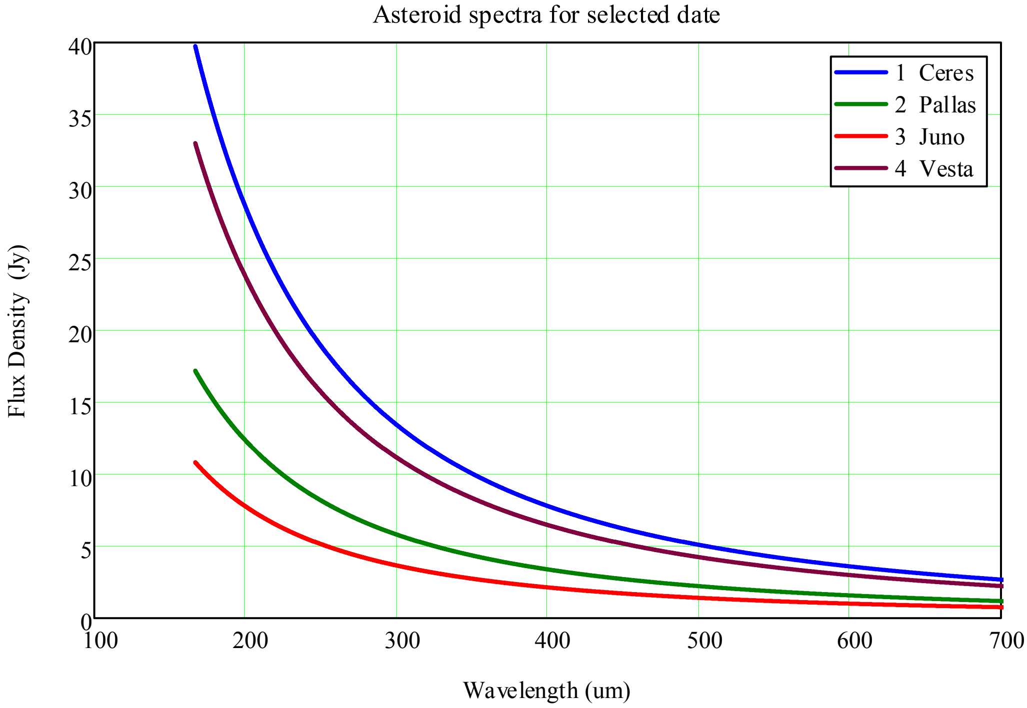

Figure 9: Standard Thermal Model spectra of 1-Ceres, 2-Pallas, 3-Juno, and 4-Vesta for Dec. 9 2009.

10. Stellar calibrators

A set of eight primary stellar calibrators has been identified by the HcalSG for use by PACS, and SPIRE will observe at least some of these for cross-calibration purposes. The eight are: αBoo, αTau, γAnd, βPeg, γDra, Sirius, and αCet.

Model spectra for these stars have been generated by Leen Decin based on the MARCS stellar atmosphere code [13], covering 2 – 200 μm, and the data are available on the HcalSG Twiki. The quoted estimated uncertainty is 1%. Figure 10 shows the model FIR SEDs for the eight stellar calibrators with extrapolations to the SPIRE photometer bands based on the spectral index in the 150 – 200 μm range. The latter is fairly uniform, varying between -1.99 and -2.03 for the eight sources. Computations covering wavelengths up to 700 μm are awaited. In the meantime, the available SEDs can be extrapolated with reasonable accuracy to SPIRE wavelengths, assuming no excess emission due to a chromospheric component or to cold dust component around the star. The presence of any such excess would lead to a higher flux density, so the extrapolated figures can be taken as lower limits.

Table 4 lists the extrapolated flux densities for the SPIRE photometer bands, together with information on the confusion levels and source visibility. The table is arranged in descending order of brightness. It includes the monochromatic flux densities at the SPIRE wavelengths and also the values that would be expected from the pipeline (i.e., not yet colour-corrected). The 1-σ confusion level is taken from HSpot, and the corresponding in-beam confusion noise is calculated by multiplying this by the beam solid angle. Typical predicted in-beam 1-σ uncertainties due to confusion are 5 – 6 mJy in all three bands with the exceptions of αTau (42, 31, 19 mJy) and Sirius (348, 28, 17 mJy).

Comments on individual sources:

- αBoo: Brightest star; not in a confused region; good S/N_{conf} even at 500 μm; visible until Aug. 22. The millimetre observations of Cohen et al. [14] show significant chromospheric emission at 1.4 mm, which could imply some excess in the SPIRE bands.
  - Suitable as a SPIRE-PACS cross calibration source.

- αTau: Nearly as bright as αBoo but much higher confusion; S/N_{conf} <20 in all bands; visible Aug./Sept. Cohen et al. [14] do not detect any chomospheric excess at 1.4 mm.
  - Not suitable as a SPIRE-PACS cross calibration source – too confused.

- βPeg: Reasonably bright; low confusion; S/N_{conf} only ~ 20 at 500 μm; disappears end July
  - Suitable as a SPIRE-PACS cross calibration source (S/N_{250} > 50)

- βAnd: Only 100 mJy at 500 μm; not a confused region but S/N_{conf} ~ 15 at 500 μm; visible until Aug. 27
  - Suitable as a SPIRE-PACS cross calibration source (S/N_{250} > 50)

- αCet: Similar to βAnd but slightly weaker and slightly higher confusion
  - Marginal suitability as a SPIRE-PACS cross calibration source (predicted S/N_{250} < 50)

- γDra: Only 60 mJy at 500 μm; S/N_{conf} ~ 10 at 500 μm; always visible
  - Marginal suitability as a SPIRE-PACS cross calibration source (predicted S/N_{250} < 50)

- Sirius: Faint and strongly confused. Low S/N_{conf} in all bands; visible Sept. – mid-Nov.
  - Not suitable as a SPIRE-PACS cross calibration source – too confused.

- βUmi: Similar S/N to γDra; always visible
  - Marginal suitability as a SPIRE-PACS cross calibration source (predicted S/N_{250} < 50)

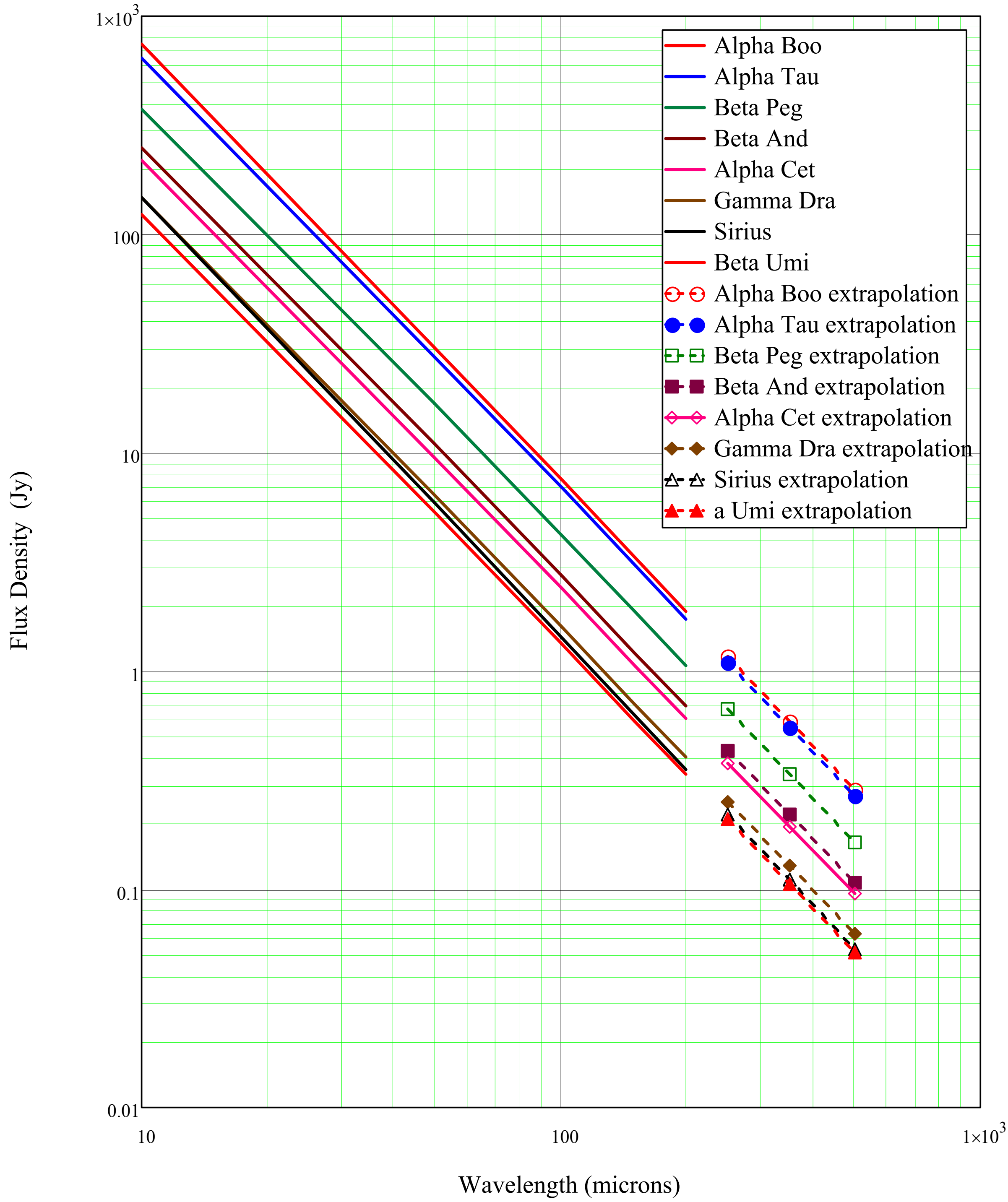

Figure 10: Decin and Eriksson's model FIR SEDs for the eight stellar calibrators with extrapolations to the SPIRE photometer bands.

Star	RA	Dec		250 µm	350 µm	500 µm
αBoo	14 15 39.67	19 10 56.7				
	Flux density		**(mJy)**	**1166**	**588**	**285**
	Calibration flux density		**(mJy)**	**1226**	**611**	**302**
	Flux density output by pipeline		**(mJy)**	**1240**	**615**	**304**
	1-σ confusion	MJy/sr		0.86	0.48	0.21
		In beam (mJy)		5.1	5.5	5.0
		S/N Conf.		160	75	40
	Background	Zodi (MJy/sr)		0.49	0.22	0.089
		ISM (MJy/sr)		2.44	1.23	0.471
		CIB (MJy/sr)		1.14	0.78	0.436
		Tot (MJy/sr)		4.07	2.32	0.996
αTau	4 35 55.24	16 30 33.5				
	Flux density		**(mJy)**	**1087**	**551**	**268**
	Calibration flux density		**(mJy)**	**1140**	**572**	**284**
	Flux density output by pipeline		**(mJy)**	**1155**	**575**	**286**
	1-σ confusion	MJy/sr		7.01	2.65	0.8
		In beam (mJy)		42	31	19
		S/N Conf.		18	13	10
	Background	Zodi (MJy/sr)		1.12	0.5	0.2
		ISM (MJy/sr)		43.7	22.1	8.4
		CIB (MJy/sr)		1.14	0.78	0.43
		Tot (MJy/sr)		46	23.4	9.1
βPeg	23 3 46.46	28 4 58.0				
	Flux density		**(mJy)**	**665**	**338**	**165**
	Calibration flux density		**(mJy)**	**699**	**351**	**174**
	Flux density output by pipeline		**(mJy)**	**707**	**353**	**175**
	1-σ confusion	MJy/sr		0.99	0.52	0.22
		In beam (mJy)		5.9	6.0	5.3
		S/N Conf.		79	40	22
	Background	Zodi (MJy/sr)		0.46	0.2	0.08
		ISM (MJy/sr)		7.5	3.79	1.44
		CIB (MJy/sr)		1.14	0.78	0.44
		Tot (MJy/sr)		9.09	4.77	1.96
βAnd	1 9 43.92	35 37 14.0				
	Flux density		**(mJy)**	**432**	**219**	**107**
	Calibration flux density		**(mJy)**			
	Flux density output by pipeline		**(mJy)**	**459**	**229**	**114**
	1-σ confusion	MJy/sr		0.88	0.49	0.21
		In beam (mJy)		5.3	5.7	5.0
		S/N Conf.		58	27	15
	Background	Zodi (MJy/sr)		0.51	0.22	0.09
		ISM (MJy/sr)		4.35	2.2	0.84
		CIB (MJy/sr)		1.14	0.78	0.44
		Tot (MJy/sr)		6	3.21	1.37
αCet	3 2 16.77	4 5 23.0				
	Flux density		**(mJy)**	**379**	**194**	**95.2**
	Calibration flux density		**(mJy)**	**398**	**201**	**101**
	Flux density output by pipeline		**(mJy)**	**403**	**202**	**101**
	1-σ confusion	MJy/sr		1.12	0.55	0.22
		In beam (mJy)		6.7	6.3	5.3
		S/N Conf.		40	22	13
	Background	Zodi (MJy/sr)		0.95	0.42	0.17
		ISM (MJy/sr)		9.73	4.93	1.88
		CIB (MJy/sr)		1.14	0.78	0.44
		Tot (MJy/sr)		11.8	6.13	2.49

Star	RA	Dec	250 µm	350 µm	500 µm
	17 56 36.37	51 29 20.0			
	Flux density	**(mJy)**	**252**	**128**	**62.1**
	Calibration flux density	**(mJy)**	**265**	**133**	**65.8**
	Flux density output by pipeline	**(mJy)**	**268**	**133**	**66.2**
	1-σ confusion	MJy/sr	0.88	0.49	0.21
γDra		In beam (mJy)	5.3	5.7	5.0
		S/N Conf.	34	16	9
	Background	Zodi (MJy/sr)	0.24	0.11	0.04
		ISM (MJy/sr)	3.99	2.02	0.77
		CIB (MJy/sr)	1.14	0.78	0.44
		Tot (MJy/sr)	5.37	2.91	1.25
	6 45 8.92	-16 42 58.0			
	Flux density	**(mJy)**	**219**	**110**	**53.3**
	Calibration flux density	**(mJy)**	**231**	**115**	**56.5**
	Flux density output by pipeline	**(mJy)**	**233**	**115**	**56.9**
	1-σ confusion	MJy/sr	6.4	2.4	0.73
Sirius		In beam (mJy)	38	28	17
		S/N Conf.	4.0	2.8	2.2
	Background	Zodi (MJy/sr)	0.44	0.2	0.08
		ISM (MJy/sr)	40.9	20.7	7.89
		CIB (MJy/sr)	1.14	0.78	0.44
		Tot (MJy/sr)	42.5	21.7	8.41
	14 50 42.33	74 9 19.8			
	Flux density	**(mJy)**	**209**	**106**	**51.5**
	Calibration flux density	**(mJy)**	**219**	**110**	**54.5**
	Flux density output by pipeline	**(mJy)**	**222**	**111**	**54.9**
	1-σ confusion	MJy/sr	0.86	0.48	0.21
βUmi		In beam (mJy)	5.1	5.5	5.0
		S/N Conf.	29	14	7
	Background	Zodi (MJy/sr)	0.24	0.11	0.04
		ISM (MJy/sr)	1.78	0.9	0.34
		CIB (MJy/sr)	1.14	0.78	0.44
		Tot (MJy/sr)	3.16	1.79	0.82

Table 4: Extrapolated SPIRE monochromatic flux densities, calibration flux densities, pipeline output flux densities, plus confusion and background levels, for the eight standard stars.

11. Calibration accuracy

SPIRE photometer observations are subject to several kinds of uncertainty.

Absolute calibration uncertainty: This component is associated with our knowledge of the brightness of the primary calibrator, Neptune, and is estimated at Â±5%. It is correlated across the three bands – i.e., flux densities in the three bands will move up or down systematically in the event of this calibration being revised.

Relative calibration uncertainty: This uncertainty arises from the process of comparing a source observation with Neptune (using the Neptune-derived voltage to flux density parameters that are implemented in the pipeline). This is a random contribution and has been estimated by careful analysis of repeated measurements of a bright source (actually Neptune itself). The results show that this component is less than 2% in all bands.

At present, we recommend that the overall calibration uncertainty for the SPIRE photometer, taking these two contributions into account, should be taken conservatively as ±7% (the direct rather than quadrature sum of the absolute and relative calibration uncertainties). It should be noted that this is dominated by the absolute component and is thus largely correlated across the three bands.

Photometric uncertainty: This component is due to the source measurement errors. The photometer pipeline produces timelines representing the in-beam flux density, and some random detector noise will be present in the timelines. Any astrometric errors will also introduce additional noise when timelines are combined in mapmaking. In addition, in order to derive estimates of, for example, the flux density of a point or compact source, users will need to employ some suitable fitting or aperture photometry technique, and additional uncertainties can be introduced due to confusion or source crowding.

Except for bright sources in uncrowded regions, such photometric uncertainties will be significant or dominant. The assessment of these uncertainties depends on the sky brightness distribution and on the source extraction or background subtraction methods, and is therefore regarded as something to be done by the user.

See Section 7 for some additional considerations relating to the process of point source extraction.

12. Future plans for photometer flux calibration

Herschel flux calibration is now in the regime of sub-10% accuracy, and for this reason small effects such as the ones treated above must be considered carefully. A Herschel calibration workshop in December 2010 will review various aspects of flux including: (i) the accuracy and compatibility of the Neptune-based calibration (used by SPIRE) and the stellar-based calibration (used by PACS); and (ii) the methods, assumptions and conventions used by both SPIRE and PACS.

Further refinements to the SPIRE photometer calibration scheme presented here may be made in the future based on (i) revision of the basic Neptune brightness model used, and/or (ii) a more detailed treatment of the extended source calibration, which is currently in development, involving a more precise method of accounting for the variation of the beam profile across the bands. We expect any such updates to produce a new calibration consistent with the current, one but with smaller uncertainties.

13. Flux density computations

Details of the flux density calculations are provided in the annex to this document.

14. References

1 *The SPIRE Analogue Signal Chain and Photometer Detector Data Processing Pipeline*, Matt Griffin, SPIRE-UCF-DOC-002890, Issue 6, November 2008.

2 *Proposed RSRF for SPIRE Photometer*, Bruce Swinyard, SPIRE-RAL-NOT- 002962, Issue 3, 28 Sept. 2007

3 Ulich, B.L. & Haas, R.W., *Absolute Calibration of Millimeter-Wavelength Spectral Lines*, Ap. J. Supp. 30, 247, 1976.

4 Lindal, G.F., et al. *The Atmosphere of Uranus: Results of Radio Occultation Measurements with Voyager 2*, J. Geophys. Res., 92, 14987, 1987.

5 Lindal, G., *The Atmosphere of Neptune: an Analysis of Radio Occultation Data Acquired with Voyager 2*, Astron. J., 103, 967, 1992.

6 Hildebrand, R. et al., *Far-infrared and Submillimeter Brightness Temperatures of the Giant Planets*, Icarus, 64, 64, 1985.

7 Orton, G.S., et al., *Submillimeter and Millimeter Observations of Uranus and Neptune*, Icarus, 67, 289, 1986

8 Marth, A., *On the Apparent Disc and on the Shadow of an Ellipsoid*, MNRAS, 57, 442, 1897

9 Griffin, M.J. & Orton, G.S., *The Near Millimeter Brightness Temperature Spectra of Uranus and Neptune*, Icarus, 105, 537, 1993.

10 Burgdorf, M. et al., *Neptune's Far-infrared Spectrum from the ISO Long-Wavelength and Short-Wavelength Spectrometers*, Icarus, 164, 244, 2003.

11 Müller, Th. & Lagerros, J.S.V., *Asteroids as Calibration Standards in the Thermal Infrared for Space Observatories*, Astron. Astrophys., 381, 324, 2002.

12 Müller, Th, *Asteroid Calibration Quality Information for COP and Early PV*, 8 May 2009, Asteroid_quality_TM_08052009.pdf (available on HCALSG Twiki)

13 Decin L., & Eriksson K., *Theoretical Model Atmosphere Spectra Used for the Calibration of Infrared Instruments*, Astron. Astrophys., 472, 1041, 2007.

14 Cohen, M., Carbon, D.F., Lim, T., Schulz, B., McMurry, A.D., Forster, J.R., and Goorvitch, D., *Far infrared and Millimeter Continuum Studies of K Giants: α Bootis and α Tauri*, Ap. J., 129, 2836, 2005.

Annex: SPIRE Photometer Flux Calibration Computation

Matt Griffin 4 November 2010

Constants $h \equiv 6.626 \cdot 10^{-34}$ $c \equiv 2.99792 \cdot 10^{8}$ $kb \equiv 1.3806 \cdot 10^{-23}$

$origin \equiv 1$ $\sigma \equiv 5.6704 \cdot 10^{-8}$ $AU := 1.4959787069 \cdot 10^{11}$

Planck function $B(nu, T) := \dfrac{2 \cdot h \cdot nu^3}{c^2 \cdot \left(e^{\frac{h \cdot nu}{kb \cdot T}} - 1 \right)}$

Photometer RSRFs

Bands $i \equiv 1, 2 .. 3$ **1 = PSW** **2 = PMW** **3 = PLW**

Read in transmission data $\begin{pmatrix} waveno \\ PSW \\ PMW \\ PLW \end{pmatrix} :=$ Worksheet

Data are from: *Proposed RSRF for SPIRE Photometer*, by Bruce Swinyard, SPIRE-RAL-NOT-002962, Issue 3, 28 Sept. 2007

Frequency (Hz) $Freq := waveno \cdot 100 \cdot c$ $rows(Freq) = 512$

Transmission

PSW $tfil_1(nu) := linterp(Freq, PSW, nu)$

PMW $tfil_2(nu) := linterp(Freq, PMW, nu)$

PLW $tfil_3(nu) := linterp(Freq, PLW, nu)$

Regrid with 0.3 GHz interval $N := 5000$ $n := 0, 1 .. N$ $\nu 0 := 3 \cdot 10^{11}$ $\Delta\nu := 0.3 \cdot 10^{9}$

$\nu_n := \nu 0 + n \cdot \Delta\nu$ $\lambda_n := \dfrac{c}{\nu_n} \cdot 10^6$ $\nu_N = 1.800 \times 10^{12}$

Plot filter profiles

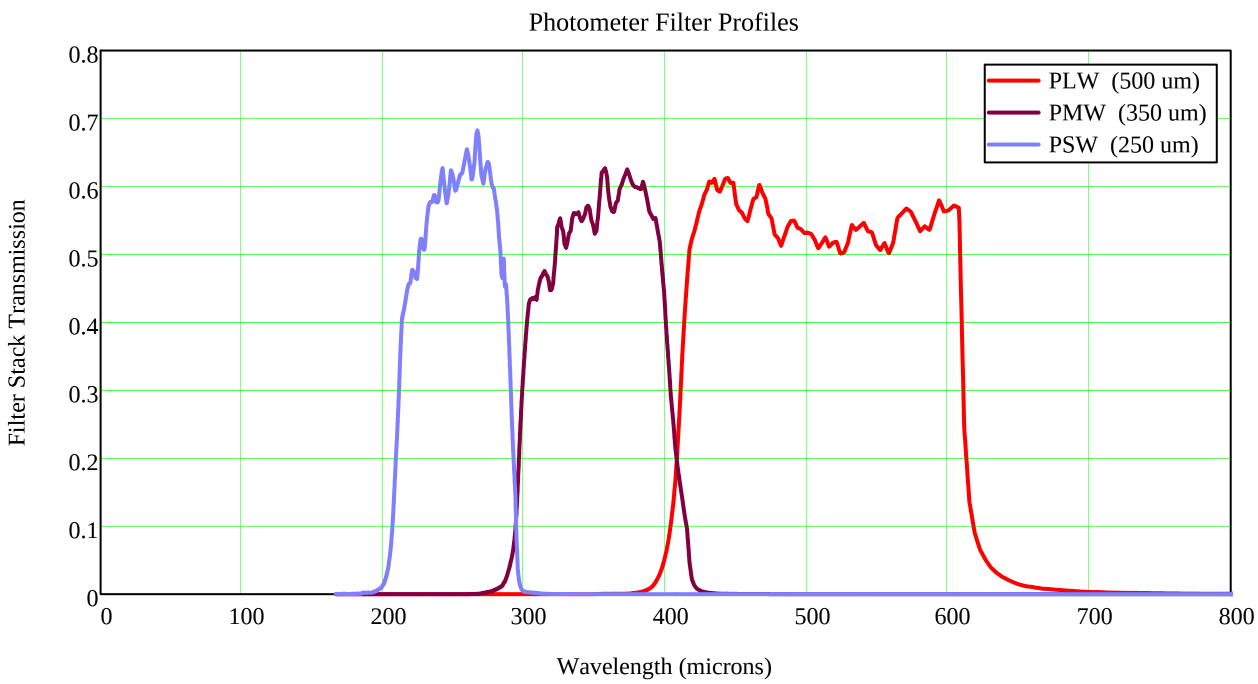

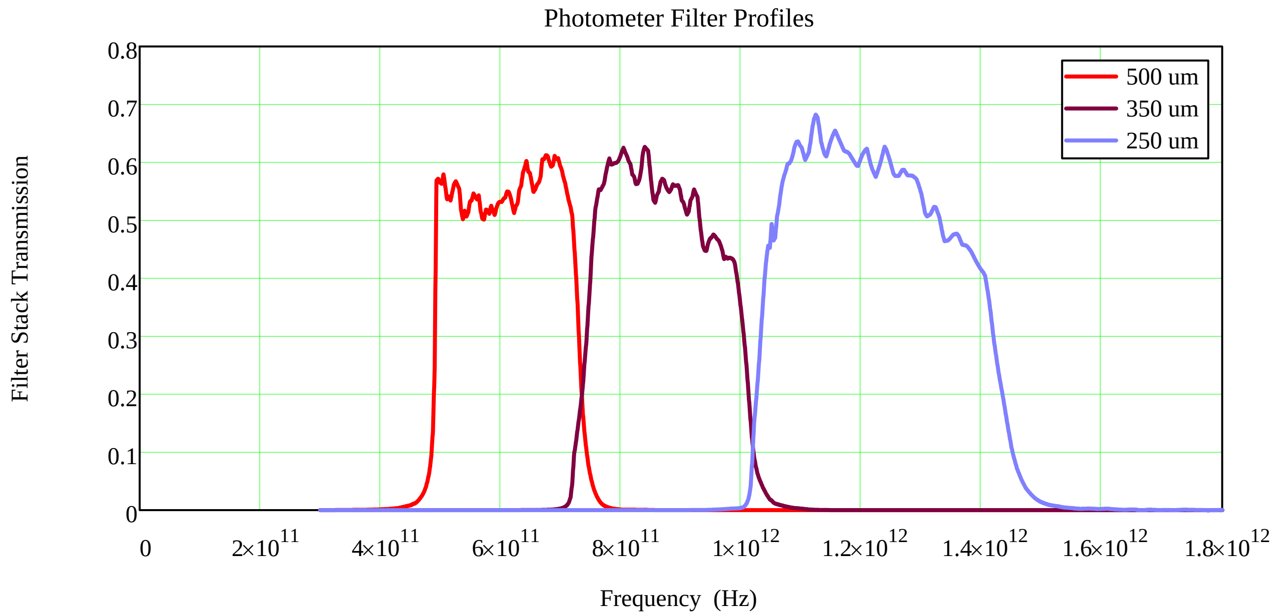

Define standard wavelengths and frequencies for the three bands

$\lambda o_i :=$ m

$250 \cdot 10^{-6}$
$350 \cdot 10^{-6}$
$500 \cdot 10^{-6}$

$\nu o_i := \dfrac{c}{\lambda o_i}$

$\nu o_i =$ Hz

$1.199 \cdot 10^{12}$
$8.565 \cdot 10^{11}$
$5.996 \cdot 10^{11}$

Weighting of filter profiles:

Point

$RP_1(nu) := tfil_1(nu) \cdot \left(\dfrac{\nu o_1}{nu}\right)^0$ $\quad RP_2(nu) := tfil_2(nu) \cdot \left(\dfrac{\nu o_2}{nu}\right)^0$ $\quad RP_3(nu) := tfil_3(nu) \cdot \left(\dfrac{\nu o_3}{nu}\right)^0$

Extended

$RE_1(nu) := tfil_1(nu) \cdot \left(\dfrac{\nu o_1}{nu}\right)^2$ $\quad RE_2(nu) := tfil_2(nu) \cdot \left(\dfrac{\nu o_2}{nu}\right)^2$ $\quad RE_3(nu) := tfil_3(nu) \cdot \left(\dfrac{\nu o_3}{nu}\right)^2$

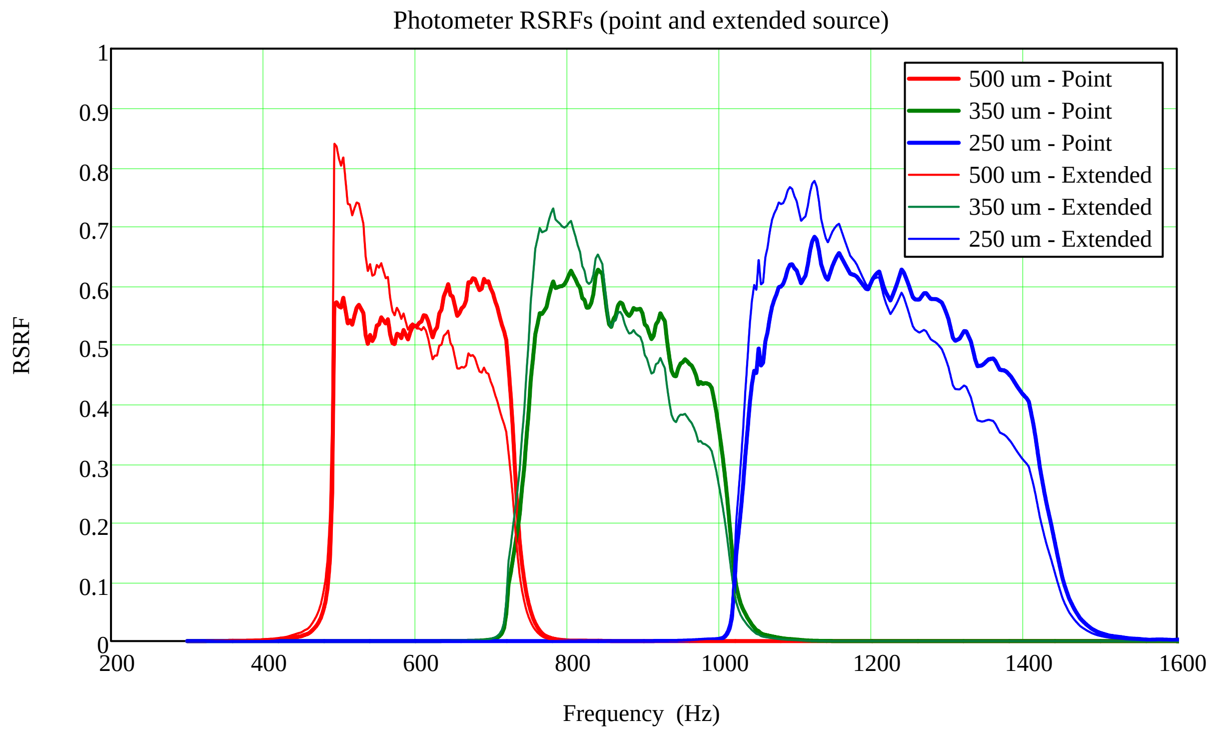

Conversion factor from RSRF-weighted flux density to monochromatic flux density

$$S_S(\nu_o) = \bar{S}_S \left[\frac{\nu_o^{\alpha_S} \int_{Passband} R(\nu)\, d\nu}{\int_{Passband} \nu^{\alpha_S} R(\nu)\, d\nu} \right] = K_4 \bar{S}_S$$

Assumed source spectrum power law index

$$\alpha_S := -4, -3.5 .. 4$$

Point source:

$$K4P_1(\alpha) := \frac{(\nu o_1)^{\alpha} \cdot \sum_{f=0}^{N-1} \left[\frac{RP_1(\nu_{f+1}) + RP_1(\nu_f)}{2} \cdot (\nu_{f+1} - \nu_f) \right]}{\sum_{f=0}^{N-1} \left[\frac{RP_1(\nu_{f+1}) + RP_1(\nu_f)}{2} \cdot \left(\frac{\nu_f + \nu_{f+1}}{2} \right)^{\alpha} \cdot (\nu_{f+1} - \nu_f) \right]}$$

$$K4P_2(\alpha) := \frac{(\nu o_2)^{\alpha} \cdot \sum_{f=0}^{N-1} \left[\frac{RP_2(\nu_{f+1}) + RP_2(\nu_f)}{2} \cdot (\nu_{f+1} - \nu_f) \right]}{\sum_{f=0}^{N-1} \left[\frac{RP_2(\nu_{f+1}) + RP_2(\nu_f)}{2} \cdot \left(\frac{\nu_f + \nu_{f+1}}{2} \right)^{\alpha} \cdot (\nu_{f+1} - \nu_f) \right]}$$

$$K4P_3(\alpha) := \frac{(\nu o_3)^{\alpha} \cdot \sum_{f=0}^{N-1} \left[\frac{RP_3(\nu_{f+1}) + RP_3(\nu_f)}{2} \cdot (\nu_{f+1} - \nu_f) \right]}{\sum_{f=0}^{N-1} \left[\frac{RP_3(\nu_{f+1}) + RP_3(\nu_f)}{2} \cdot \left(\frac{\nu_f + \nu_{f+1}}{2} \right)^{\alpha} \cdot (\nu_{f+1} - \nu_f) \right]}$$

Extended source

$$K4E_1(\alpha) := \frac{(\nu o_1)^{\alpha} \cdot \sum_{f=0}^{N-1} \left[\frac{RE_1(\nu_{f+1}) + RE_1(\nu_f)}{2} \cdot (\nu_{f+1} - \nu_f) \right]}{\sum_{f=0}^{N-1} \left[\frac{RE_1(\nu_{f+1}) + RE_1(\nu_f)}{2} \cdot \left(\frac{\nu_f + \nu_{f+1}}{2} \right)^{\alpha} \cdot (\nu_{f+1} - \nu_f) \right]}$$

$$K4E_2(\alpha) := \frac{(\nu o_2)^{\alpha} \cdot \sum_{f=0}^{N-1} \left[\frac{RE_2(\nu_{f+1}) + RE_2(\nu_f)}{2} \cdot (\nu_{f+1} - \nu_f) \right]}{\sum_{f=0}^{N-1} \left[\frac{RE_2(\nu_{f+1}) + RE_2(\nu_f)}{2} \cdot \left(\frac{\nu_f + \nu_{f+1}}{2} \right)^{\alpha} \cdot (\nu_{f+1} - \nu_f) \right]}$$

$$K4E_3(\alpha) := \frac{(\nu o_3)^{\alpha} \cdot \sum_{f=0}^{N-1} \left[\frac{RE_3(\nu_{f+1}) + RE_3(\nu_f)}{2} \cdot (\nu_{f+1} - \nu_f) \right]}{\sum_{f=0}^{N-1} \left[\frac{RE_3(\nu_{f+1}) + RE_3(\nu_f)}{2} \cdot \left(\frac{\nu_f + \nu_{f+1}}{2} \right)^{\alpha} \cdot (\nu_{f+1} - \nu_f) \right]}$$

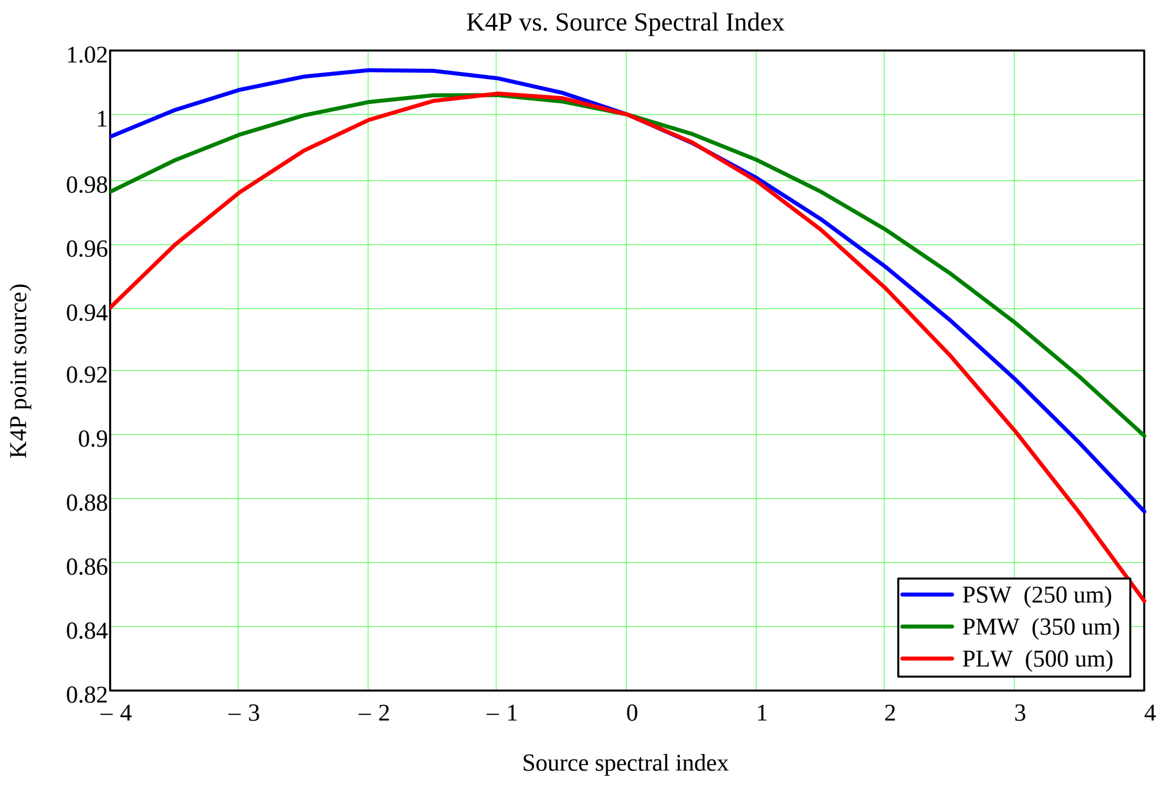
K4P vs. Source Spectral Index
K4P point source)
Source spectral index
1.02
1
0.98
0.96
0.94
0.92
0.9
0.88
0.86
0.84
0.82
– 4
– 3
– 2
– 1
0
1
2
3
4
PSW (250 um)
PMW (350 um)
PLW (500 um)

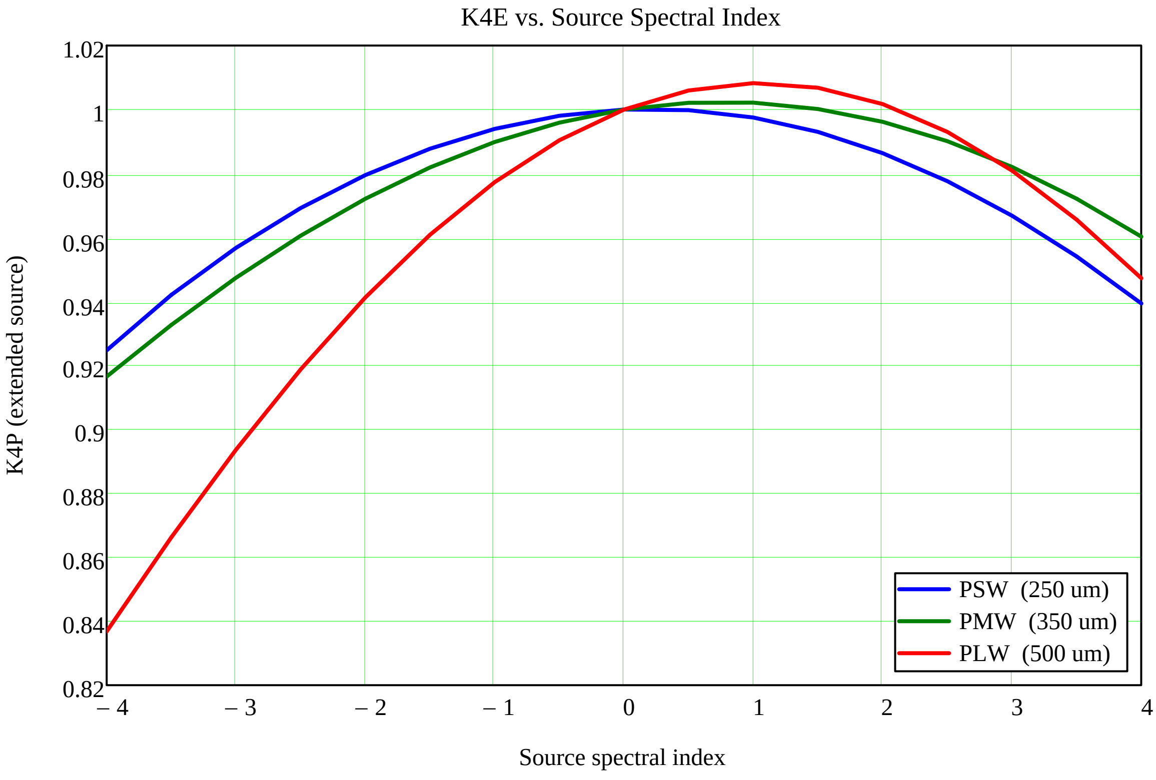
K4E vs. Source Spectral Index
K4P (extended source)
Source spectral index
1.02
1
0.98
0.96
0.94
0.92
0.9
0.88
0.86
0.84
0.82
– 4
– 3
– 2
– 1
0
1
2
3
4
PSW (250 um)
PMW (350 um)
PLW (500 um)

Tabulation of K4P vs. spectral index

$\alpha_S =$	$K4P_1(\alpha_S) =$	$K4P_2(\alpha_S) =$	$K4P_3(\alpha_S) =$
-4.000	0.9931	0.9759	0.9397
-3.500	1.0014	0.9857	0.9592
-3.000	1.0077	0.9937	0.9757
-2.500	1.0118	0.9998	0.9887
-2.000	1.0138	1.0039	0.9983
-1.500	1.0137	1.0060	1.0043
-1.000	1.0113	1.0060	1.0065
-0.500	1.0067	1.0040	1.0051
0.000	1.0000	1.0000	1.0000
0.500	0.9911	0.9939	0.9913
1.000	0.9802	0.9859	0.9793
1.500	0.9672	0.9759	0.9640
2.000	0.9524	0.9640	0.9456
2.500	0.9357	0.9503	0.9246
3.000	0.9173	0.9350	0.9011
3.500	0.8973	0.9180	0.8754
4.000	0.8759	0.8996	0.8480

Tabulation of K4E vs. spectral index

$K4E_1(\alpha_S) =$	$K4E_2(\alpha_S) =$	$K4E_3(\alpha_S) =$
0.9247	0.9165	0.8368
0.9421	0.9327	0.8662
0.9568	0.9474	0.8937
0.9692	0.9606	0.9188
0.9795	0.9721	0.9413
0.9877	0.9819	0.9608
0.9939	0.9898	0.9773
0.9980	0.9959	0.9904
1.0000	1.0000	1.0000
0.9998	1.0021	1.0060
0.9975	1.0022	1.0082
0.9930	1.0002	1.0068
0.9863	0.9961	1.0017
0.9776	0.9901	0.9930
0.9668	0.9821	0.9809
0.9540	0.9721	0.9656
0.9394	0.9603	0.9472

Nominal spectral index

$\alpha_{So} := -1$

$K4P_1(\alpha_{So}) = 1.0113$ $\quad$ $K4E_1(\alpha_{So}) = 0.9939$

$K4P_2(\alpha_{So}) = 1.0060$ $\quad$ $K4E_2(\alpha_{So}) = 0.9898$

$K4P_3(\alpha_{So}) = 1.0065$ $\quad$ $K4E_3(\alpha_{So}) = 0.9773$

$$\frac{K4E_1(\alpha_{So})}{K4P_1(\alpha_{So})} = 0.9828 \qquad \frac{K4E_2(\alpha_{So})}{K4P_2(\alpha_{So})} = 0.9839 \qquad \frac{K4E_3(\alpha_{So})}{K4P_3(\alpha_{So})} = 0.9710$$

Colour correction factor vs. source power-law spectral index

$$S'_S(\nu_o) = \nu_o^{(\alpha_{Snew} - \alpha_{So})} \left[\frac{\int_{Passband} R(\nu)\nu^{\alpha_{So}}\, d\nu}{\int_{Passband} R(\nu)\,\nu^{\alpha_{Snew}}\, d\nu} \right] S_S(\nu_o) = K_C(\alpha_{Snew}) S_S(\nu_o)$$

Nominal spectral index

$\alpha_{So} = -1.000$

Point source:

$$KPc_1(\alpha) := (\nu o_1)^{(\alpha - \alpha_{So})} \cdot \frac{\left[\sum_{f=0}^{N-1} \left[\left[\frac{(RP_1(\nu_{f+1}) + RP_1(\nu_f))}{2} \cdot (\nu_{f+1} - \nu_f)\right] \cdot \left(\frac{\nu_{f+1} + \nu_f}{2}\right)^{\alpha_{So}}\right]\right]}{\left[\sum_{f=0}^{N-1} \left[\left[\frac{(RP_1(\nu_{f+1}) + RP_1(\nu_f))}{2} \cdot (\nu_{f+1} - \nu_f)\right] \cdot \left(\frac{\nu_{f+1} + \nu_f}{2}\right)^{\alpha}\right]\right]}$$

$$KPc_2(\alpha) := (\nu o_2)^{(\alpha - \alpha_{So})} \cdot \frac{\left[\sum_{f=0}^{N-1} \left[\left[\frac{(RP_2(\nu_{f+1}) + RP_2(\nu_f))}{2} \cdot (\nu_{f+1} - \nu_f)\right] \cdot \left(\frac{\nu_{f+1} + \nu_f}{2}\right)^{\alpha_{So}}\right]\right]}{\left[\sum_{f=0}^{N-1} \left[\left[\frac{(RP_2(\nu_{f+1}) + RP_2(\nu_f))}{2} \cdot (\nu_{f+1} - \nu_f)\right] \cdot \left(\frac{\nu_{f+1} + \nu_f}{2}\right)^{\alpha}\right]\right]}$$

$$KPc_3(\alpha) := (\nu o_3)^{(\alpha - \alpha_{So})} \cdot \frac{\left[\sum_{f=0}^{N-1} \left[\left[\frac{(RP_3(\nu_{f+1}) + RP_3(\nu_f))}{2} \cdot (\nu_{f+1} - \nu_f)\right] \cdot \left(\frac{\nu_{f+1} + \nu_f}{2}\right)^{\alpha_{So}}\right]\right]}{\left[\sum_{f=0}^{N-1} \left[\left[\frac{(RP_3(\nu_{f+1}) + RP_3(\nu_f))}{2} \cdot (\nu_{f+1} - \nu_f)\right] \cdot \left(\frac{\nu_{f+1} + \nu_f}{2}\right)^{\alpha}\right]\right]}$$

Extended source:

$$KEc_1(\alpha) := (\nu o_1)^{(\alpha - \alpha_{So})} \cdot \frac{\left[\sum_{f=0}^{N-1} \left[\left[\frac{(RE_1(\nu_{f+1}) + RE_1(\nu_f))}{2} \cdot (\nu_{f+1} - \nu_f)\right] \cdot \left(\frac{\nu_{f+1} + \nu_f}{2}\right)^{\alpha_{So}}\right]\right]}{\left[\sum_{f=0}^{N-1} \left[\left[\frac{(RE_1(\nu_{f+1}) + RE_1(\nu_f))}{2} \cdot (\nu_{f+1} - \nu_f)\right] \cdot \left(\frac{\nu_{f+1} + \nu_f}{2}\right)^{\alpha}\right]\right]}$$

$$KEc_2(\alpha) := (\nu o_2)^{(\alpha - \alpha_{So})} \cdot \frac{\left[\sum_{f=0}^{N-1} \left[\left[\frac{(RE_2(\nu_{f+1}) + RE_2(\nu_f))}{2} \cdot (\nu_{f+1} - \nu_f)\right] \cdot \left(\frac{\nu_{f+1} + \nu_f}{2}\right)^{\alpha_{So}}\right]\right]}{\left[\sum_{f=0}^{N-1} \left[\left[\frac{(RE_2(\nu_{f+1}) + RE_2(\nu_f))}{2} \cdot (\nu_{f+1} - \nu_f)\right] \cdot \left(\frac{\nu_{f+1} + \nu_f}{2}\right)^{\alpha}\right]\right]}$$

$$KEc_3(\alpha) := (\nu o_3)^{(\alpha - \alpha_{So})} \cdot \frac{\left[\sum_{f=0}^{N-1} \left[\left[\frac{(RE_3(\nu_{f+1}) + RE_3(\nu_f))}{2} \cdot (\nu_{f+1} - \nu_f)\right] \cdot \left(\frac{\nu_{f+1} + \nu_f}{2}\right)^{\alpha_{So}}\right]\right]}{\left[\sum_{f=0}^{N-1} \left[\left[\frac{(RE_3(\nu_{f+1}) + RE_3(\nu_f))}{2} \cdot (\nu_{f+1} - \nu_f)\right] \cdot \left(\frac{\nu_{f+1} + \nu_f}{2}\right)^{\alpha}\right]\right]}$$

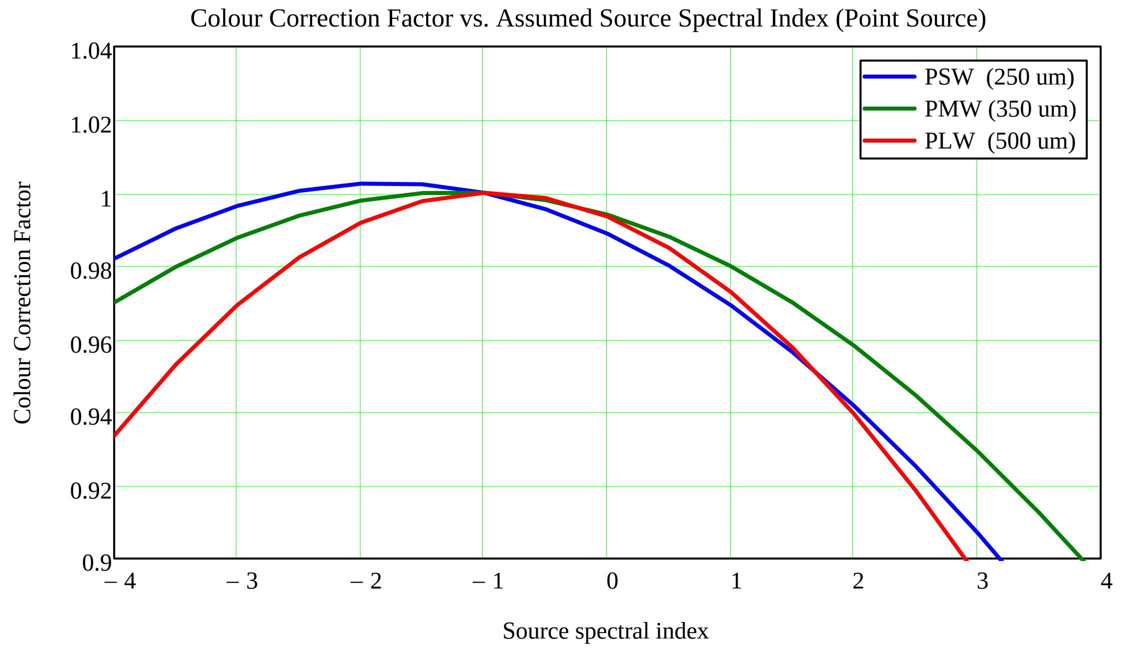

Colour Correction Factor vs. Assumed Source Spectral Index (Point Source)
Colour Correction Factor
Source spectral index
PSW (250 um)
PMW (350 um)
PLW (500 um)
1.04
1.02
1
0.98
0.96
0.94
0.92
0.9
– 4
– 3
– 2
– 1
0
1
2
3
4

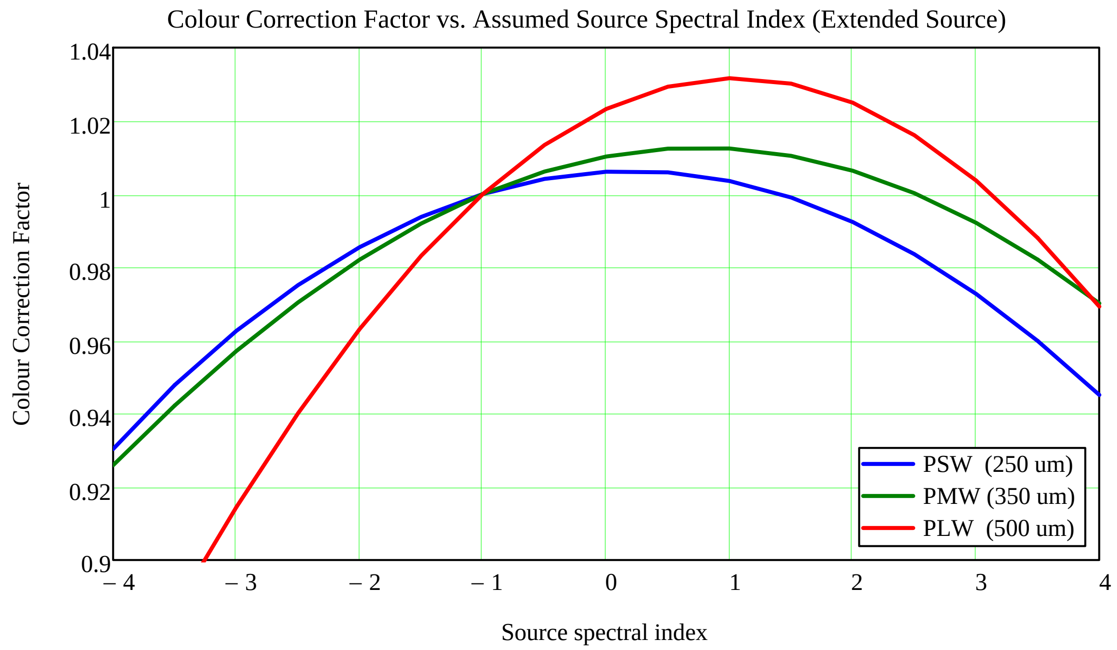

Colour Correction Factor vs. Assumed Source Spectral Index (Extended Source)
Colour Correction Factor
Source spectral index
PSW (250 um)
PMW (350 um)
PLW (500 um)
1.04
1.02
1
0.98
0.96
0.94
0.92
0.9
– 4
– 3
– 2
– 1
0
1
2
3
4

Tabulation of KC vs. spectral index

	Point source			Extended source		
$\alpha_S =$	$KPc_1(\alpha_S) =$	$KPc_2(\alpha_S) =$	$KPc_3(\alpha_S) =$	$KEc_1(\alpha_S) =$	$KEc_2(\alpha_S) =$	$KEc_3(\alpha_S) =$
-4.000	0.9820	0.9700	0.9336	0.9303	0.9259	0.8562
-3.500	0.9902	0.9798	0.9530	0.9478	0.9422	0.8864
-3.000	0.9964	0.9877	0.9693	0.9626	0.9571	0.9144
-2.500	1.0005	0.9938	0.9823	0.9751	0.9704	0.9401
-2.000	1.0025	0.9978	0.9918	0.9855	0.9821	0.9631
-1.500	1.0023	0.9999	0.9978	0.9938	0.9920	0.9832
-1.000	1.0000	1.0000	1.0000	1.0000	1.0000	1.0000
-0.500	0.9955	0.9980	0.9986	1.0041	1.0061	1.0134
0.000	0.9888	0.9940	0.9935	1.0061	1.0103	1.0232
0.500	0.9801	0.9880	0.9849	1.0059	1.0124	1.0293
1.000	0.9692	0.9799	0.9729	1.0036	1.0124	1.0316
1.500	0.9564	0.9700	0.9577	0.9990	1.0104	1.0302
2.000	0.9417	0.9582	0.9395	0.9924	1.0064	1.0249
2.500	0.9252	0.9446	0.9186	0.9836	1.0003	1.0161
3.000	0.9070	0.9293	0.8952	0.9727	0.9921	1.0037
3.500	0.8873	0.9125	0.8698	0.9598	0.9821	0.9880
4.000	0.8662	0.8942	0.8424	0.9451	0.9701	0.9692

Beam areas

Measured beam areas (sq. arcsec)

$A_{beam\_sq\_arcsec\_1\_arcsec\_pix_i} :=$

426
771
1626

$A_{beam\_sq\_arcsec\_6\_10\_14\_arcsec\_pix_i} :=$

450
805
1682

Measured beam area for 1" pixels (sr)

$$Conv\_sq\_arcsec\_to\_sr := \left(\frac{2\cdot\pi}{60\cdot 60\cdot 360}\right)^2$$

$$A_{beam_i} := A_{beam\_sq\_arcsec\_1\_arcsec\_pix_i}\cdot Conv\_sq\_arcsec\_to\_sr$$

$A_{beam_i} =$

$1.001\cdot 10^{-8}$
$1.812\cdot 10^{-8}$
$3.822\cdot 10^{-8}$

$\nu o_i =$

$1.199\cdot 10^{12}$
$8.565\cdot 10^{11}$
$5.996\cdot 10^{11}$

Example extended source calibration

Define a v^3 spectrum and 100 MJy/sr intensity at 250 μm:

$$B_{source}(nu) := 100\cdot\left(\frac{nu}{\nu o_1}\right)^3$$

$B_{source}(\nu o_i) =$

100.00
36.44
12.50

Corresponding in-beam flux densities (Jy)

$$S_{source_i} := B_{source}(\nu o_i)\cdot 10^6\cdot A_{beam_i}$$

$S_{source_i} =$

1.0013
0.6604
0.4777

$S_{source1}(nu) := B_{source}(nu)\cdot 10^6\cdot A_{beam_1}$ $\qquad S_{source1}(\nu o_1) = 1.0013$

$S_{source2}(nu) := B_{source}(nu)\cdot 10^6\cdot A_{beam_2}$ $\qquad S_{source2}(\nu o_2) = 0.6604$

$S_{source3}(nu) := B_{source}(nu)\cdot 10^6\cdot A_{beam_3}$ $\qquad S_{source3}(\nu o_3) = 0.4777$

Corresponding RSRF-weighted flux densities:

$$\bar{S}_{source} = \frac{\int_{Passband} S_{source}(\nu) R(\nu)\, d\nu}{\int_{Passband} R(\nu)\, d\nu}$$

Point source:

$$SbarP_1 := \frac{\sum_{f=0}^{N-1}\left[\frac{S_{source1}(\nu_{f+1}) + S_{source1}(\nu_f)}{2}\cdot\frac{RP_1(\nu_{f+1}) + RP_1(\nu_f)}{2}\cdot(\nu_{f+1}-\nu_f)\right]}{\sum_{f=0}^{N-1}\left[\frac{RP_1(\nu_{f+1}) + RP_1(\nu_f)}{2}\cdot(\nu_{f+1}-\nu_f)\right]}$$

$SbarP_1 = 1.0916$

$$SbarP_2 := \frac{\sum_{f=0}^{N-1}\left[\frac{S_{source2}(\nu_{f+1})+S_{source2}(\nu_f)}{2}\cdot\frac{RP_2(\nu_{f+1})+RP_2(\nu_f)}{2}\cdot(\nu_{f+1}-\nu_f)\right]}{\sum_{f=0}^{N-1}\left[\frac{RP_2(\nu_{f+1})+RP_2(\nu_f)}{2}\cdot(\nu_{f+1}-\nu_f)\right]} \qquad SbarP_2 = 0.7064$$

$$SbarP_3 := \frac{\sum_{f=0}^{N-1}\left[\frac{S_{source3}(\nu_{f+1})+S_{source3}(\nu_f)}{2}\cdot\frac{RP_3(\nu_{f+1})+RP_3(\nu_f)}{2}\cdot(\nu_{f+1}-\nu_f)\right]}{\sum_{f=0}^{N-1}\left[\frac{RP_3(\nu_{f+1})+RP_3(\nu_f)}{2}\cdot(\nu_{f+1}-\nu_f)\right]} \qquad SbarP_3 = 0.5302$$

Extended source:

$$SbarE_1 := \frac{\sum_{f=0}^{N-1}\left[\frac{S_{source1}(\nu_{f+1})+S_{source1}(\nu_f)}{2}\cdot\frac{RE_1(\nu_{f+1})+RE_1(\nu_f)}{2}\cdot(\nu_{f+1}-\nu_f)\right]}{\sum_{f=0}^{N-1}\left[\frac{RE_1(\nu_{f+1})+RE_1(\nu_f)}{2}\cdot(\nu_{f+1}-\nu_f)\right]} \qquad SbarE_1 = 1.0357$$

$$SbarE_2 := \frac{\sum_{f=0}^{N-1}\left[\frac{S_{source2}(\nu_{f+1})+S_{source2}(\nu_f)}{2}\cdot\frac{RE_2(\nu_{f+1})+RE_2(\nu_f)}{2}\cdot(\nu_{f+1}-\nu_f)\right]}{\sum_{f=0}^{N-1}\left[\frac{RE_2(\nu_{f+1})+RE_2(\nu_f)}{2}\cdot(\nu_{f+1}-\nu_f)\right]} \qquad SbarE_2 = 0.6725$$

$$SbarE_3 := \frac{\sum_{f=0}^{N-1}\left[\frac{S_{source3}(\nu_{f+1})+S_{source3}(\nu_f)}{2}\cdot\frac{RE_3(\nu_{f+1})+RE_3(\nu_f)}{2}\cdot(\nu_{f+1}-\nu_f)\right]}{\sum_{f=0}^{N-1}\left[\frac{RE_3(\nu_{f+1})+RE_3(\nu_f)}{2}\cdot(\nu_{f+1}-\nu_f)\right]} \qquad SbarE_3 = 0.4870$$

Assume extended source calibration:

Correct to monochromatic flux densities assuming αs = -1 by multiplying by K4 for extended source:

$K4E_1(\alpha_{So}) = 0.9939 \qquad K4E_1(\alpha_{So})\cdot SbarE_1 = 1.0294$

$K4E_2(\alpha_{So}) = 0.9898 \qquad K4E_2(\alpha_{So})\cdot SbarE_2 = 0.6657$

$K4E_3(\alpha_{So}) = 0.9773 \qquad K4E_3(\alpha_{So})\cdot SbarE_3 = 0.4760$

Apply extended source colour correction for αs = 3

$KEc_1(3) = 0.9727 \qquad KEc_1(3)\cdot K4E_1(\alpha_{So})\cdot SbarE_1 = 1.0013$

$KEc_2(3) = 0.9921 \qquad KEc_2(3)\cdot K4E_2(\alpha_{So})\cdot SbarE_2 = 0.6604$

$KEc_3(3) = 1.0037 \qquad KEc_3(3)\cdot K4E_3(\alpha_{So})\cdot SbarE_3 = 0.4777$

Check: this recovers the correct monochromatic flux densities

$S_{source_i} =$

1.001
0.660
0.478

But the pipeline assumes point source calibration and returns the following values of Jy in beam:

$K4P_1(\alpha_{So}) = 1.0113$ $\quad K4P_1(\alpha_{So}) \cdot SbarE_1 = 1.0474$

$K4P_2(\alpha_{So}) = 1.0060$ $\quad K4P_2(\alpha_{So}) \cdot SbarE_2 = 0.6766$

$K4P_3(\alpha_{So}) = 1.0065$ $\quad K4P_3(\alpha_{So}) \cdot SbarE_3 = 0.4902$

These values are higher than the true source in-beam monochromatic flux densities by

$$\frac{K4P_1(\alpha_{So}) \cdot SbarE_1}{S_{source_1}} = 1.046 \qquad \frac{K4P_2(\alpha_{So}) \cdot SbarE_2}{S_{source_2}} = 1.024 \qquad \frac{K4P_3(\alpha_{So}) \cdot SbarE_3}{S_{source_3}} = 1.026$$

Knowing that it's an extended rather than a point source, the user corrects by multiplying by K4E/K4P:

$$\frac{K4E_1(\alpha_{So})}{K4P_1(\alpha_{So})} = 0.9828 \qquad \frac{K4E_1(\alpha_{So})}{K4P_1(\alpha_{So})} \cdot K4P_1(\alpha_{So}) \cdot SbarE_1 = 1.0294$$

$$\frac{K4E_2(\alpha_{So})}{K4P_2(\alpha_{So})} = 0.9839 \qquad \frac{K4E_2(\alpha_{So})}{K4P_2(\alpha_{So})} \cdot K4P_2(\alpha_{So}) \cdot SbarE_2 = 0.6657$$

$$\frac{K4E_3(\alpha_{So})}{K4P_3(\alpha_{So})} = 0.9710 \qquad \frac{K4E_3(\alpha_{So})}{K4P_3(\alpha_{So})} \cdot K4P_3(\alpha_{So}) \cdot SbarE_3 = 0.4760$$

These values are higher than the true source in-beam monochromatic flux densities by

$$\frac{K4E_1(\alpha_{So}) \cdot SbarE_1}{S_{source_1}} = 1.028 \qquad \frac{K4E_2(\alpha_{So}) \cdot SbarE_2}{S_{source_2}} = 1.008 \qquad \frac{K4E_3(\alpha_{So}) \cdot SbarE_3}{S_{source_3}} = 0.996$$

but are still based on an assumes nu^-1 spectrum

Now the extended source colour correction can be applied as above, returning the correct values of monochromatic flux density (Jy in beam):

$$\frac{K4E_1(\alpha_{So})}{K4P_1(\alpha_{So})} \cdot K4P_1(\alpha_{So}) \cdot SbarE_1 \cdot KEc_1(3) = 1.0013$$

$$\frac{K4E_2(\alpha_{So})}{K4P_2(\alpha_{So})} \cdot K4P_2(\alpha_{So}) \cdot SbarE_2 \cdot KEc_2(3) = 0.6604$$

$$\frac{K4E_3(\alpha_{So})}{K4P_3(\alpha_{So})} \cdot K4P_3(\alpha_{So}) \cdot SbarE_3 \cdot KEc_3(3) = 0.4777$$

What if the point source calibration and colour correction are applied incorrectly?
Then the following flux densities are derived:

$KPc_1(3) = 0.9070$ $\quad K4P_1(\alpha_{So}) \cdot KPc_1(3) = 0.9173$ $\quad K4E_1(\alpha_{So}) \cdot KEc_1(3) = 0.9668$ $\quad K4P_1(\alpha_{So}) \cdot SbarE_1 \cdot KPc_1(3) = 0.9500$

$KPc_2(3) = 0.9293$ $\quad K4P_2(\alpha_{So}) \cdot KPc_2(3) = 0.9350$ $\quad K4E_2(\alpha_{So}) \cdot KEc_2(3) = 0.9821$ $\quad K4P_2(\alpha_{So}) \cdot SbarE_2 \cdot KPc_2(3) = 0.6288$

$KPc_3(3) = 0.8952$ $\quad K4P_3(\alpha_{So}) \cdot KPc_3(3) = 0.9011$ $\quad K4E_3(\alpha_{So}) \cdot KEc_3(3) = 0.9809$ $\quad K4P_3(\alpha_{So}) \cdot SbarE_3 \cdot KPc_3(3) = 0.4389$

So this produces flux densities lower by about 5%

$$\frac{KEc_1(3)\cdot K4E_1(\alpha_{So})\cdot SbarE_1}{K4P_1(\alpha_{So})\cdot SbarE_1\cdot KPc_1(3)} = 1.054 \qquad \frac{KEc_1(3)\cdot K4E_1(\alpha_{So})}{K4P_1(\alpha_{So})\cdot KPc_1(3)} = 1.054$$

$$\frac{KEc_2(3)\cdot K4E_2(\alpha_{So})\cdot SbarE_2}{K4P_2(\alpha_{So})\cdot SbarE_2\cdot KPc_2(3)} = 1.050 \qquad \frac{KEc_2(3)\cdot K4E_2(\alpha_{So})}{K4P_2(\alpha_{So})\cdot KPc_2(3)} = 1.050$$

$$\frac{KEc_2(3)\cdot K4E_2(\alpha_{So})\cdot SbarE_2}{K4P_2(\alpha_{So})\cdot SbarE_2\cdot KPc_2(3)} = 1.050 \qquad \frac{KEc_2(3)\cdot K4E_2(\alpha_{So})}{K4P_2(\alpha_{So})\cdot KPc_2(3)} = 1.050$$

Definition of observing date

$JD\_Launch := 2454965.5$

Select observation date (range = Mar 01 2009 - Jan 01 2011) $Y \equiv 2010$ $M \equiv 4$ $D \equiv 5$

Calculate corresponding JD for 0 hrs (range = 245022 - 2455582)

$y := if(M > 2, Y, Y - 1)$ $m := if(M > 2, M, M + 12)$ $jd := floor(365.25 \cdot y) + floor[30.6001 \cdot (m + 1)] + D + 1720994.5$

$aa := floor\left(\frac{y}{100}\right)$ $bb := 2 - aa + floor\left(\frac{aa}{4}\right)$ $JD\_Selected := jd + bb$ $JD\_Selected = 2455291.5$

Calculate corresponding OD (based on 14 May 2009 = OD0)

$OD\_Selected := JD\_Selected - JD\_Launch$

$OD\_Selected = 326$

Uranus and Neptune Brightness Temperature Spectra

Modified Griffin & Orton Models

Uranus spectrum:
- **Griffin & Orton (1993) * 0.96 for λ >100 um**
- **IRIS whole disk *0.953 for λ < 100 um**

Neptune spectrum
- **Griffin & Orton (1993) for λ > 100 um**
- **Burgdorf et al. (2004) - 3.7 K for λ < 100 um**

$$\begin{pmatrix} waveno\_N \\ TBN \\ waveno\_U \\ TBU \end{pmatrix} :=$$

Worksheet

Frequency (Hz) and wavelength (μm)

$\nu\_Nep := waveno\_N \cdot 100 \cdot c$ $\nu\_Ur := waveno\_U \cdot 100 \cdot c$

$\lambda\_Nep := \frac{c \cdot 10^6}{\nu\_Nep}$ $\lambda\_Ur := \frac{c \cdot 10^6}{\nu\_Ur}$

$rows(\nu\_Nep) = 102$ $rows(\nu\_Ur) = 151$

Raphael Moreno Models (April 2009)

$$\begin{pmatrix} GHzm \\ Micronsm \\ TBUm \\ TBNm \end{pmatrix} :=$$

Worksheet

$\nu m := GHzm \cdot 10^9$ $rows(\nu m) = 4995$

Glenn Orton's Models (April 13 2009)

$$\begin{pmatrix} Waveno\_GSO\_U \\ TBU\_GSO \\ Waveno\_GSO\_N \\ TBN\_GSO \end{pmatrix} :=$$

Worksheet

$rows(Waveno\_GSO\_U) = 9955$ $rows(Waveno\_GSO\_N) = 9956$

$\nu\_U\_GSO := Waveno\_GSO\_U \cdot 100 \cdot c$ $\nu\_N\_GSO := Waveno\_GSO\_N \cdot 100 \cdot c$

$\lambda\_U\_GSO := \frac{c \cdot 10^6}{\nu\_U\_GSO}$ $\lambda\_N\_GSO := \frac{c \cdot 10^6}{\nu\_N\_GSO}$

Modified G&O

Moreno

GSO Uranus April 13

GSO Neptune April 16

$TB\_Nep(nu) := linterp(\nu\_Nep, TBN, nu)$

$TB\_Nepm(nu) := linterp(\nu m, TBNm, nu)$

$TB\_Ur(nu) := linterp(\nu\_Ur, TBU, nu)$

$TB\_Urm(nu) := linterp(\nu m, TBUm, nu)$

$TB\_U\_GSO(nu) := linterp(\nu\_U\_GSO, TBU\_GSO, nu)$

$TB\_N\_GSO(nu) := linterp(\nu\_N\_GSO, TBN\_GSO, nu)$

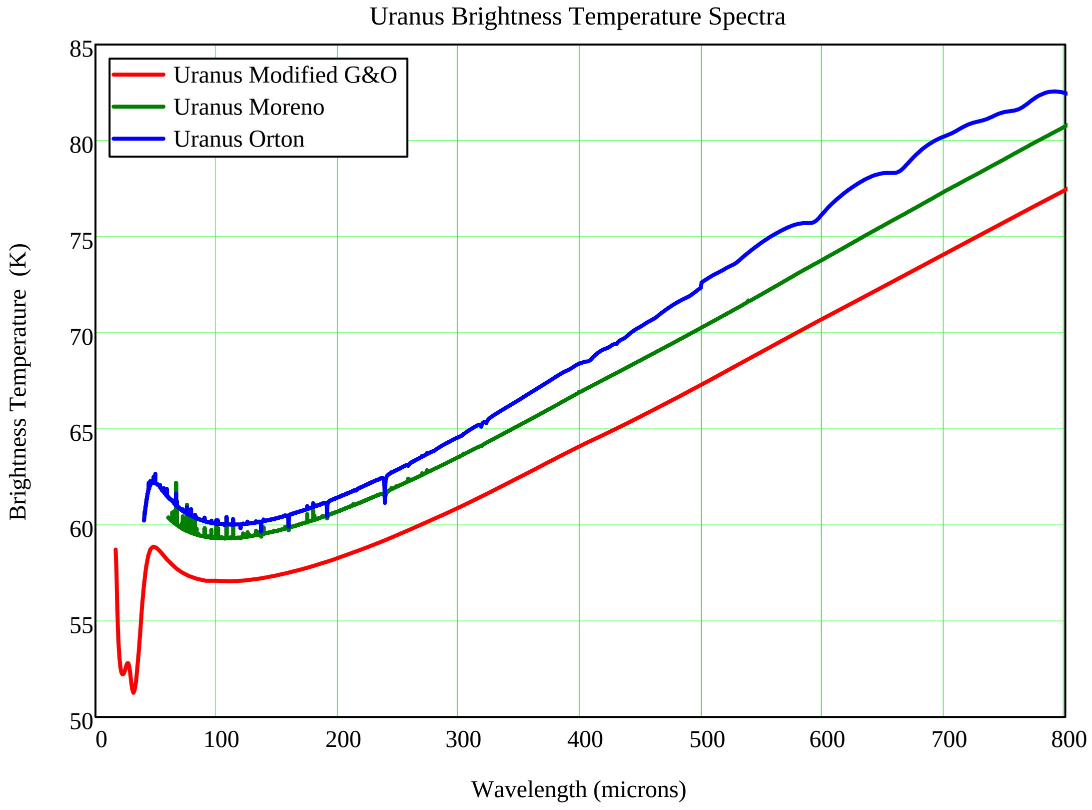

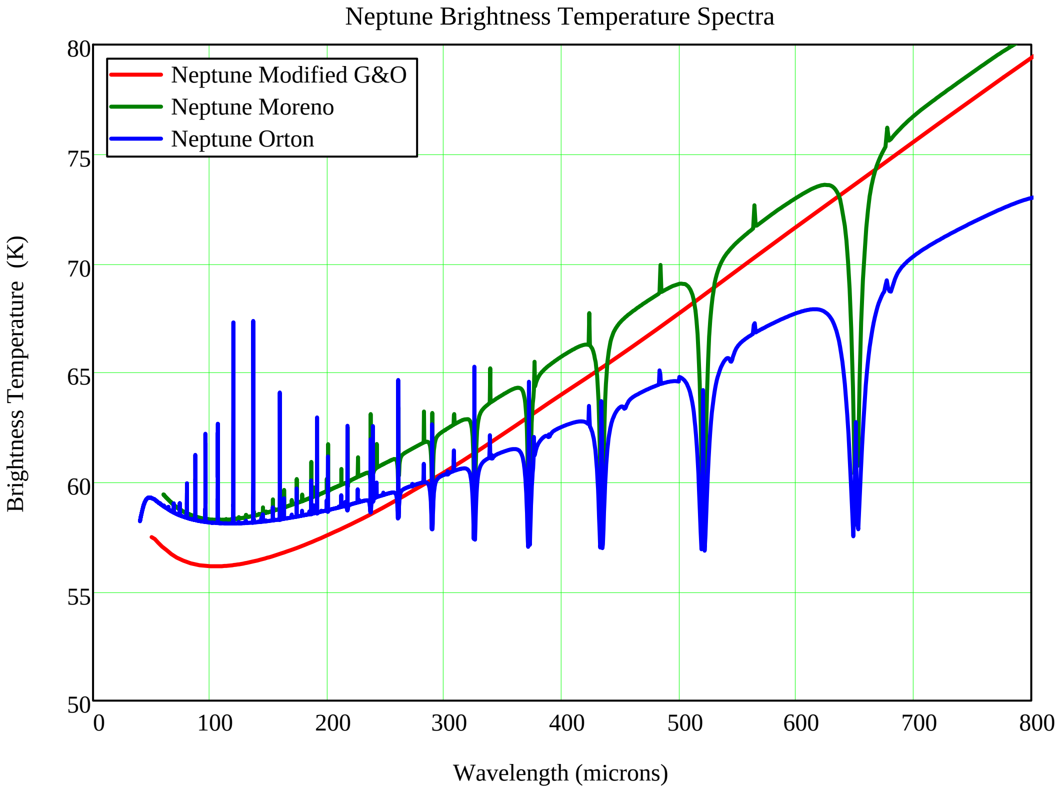

Planetary distance and size data

Year
Month
Day
Julian Date
Neptune-Herschel Distance (AU)
Neptune SEL (deg.)
Neptune eq. dia. (")
Uranus-Herschel Distance (AU)
Uranus SEL (deg.)
Uranus eq. dia. (")

$$\begin{pmatrix} Yr \\ Mo \\ Day \\ JD \\ D\_HN \\ SEL\_N \\ \theta eq\_N \\ D\_HU \\ SEL\_U \\ \theta eq\_U \end{pmatrix} :=$$

$OD := JD - JD\_Launch$

Interpolations

$D_{HN}(J\_Date) := linterp(JD, D\_HN, J\_Date)$

$D_{HU}(J\_Date) := linterp(JD, D\_HU, J\_Date)$

$SEL_N(J\_Date) := linterp(JD, SEL\_N, J\_Date)$

$SEL_U(J\_Date) := linterp(JD, SEL\_U, J\_Date)$

$\theta_{eqN}(J\_Date) := linterp(JD, \theta eq\_N, J\_Date)$

$\theta_{eqU}(J\_Date) := linterp(JD, \theta eq\_U, J\_Date)$

Values on selected date

$D_{HN}(JD\_Selected) = 30.694$

$D_{HU}(JD\_Selected) = 21.054$

$SEL_N(JD\_Selected) = -28.520$

$SEL_U(JD\_Selected) = 10.330$

$\theta_{eqN}(JD\_Selected) = 2.225$

$\theta_{eqU}(JD\_Selected) = 3.348$

Radii and ellipticities

One-bar radii (m) from Lindal et al (1987) and Lindal (1992)

$r_{Ueq} := 25559 \cdot 10^3$ $\quad r_{Neq} := 24766 \cdot 10^3$

$r_{Up} := 24973 \cdot 10^3$ $\quad r_{Np} := 24342 \cdot 10^3$

$25563 \cdot (1 - 0.024) = 24949$

$$e_U := \left(\frac{r_{Ueq}^2 - r_{Up}^2}{r_{Ueq}^2} \right)^{0.5} \qquad e_N := \left(\frac{r_{Neq}^2 - r_{Np}^2}{r_{Neq}^2} \right)^{0.5}$$

$24760 \cdot (1 - 0.021) = 24240$

$e_U = 0.2129$ $\quad e_N = 0.1842$

Disk sizes and solid angles for selected date

Neptune | **Uranus**

Seb-Earth Latitude (rad)

$\phi_N(J\_Date) := (SEL_N(J\_Date))\cdot\frac{2\cdot\pi}{360}$

$\phi_N(JD\_Selected) = -0.498$

$\phi_U(J\_Date) := (SEL_U(J\_Date))\cdot\frac{2\cdot\pi}{360}$

$\phi_U(JD\_Selected) = 0.180$

Apparent polar radius (m)

$r_{paN}(J\_Date) := r_{Neq}\cdot\left(1 - \cos(\phi_N(J\_Date))^2\cdot e_N^{\,2}\right)^{0.5}$

$r_{paN}(JD\_Selected) = 2.44393 \times 10^7$

$r_{paU}(J\_Date) := r_{Ueq}\cdot\left(1 - \cos(\phi_U(J\_Date))^2\cdot e_U^{\,2}\right)^{0.5}$

$r_{paU}(JD\_Selected) = 2.499206 \times 10^7$

Geometric mean radius (m)

$r_{Ngm}(J\_Date) := \left(r_{Neq}\cdot r_{paN}(J\_Date)\right)^{0.5}$

$r_{Ngm}(JD\_Selected) = 2.46021 \times 10^7$

$r_{Ugm}(J\_Date) := \left(r_{Ueq}\cdot r_{paU}(J\_Date)\right)^{0.5}$

$r_{Ugm}(JD\_Selected) = 2.52739 \times 10^7$

Angular radius (")

$\theta_N(J\_Date) := \frac{r_{Ngm}(J\_Date)}{D_{HN}(J\_Date)\cdot AU}\cdot\frac{360}{2\cdot\pi}\cdot 3600$

$\theta_N(JD\_Selected) = 1.105$

$\theta_U(J\_Date) := \frac{r_{Ugm}(J\_Date)}{D_{HU}(J\_Date)\cdot AU}\cdot\frac{360}{2\cdot\pi}\cdot 3600$

$\theta_U(JD\_Selected) = 1.655$

Solid angle (sr)

$\Omega_N(J\_Date) := \pi\cdot\left(\frac{r_{Ngm}(J\_Date)}{D_{HN}(J\_Date)\cdot AU}\right)^2$

$\Omega_N(JD\_Selected) = 9.018 \times 10^{-11}$

$\Omega_U(J\_Date) := \pi\cdot\left(\frac{r_{Ugm}(J\_Date)}{D_{HU}(J\_Date)\cdot AU}\right)^2$

$\Omega_U(JD\_Selected) = 2.023 \times 10^{-10}$

Check: Raphael Moreno's method:

$r_{NN\_Moreno}(J\_Date) := \left(\sin(\phi_N(J\_Date))^2\cdot r_{Neq}^{\,2} + \cos(\phi_N(J\_Date))^2\cdot r_{Np}^{\,2}\right)^{0.5}$

$r_{NU\_Moreno}(J\_Date) := \left(\sin(\phi_U(J\_Date))^2\cdot r_{Ueq}^{\,2} + \cos(\phi_U(J\_Date))^2\cdot r_{Up}^{\,2}\right)^{0.5}$

$r_{NN\_Moreno}(JD\_Selected) = 2.443931 \times 10^7$

$r_{NU\_Moreno}(JD\_Selected) = 2.499206 \times 10^7$

Beam correction factors for selected date

$d := 0, 1 .. rows(JD) - 1$

Correction factor for a disk of angular radius θ_p observed by a beam of FWHM θ_{FWHM} (the observed flux density is reduced with respect to the source flux density by this factor):

$$K_{Beam}(\theta_p, \theta_{FWHM}) := \frac{\left(1 - e^{-\frac{\theta_p^{\,2}\cdot 4\cdot\ln(2)}{\theta_{FWHM}^{\,2}}}\right)}{\frac{\theta_p^{\,2}\cdot 4\cdot\ln(2)}{\theta_{FWHM}^{\,2}}}$$

Beam FWHM (")

$\theta_{FWHM_i} :=$

18
25
36

Neptune

$K_{Beam}(\theta_N(JD\_Selected), \theta_{FWHM_i}) =$

0.995
0.997
0.999

Uranus

$K_{Beam}(\theta_U(JD\_Selected), \theta_{FWHM_i}) =$

0.988
0.994
0.997

Uranus and Neptune flux density spectra (Jy) for selected observation date

$\Omega_N(\text{JD\_Selected}) = 9.018 \times 10^{-11}$

$\text{Snu\_Nep}(nu) := B(nu, \text{TB\_Nep}(nu)) \cdot \Omega_N(\text{JD\_Selected}) \cdot 10^{26}$ **G&O**

$\text{Snu\_Nepm}(nu) := B(nu, \text{TB\_Nepm}(nu)) \cdot \Omega_N(\text{JD\_Selected}) \cdot 10^{26}$ **Moreno**

$\Omega_U(\text{JD\_Selected}) = 2.023 \times 10^{-10}$

$\text{Snu\_Ur}(nu) := B(nu, \text{TB\_Ur}(nu)) \cdot \Omega_U(\text{JD\_Selected}) \cdot 10^{26}$ **G&O**

$\text{Snu\_Urm}(nu) := B(nu, \text{TB\_Urm}(nu)) \cdot \Omega_U(\text{JD\_Selected}) \cdot 10^{26}$ **Moreno**

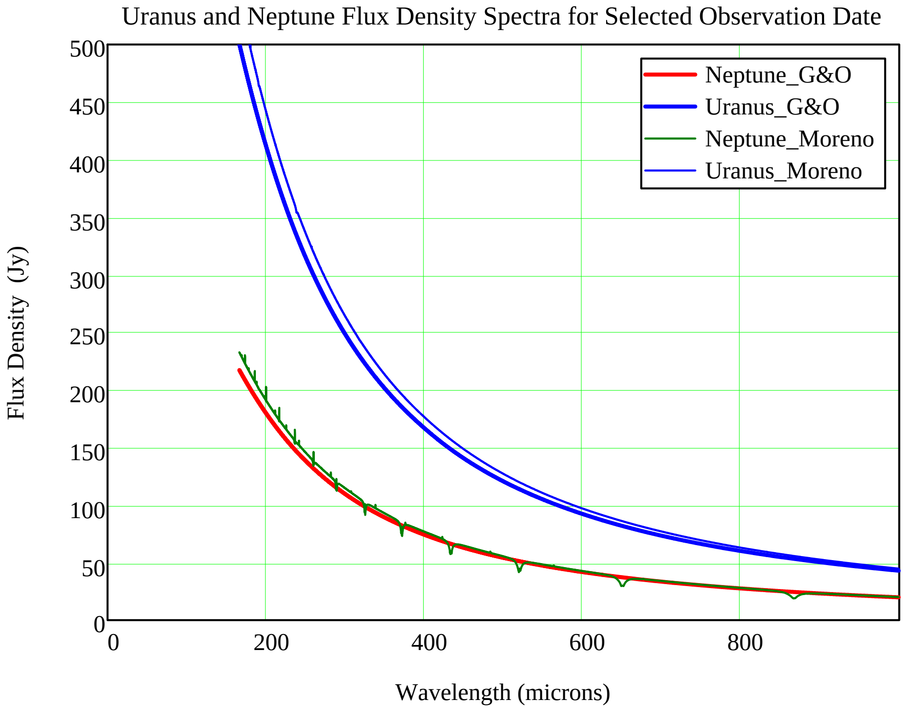

Date

$Y = 2010 \quad M = 4 \quad D = 5$

$\text{OD\_Selected} = 326$

$\text{JD\_Selected} = 2455291.5$

$\text{SUR}_n := \text{Snu\_Urm}(\nu_n)$

$\text{SNEP}_n := \text{Snu\_Nepm}(\nu_n)$

$\text{TBUR}_n := \text{TB\_Ur}(\nu_n)$

$\text{TBNEP}_n := \text{TB\_Nepm}(\nu_n)$

$\text{OD\_Selected} = 326$

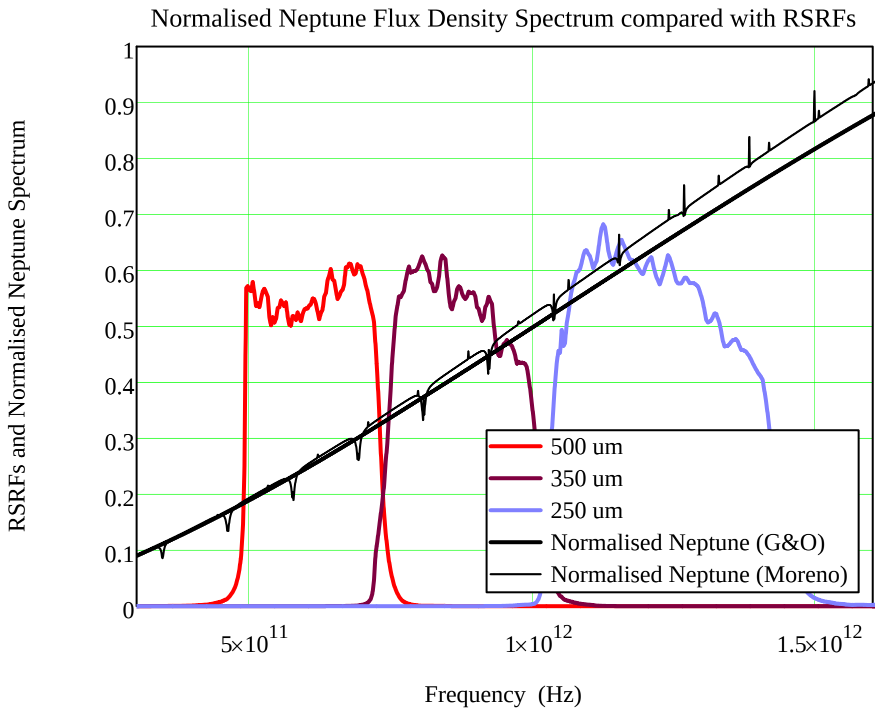

$\left(\frac{\nu}{10^9} \quad \frac{\nu}{100 \cdot c} \quad \text{SNEP} \quad \text{TBNEP} \right)$

$\left(\frac{\nu}{10^9} \quad \frac{\nu}{100 \cdot c} \quad \text{SUR} \quad \text{TBUR} \right)$

Neptune and Uranus calibration flux densities (Jy) for selected date; without correction for beam dilution

$$\bar{S}_{\mathrm{Calib}} = \frac{\int_{Passband} S_{\mathrm{C}}(\nu) R(\nu)\, d\nu}{\int_{Passband} R(\nu)\, d\nu}$$

Neptune: G&O Models

$$\mathrm{SCal\_noBCF\_NepGO}_1 := \frac{\sum_{f=0}^{N-1} \left[\frac{\mathrm{Snu\_Nep}(\nu_{f+1}) + \mathrm{Snu\_Nep}(\nu_f)}{2} \cdot \frac{\mathrm{RP}_1(\nu_{f+1}) + \mathrm{RP}_1(\nu_f)}{2} \cdot (\nu_{f+1} - \nu_f) \right]}{\sum_{f=0}^{N-1} \left[\frac{\mathrm{RP}_1(\nu_{f+1}) + \mathrm{RP}_1(\nu_f)}{2} \cdot (\nu_{f+1} - \nu_f) \right]}$$

$$\mathrm{SCal\_noBCF\_NepGO}_2 := \frac{\sum_{f=0}^{N-1} \left[\frac{\mathrm{Snu\_Nep}(\nu_{f+1}) + \mathrm{Snu\_Nep}(\nu_f)}{2} \cdot \frac{\mathrm{RP}_2(\nu_{f+1}) + \mathrm{RP}_2(\nu_f)}{2} \cdot (\nu_{f+1} - \nu_f) \right]}{\sum_{f=0}^{N-1} \left[\frac{\mathrm{RP}_2(\nu_{f+1}) + \mathrm{RP}_2(\nu_f)}{2} \cdot (\nu_{f+1} - \nu_f) \right]}$$

$$\mathrm{SCal\_noBCF\_NepGO}_3 := \frac{\sum_{f=0}^{N-1} \left[\frac{\mathrm{Snu\_Nep}(\nu_{f+1}) + \mathrm{Snu\_Nep}(\nu_f)}{2} \cdot \frac{\mathrm{RP}_3(\nu_{f+1}) + \mathrm{RP}_3(\nu_f)}{2} \cdot (\nu_{f+1} - \nu_f) \right]}{\sum_{f=0}^{N-1} \left[\frac{\mathrm{RP}_3(\nu_{f+1}) + \mathrm{RP}_3(\nu_f)}{2} \cdot (\nu_{f+1} - \nu_f) \right]}$$

Neptune: Moreno Models

$$\mathrm{SCal\_noBCF\_NepM}_1 := \frac{\sum_{f=0}^{N-1} \left[\frac{\mathrm{Snu\_Nepm}(\nu_{f+1}) + \mathrm{Snu\_Nepm}(\nu_f)}{2} \cdot \frac{\mathrm{RP}_1(\nu_{f+1}) + \mathrm{RP}_1(\nu_f)}{2} \cdot (\nu_{f+1} - \nu_f) \right]}{\sum_{f=0}^{N-1} \left[\frac{\mathrm{RP}_1(\nu_{f+1}) + \mathrm{RP}_1(\nu_f)}{2} \cdot (\nu_{f+1} - \nu_f) \right]}$$

$$\mathrm{SCal\_noBCF\_NepM}_2 := \frac{\sum_{f=0}^{N-1} \left[\frac{\mathrm{Snu\_Nepm}(\nu_{f+1}) + \mathrm{Snu\_Nepm}(\nu_f)}{2} \cdot \frac{\mathrm{RP}_2(\nu_{f+1}) + \mathrm{RP}_2(\nu_f)}{2} \cdot (\nu_{f+1} - \nu_f) \right]}{\sum_{f=0}^{N-1} \left[\frac{\mathrm{RP}_2(\nu_{f+1}) + \mathrm{RP}_2(\nu_f)}{2} \cdot (\nu_{f+1} - \nu_f) \right]}$$

$$\mathrm{SCal\_noBCF\_NepM}_3 := \frac{\sum_{f=0}^{N-1} \left[\frac{\mathrm{Snu\_Nepm}(\nu_{f+1}) + \mathrm{Snu\_Nepm}(\nu_f)}{2} \cdot \frac{\mathrm{RP}_3(\nu_{f+1}) + \mathrm{RP}_3(\nu_f)}{2} \cdot (\nu_{f+1} - \nu_f) \right]}{\sum_{f=0}^{N-1} \left[\frac{\mathrm{RP}_3(\nu_{f+1}) + \mathrm{RP}_3(\nu_f)}{2} \cdot (\nu_{f+1} - \nu_f) \right]}$$

Uranus: G&O Models

$$SCal\_noBCF\_UrGO_1 := \frac{\sum_{f=0}^{N-1}\left[\frac{Snu\_Ur(\nu_{f+1}) + Snu\_Ur(\nu_f)}{2}\cdot\frac{RP_1(\nu_{f+1}) + RP_1(\nu_f)}{2}\cdot(\nu_{f+1} - \nu_f)\right]}{\sum_{f=0}^{N-1}\left[\frac{RP_1(\nu_{f+1}) + RP_1(\nu_f)}{2}\cdot(\nu_{f+1} - \nu_f)\right]}$$

$$SCal\_noBCF\_UrGO_2 := \frac{\sum_{f=0}^{N-1}\left[\frac{Snu\_Ur(\nu_{f+1}) + Snu\_Ur(\nu_f)}{2}\cdot\frac{RP_2(\nu_{f+1}) + RP_2(\nu_f)}{2}\cdot(\nu_{f+1} - \nu_f)\right]}{\sum_{f=0}^{N-1}\left[\frac{RP_2(\nu_{f+1}) + RP_2(\nu_f)}{2}\cdot(\nu_{f+1} - \nu_f)\right]}$$

$$SCal\_noBCF\_UrGO_3 := \frac{\sum_{f=0}^{N-1}\left[\frac{Snu\_Ur(\nu_{f+1}) + Snu\_Ur(\nu_f)}{2}\cdot\frac{RP_3(\nu_{f+1}) + RP_3(\nu_f)}{2}\cdot(\nu_{f+1} - \nu_f)\right]}{\sum_{f=0}^{N-1}\left[\frac{RP_3(\nu_{f+1}) + RP_3(\nu_f)}{2}\cdot(\nu_{f+1} - \nu_f)\right]}$$

Uranus: Moreno Models

$$SCal\_noBCF\_UrM_1 := \frac{\sum_{f=0}^{N-1}\left[\frac{Snu\_Urm(\nu_{f+1}) + Snu\_Urm(\nu_f)}{2}\cdot\frac{RP_1(\nu_{f+1}) + RP_1(\nu_f)}{2}\cdot(\nu_{f+1} - \nu_f)\right]}{\sum_{f=0}^{N-1}\left[\frac{RP_1(\nu_{f+1}) + RP_1(\nu_f)}{2}\cdot(\nu_{f+1} - \nu_f)\right]}$$

$$SCal\_noBCF\_UrM_2 := \frac{\sum_{f=0}^{N-1}\left[\frac{Snu\_Urm(\nu_{f+1}) + Snu\_Urm(\nu_f)}{2}\cdot\frac{RP_2(\nu_{f+1}) + RP_2(\nu_f)}{2}\cdot(\nu_{f+1} - \nu_f)\right]}{\sum_{f=0}^{N-1}\left[\frac{RP_2(\nu_{f+1}) + RP_2(\nu_f)}{2}\cdot(\nu_{f+1} - \nu_f)\right]}$$

$$SCal\_noBCF\_UrM_3 := \frac{\sum_{f=0}^{N-1}\left[\frac{Snu\_Urm(\nu_{f+1}) + Snu\_Urm(\nu_f)}{2}\cdot\frac{RP_3(\nu_{f+1}) + RP_3(\nu_f)}{2}\cdot(\nu_{f+1} - \nu_f)\right]}{\sum_{f=0}^{N-1}\left[\frac{RP_3(\nu_{f+1}) + RP_3(\nu_f)}{2}\cdot(\nu_{f+1} - \nu_f)\right]}$$

Calibration flux densities for selected date (without beam correction)

$Y = 2010$ $M = 4$ $D = 5$ $OD\_Selected = 326$

		G&O Models	Moreno Models
Neptune	PSW	$SCal\_noBCF\_NepGO_1 = 141.7$	$SCal\_noBCF\_NepM_1 = 149.2$
	PMW	$SCal\_noBCF\_NepGO_2 = 91.05$	$SCal\_noBCF\_NepM_2 = 94.04$
	PLW	$SCal\_noBCF\_NepGO_3 = 56.00$	$SCal\_noBCF\_NepM_3 = 56.73$
Uranus	PSW	$SCal\_noBCF\_UrGO_1 = 323.2$	$SCal\_noBCF\_UrM_1 = 344.9$
	PMW	$SCal\_noBCF\_UrGO_2 = 205.6$	$SCal\_noBCF\_UrM_2 = 218.0$
	PLW	$SCal\_noBCF\_UrGO_3 = 124.8$	$SCal\_noBCF\_UrM_3 = 131.7$

Note that these values are not very different from the values at the nominal band frequencies

$Snu\_Nepm(\nu o_i) =$ $Snu\_Urm(\nu o_i) =$

$Snu\_Nepm(\nu o_i)$	$Snu\_Urm(\nu o_i)$
145.74	336.4
92.79	213.4
55.45	127.1

Beam-corrected calibration flux densities for selected date (Jy):

$Y = 2010$

$M = 4$

$D = 5$

$OD\_Selected = 326$

$$SCalib\_NepM_1 := SCal\_noBCF\_NepM_1 \cdot K_{Beam}\left(\theta_N(JD\_Selected), \theta_{FWHM_1}\right)$$

$$SCalib\_NepM_2 := SCal\_noBCF\_NepM_2 \cdot K_{Beam}\left(\theta_N(JD\_Selected), \theta_{FWHM_2}\right)$$

$$SCalib\_NepM_3 := SCal\_noBCF\_NepM_3 \cdot K_{Beam}\left(\theta_N(JD\_Selected), \theta_{FWHM_3}\right)$$

$$SCalib\_UrM_1 := SCal\_noBCF\_UrM_1 \cdot K_{Beam}\left(\theta_U(JD\_Selected), \theta_{FWHM_1}\right)$$

$$SCalib\_UrM_2 := SCal\_noBCF\_UrM_2 \cdot K_{Beam}\left(\theta_U(JD\_Selected), \theta_{FWHM_2}\right)$$

$$SCalib\_UrM_3 := SCal\_noBCF\_UrM_3 \cdot K_{Beam}\left(\theta_U(JD\_Selected), \theta_{FWHM_3}\right)$$

Neptune		Uranus	
	$SCalib\_NepM_1 = 148.5$		$SCalib\_UrM_1 = 340.9$
	$SCalib\_NepM_2 = 93.8$		$SCalib\_UrM_2 = 216.6$
	$SCalib\_NepM_3 = 56.7$		$SCalib\_UrM_3 = 131.3$

Check for consistency

Actual spectral indices for Neptune

$$\alpha Nep_i := \frac{\log\left[\frac{Snu\_Nepm\left[(1.1 \cdot \nu o)_i\right]}{Snu\_Nepm\left[(0.9 \cdot \nu o)_i\right]}\right]}{\log\left(\frac{1.1}{0.9}\right)}$$

$\alpha Nep_i =$

αNep_i
1.277
1.385
1.454

$KPc_1(\alpha Nep_1) = 0.962$ $KPc_2(\alpha Nep_1) = 0.975$ $KPc_3(\alpha Nep_1) = 0.965$

$K4P_1(-1) = 1.011$ $K4P_2(-1) = 1.006$ $K4P_3(-1) = 1.007$

Agreement not perfect - attributable to the fact that the Neptune spectrum is not a pure power law across the bands

$$\frac{SCal\_noBCF\_NepM_1 \cdot K4P_1(-1) \cdot KPc_1(\alpha Nep_1)}{Snu\_Nepm(\nu o_1)} = 0.997$$

$$\frac{SCal\_noBCF\_NepM_2 \cdot K4P_2(-1) \cdot KPc_2(\alpha Nep_2)}{Snu\_Nepm(\nu o_2)} = 0.991$$

$$\frac{SCal\_noBCF\_NepM_3 \cdot K4P_3(-1) \cdot KPc_3(\alpha Nep_3)}{Snu\_Nepm(\nu o_3)} = 0.988$$

$d := 0, 1 .. rows(JD) - 1$

Angular radius and solid angle vs. date

Year	Day	Month	Julian Date	OD	Neptune Angular Radius (")	Uranus Angular Radius (")	Neptune Solid Angle (sr)	Neptune Solid Angle (sr)
$Yr_d =$	$Day_d =$	$Mo_d =$	$JD_d =$	$OD_d =$	$\theta_N(JD_d) =$	$\theta_U(JD_d) =$	$\Omega_N(JD_d) \cdot 10^{11} =$	$\Omega_U(JD_d) \cdot 10^{10} =$
2009	1	"Jun"	2454983.5	18	1.140	1.712	9.591	2.165
2009	2	"Jun"	2454984.5	19	1.140	1.714	9.602	2.168
2009	3	"Jun"	2454985.5	20	1.141	1.715	9.612	2.172
2009	4	"Jun"	2454986.5	21	1.142	1.716	9.623	2.175
2009	5	"Jun"	2454987.5	22	1.142	1.718	9.633	2.179
2009	6	"Jun"	2454988.5	23	1.143	1.719	9.644	2.182
2009	7	"Jun"	2454989.5	24	1.143	1.721	9.654	2.186
2009	8	"Jun"	2454990.5	25	1.144	1.722	9.665	2.189
2009	9	"Jun"	2454991.5	26	1.145	1.723	9.675	2.193
2009	10	"Jun"	2454992.5	27	1.145	1.725	9.685	2.197
2009	11	"Jun"	2454993.5	28	1.146	1.726	9.695	2.200
2009	12	"Jun"	2454994.5	29	1.146	1.728	9.705	2.204
2009	13	"Jun"	2454995.5	30	1.147	1.729	9.716	2.208
2009	14	"Jun"	2454996.5	31	1.148	1.730	9.726	2.211
2009	15	"Jun"	2454997.5	32	1.148	1.732	9.736	2.215
2009	16	"Jun"	2454998.5	33	1.149	1.733	9.745	2.219
2009	17	"Jun"	2454999.5	34	1.149	1.735	9.755	2.222
2009	18	"Jun"	2455000.5	35	1.150	1.736	9.765	2.226
2009	19	"Jun"	2455001.5	36	1.151	1.738	9.775	2.230
2009	20	"Jun"	2455002.5	37	1.151	1.739	9.784	2.234
2009	21	"Jun"	2455003.5	38	1.152	1.741	9.794	2.237
2009	22	"Jun"	2455004.5	39	1.152	1.742	9.803	2.241
...	...	...	...	...	...	...	...	...

Beam correction factors vs. date

Year	Day	Julian Date	Neptune Beam Correction Factors PSW	PMW	PLW
$Yr_d =$	$Day_d =$	$JD_d =$	$K_{Beam}(\theta_N(JD_d), \theta_{FWHM_1})$	$K_{Beam}(\theta_N(JD_d), \theta_{FWHM_2})$	$K_{Beam}(\theta_N(JD_d), \theta_{FWHM_3}) =$
2009	1	2454983.5	0.994	0.997	0.999
2009	2	2454984.5	0.994	0.997	0.999
2009	3	2454985.5	0.994	0.997	0.999
2009	4	2454986.5	0.994	0.997	0.999
2009	5	2454987.5	0.994	0.997	0.999
2009	6	2454988.5	0.994	0.997	0.999
2009	7	2454989.5	0.994	0.997	0.999
2009	8	2454990.5	0.994	0.997	0.999
2009	9	2454991.5	0.994	0.997	0.999
2009	10	2454992.5	0.994	0.997	0.999
2009	11	2454993.5	0.994	0.997	0.999
2009	12	2454994.5	0.994	0.997	0.999
2009	13	2454995.5	0.994	0.997	0.999
2009	14	2454996.5	0.994	0.997	0.999
2009	15	2454997.5	0.994	0.997	0.999
2009	16	2454998.5	0.994	0.997	0.999
2009	17	2454999.5	0.994	0.997	0.999
2009	18	2455000.5	0.994	0.997	0.999
2009	19	2455001.5	0.994	0.997	0.999
2009	20	2455002.5	0.994	0.997	0.999
2009	21	2455003.5	0.994	0.997	0.999
...	...	...	...	...	...

Neptune calibration fluxes vs. date (corrected for beam dilution)

$$SCalib\_Nep\_PSW_d := SCalib\_NepM_1 \cdot \left(\frac{\Omega_N(JD_d)}{\Omega_N(JD\_Selected)} \right) \cdot \left(\frac{K_{Beam}(\theta_N(JD_d), \theta_{FWHM_1})}{K_{Beam}(\theta_N(JD\_Selected), \theta_{FWHM_1})} \right)$$

$$SCalib\_Nep\_PMW_d := SCalib\_NepM_2 \cdot \left(\frac{\Omega_N(JD_d)}{\Omega_N(JD\_Selected)} \right) \cdot \left(\frac{K_{Beam}(\theta_N(JD_d), \theta_{FWHM_2})}{K_{Beam}(\theta_N(JD\_Selected), \theta_{FWHM_2})} \right)$$

$$SCalib\_Nep\_PLW_d := SCalib\_NepM_3 \cdot \left(\frac{\Omega_N(JD_d)}{\Omega_N(JD\_Selected)} \right) \cdot \left(\frac{K_{Beam}(\theta_N(JD_d), \theta_{FWHM_3})}{K_{Beam}(\theta_N(JD\_Selected), \theta_{FWHM_3})} \right)$$

Moreno Neptune Calibration Flux Density (Jy)

Year	Day	Month	Julian Date	PSW	PMW	PLW
Yr_d =	Mo_d =	Day_d =	JD_d =	$SCalib\_Nep\_PSW_d$ =	$SCalib\_Nep\_PMW_d$ =	$SCalib\_Nep\_PLW_d$ =
2009	"Jun"	1	2454983.5	157.85	99.72	60.25
2009	"Jun"	2	2454984.5	158.02	99.83	60.32
2009	"Jun"	3	2454985.5	158.19	99.94	60.38
2009	"Jun"	4	2454986.5	158.37	100.05	60.45
2009	"Jun"	5	2454987.5	158.54	100.16	60.52
2009	"Jun"	6	2454988.5	158.71	100.27	60.58
2009	"Jun"	7	2454989.5	158.88	100.38	60.65
2009	"Jun"	8	2454990.5	159.05	100.48	60.71
2009	"Jun"	9	2454991.5	159.22	100.59	60.78
2009	"Jun"	10	2454992.5	159.39	100.70	60.84
2009	"Jun"	11	2454993.5	159.55	100.80	60.91
2009	"Jun"	12	2454994.5	159.72	100.91	60.97
2009	"Jun"	13	2454995.5	159.88	101.01	61.03
2009	"Jun"	14	2454996.5	160.05	101.12	61.10
2009	"Jun"	15	2454997.5	160.21	101.22	61.16
2009	"Jun"	16	2454998.5	160.37	101.32	61.22
2009	"Jun"	17	2454999.5	160.53	101.42	61.28
2009	"Jun"	18	2455000.5	160.69	101.52	61.34
2009	"Jun"	19	2455001.5	160.85	101.62	61.40
2009	"Jun"	20	2455002.5	161.01	101.72	61.46
2009	"Jun"	21	2455003.5	161.16	101.82	61.52
2009	"Jun"	22	2455004.5	161.31	101.92	61.58
2009	"Jun"	23	2455005.5	161.47	102.01	61.64
2009	"Jun"	24	2455006.5	161.62	102.11	61.70
2009	"Jun"	25	2455007.5	161.77	102.20	61.75
2009	"Jun"	26	2455008.5	161.91	102.30	61.81
2009	"Jun"	27	2455009.5	162.06	102.39	61.87
2009	"Jun"	28	2455010.5	162.20	102.48	61.92
2009	"Jun"	29	2455011.5	162.34	102.57	61.98
2009	"Jun"	30	2455012.5	162.48	102.66	62.03
...	...	...	...	...	...	...

Uranus calibration fluxes vs. date (corrected for beam dilution)

$$SCalib\_Ur\_PSW_d := SCalib\_UrM_1 \cdot \left(\frac{\Omega_U(JD_d)}{\Omega_U(JD\_Selected)}\right) \cdot \left(\frac{K_{Beam}(\theta_U(JD_d), \theta_{FWHM_2})}{K_{Beam}(\theta_U(JD\_Selected), \theta_{FWHM_2})}\right)$$

$$SCalib\_Ur\_PMW_d := SCalib\_UrM_2 \cdot \left(\frac{\Omega_U(JD_d)}{\Omega_U(JD\_Selected)}\right) \cdot \left(\frac{K_{Beam}(\theta_U(JD_d), \theta_{FWHM_2})}{K_{Beam}(\theta_U(JD\_Selected), \theta_{FWHM_2})}\right)$$

$$SCalib\_Ur\_PLW_d := SCalib\_UrM_3 \cdot \left(\frac{\Omega_U(JD_d)}{\Omega_U(JD\_Selected)}\right) \cdot \left(\frac{K_{Beam}(\theta_U(JD_d), \theta_{FWHM_2})}{K_{Beam}(\theta_U(JD\_Selected), \theta_{FWHM_2})}\right)$$

$SCalib\_UrM_1 = 340.885$

$OD\_Selected = 326.000$

$JD\_Selected = 2455291.50$

Moreno Uranus Calibration Flux Density (Jy)

Year	Day	Month	Julian Date	PSW	PMW	PLW
$Yr_d =$	$Mo_d =$	$Day_d =$	$JD_d =$	$SCalib\_Ur\_PSW_d =$	$SCalib\_Ur\_PMW_d =$	$SCalib\_Ur\_PLW_d =$
2009	"Jun"	1	2454983.5	364.66	231.75	140.46
2009	"Jun"	2	2454984.5	365.24	232.12	140.69
2009	"Jun"	3	2454985.5	365.82	232.48	140.91
2009	"Jun"	4	2454986.5	366.40	232.86	141.13
2009	"Jun"	5	2454987.5	366.99	233.23	141.36
2009	"Jun"	6	2454988.5	367.58	233.60	141.59
2009	"Jun"	7	2454989.5	368.17	233.98	141.82
2009	"Jun"	8	2454990.5	368.77	234.36	142.05
2009	"Jun"	9	2454991.5	369.37	234.74	142.28
2009	"Jun"	10	2454992.5	369.98	235.13	142.51
2009	"Jun"	11	2454993.5	370.58	235.51	142.74
2009	"Jun"	12	2454994.5	371.19	235.90	142.98
2009	"Jun"	13	2454995.5	371.80	236.29	143.21
2009	"Jun"	14	2454996.5	372.42	236.68	143.45
2009	"Jun"	15	2454997.5	373.03	237.07	143.69
2009	"Jun"	16	2454998.5	373.65	237.46	143.93
2009	"Jun"	17	2454999.5	374.27	237.86	144.17
2009	"Jun"	18	2455000.5	374.90	238.25	144.41
2009	"Jun"	19	2455001.5	375.52	238.65	144.65
2009	"Jun"	20	2455002.5	376.14	239.05	144.89
2009	"Jun"	21	2455003.5	376.77	239.44	145.13
2009	"Jun"	22	2455004.5	377.40	239.84	145.37
2009	"Jun"	23	2455005.5	378.02	240.24	145.61
2009	"Jun"	24	2455006.5	378.65	240.64	145.85
2009	"Jun"	25	2455007.5	379.28	241.04	146.10
2009	"Jun"	26	2455008.5	379.91	241.44	146.34
2009	"Jun"	27	2455009.5	380.54	241.84	146.58
2009	"Jun"	28	2455010.5	381.17	242.24	146.82
2009	"Jun"	29	2455011.5	381.80	242.64	147.07
2009	"Jun"	30	2455012.5	382.43	243.04	147.31
...	...	...	...	...	...	...

Tabulation of Uranus and Neptune beam-corrected calibration flux densities

(Yr   Mo   Day   OD   SCalib_Nep_PSW   SCalib_Nep_PMW   SCalib_Nep_PLW   SCalib_Ur_PSW   SCalib_Ur_PMW   SCalib_Ur_PLW

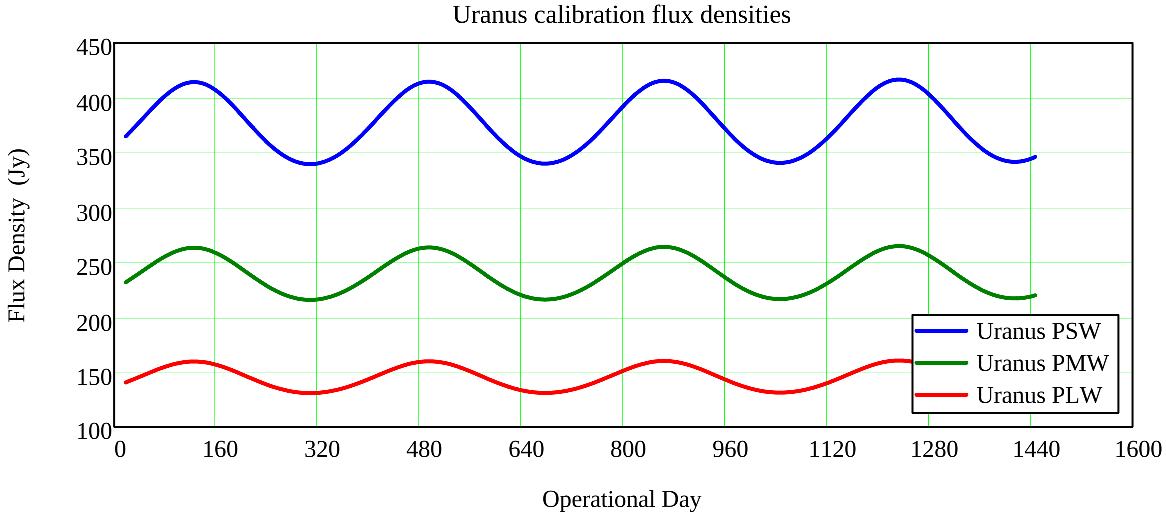

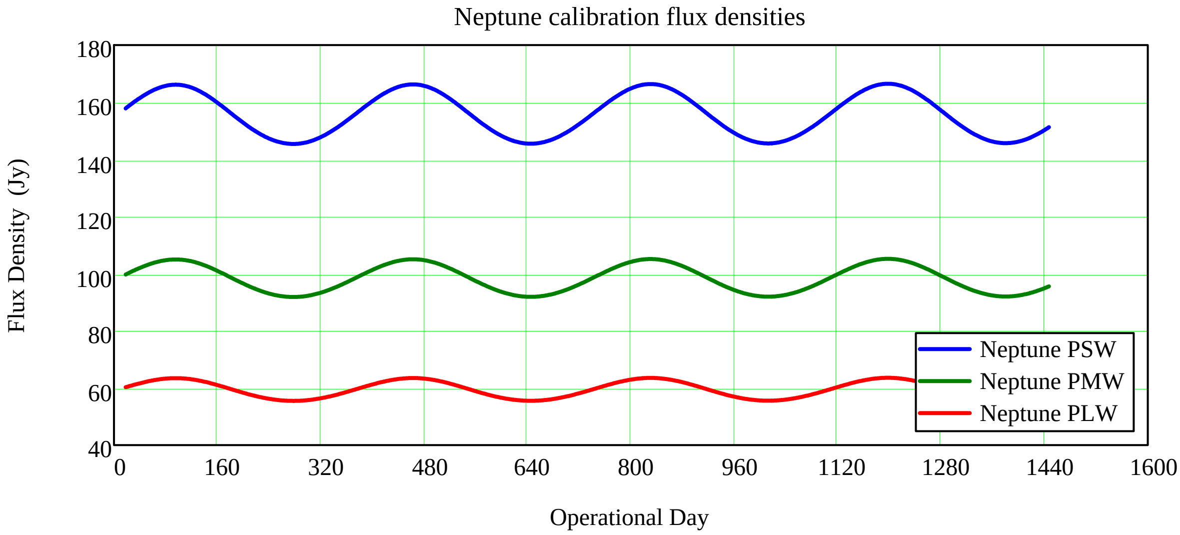

Asteroid Properties

Astrometric Data (from Thomas Mueller's ephemeris files on HCALSG wiki)

$Ceres :=$	$Pallas :=$	$Juno :=$	$Vesta :=$

pV (visual geometric albedo) and G (slope parameter) values also from Thomas Mueller

$pV_1 := 0.098$	$pV_2 := 0.152$	$pV_3 := 0.207$	$pV_4 := 0.328$
$G_1 := 0.05$	$G_2 := 0.08$	$G_3 := 0.31$	$G_4 := 0.34$
$A_1 := \left(0.29 + 0.684 \cdot G_1\right) \cdot pV_1$	$A_2 := \left(0.29 + 0.684 \cdot G_2\right) \cdot pV_2$	$A_3 := \left(0.29 + 0.684 \cdot G_3\right) \cdot pV_3$	$A_4 := \left(0.29 + 0.684 \cdot G_4\right) \cdot pV_4$
$A_1 = 0.032$	$A_2 = 0.052$	$A_3 = 0.104$	$A_4 = 0.171$
$Date_1 := Ceres^{\langle 0 \rangle}$	$Date_2 := Pallas^{\langle 0 \rangle}$	$Date_3 := Juno^{\langle 0 \rangle}$	$Date_4 := Vesta^{\langle 0 \rangle}$
$JD_1 := Ceres^{\langle 2 \rangle}$	$JD_2 := Pallas^{\langle 2 \rangle}$	$JD_3 := Juno^{\langle 2 \rangle}$	$JD_4 := Vesta^{\langle 2 \rangle}$
$DSun_1 := Ceres^{\langle 9 \rangle}$	$DSun_2 := Pallas^{\langle 9 \rangle}$	$DSun_3 := Juno^{\langle 9 \rangle}$	$DSun_4 := Vesta^{\langle 9 \rangle}$
$DL2_1 := Ceres^{\langle 11 \rangle}$	$DL2_2 := Pallas^{\langle 11 \rangle}$	$DL2_3 := Juno^{\langle 11 \rangle}$	$DL2_4 := Vesta^{\langle 11 \rangle}$
$\phi Sun_1 := Ceres^{\langle 14 \rangle}$	$\phi Sun_2 := Pallas^{\langle 14 \rangle}$	$\phi Sun_3 := Juno^{\langle 14 \rangle}$	$\phi Sun_4 := Vesta^{\langle 14 \rangle}$
$TMS70_1 := Ceres^{\langle 21 \rangle}$	$TMS70_2 := Pallas^{\langle 21 \rangle}$	$TMS70_3 := Juno^{\langle 21 \rangle}$	$TMS70_4 := Vesta^{\langle 21 \rangle}$
$TMS500_1 := Ceres^{\langle 26 \rangle}$	$TMS500_2 := Pallas^{\langle 26 \rangle}$	$TMS500_3 := Juno^{\langle 26 \rangle}$	$TMS500_4 := Vesta^{\langle 26 \rangle}$

Ceres visibility:	**Pallas visibility:**	**Juno visibility:**	**Vesta visibility:**
20 Apr - 14 July 2009	**Dec 29 2008 - May 9 2009**	**1 May - 26 July 2009**	**11 Oct - 27 Dec. 2009**
8 Feb - 25 Apr 2010	**Dec 27 2009 - Mar. 20 2010**	**14 Nov 2009 - 14 Feb 2010**	**12 Apr. 2010 - 7 July 2011**
14 Aug - 30 Oct 2010	**Jun. 14 2011 - Dec. 22 2011**	**7 Nov. 2010 - 20 Jan. 2011**	**12 Mar. 2011 - 9 June 2011**

$Hebe :=$

$pV_6 := 0.268$

$G_6 := 0.24$

$A_6 := (0.29 + 0.684 \cdot G_6) \cdot pV_6$

$A_6 = 0.122$

$Date_6 := Hebe^{\langle 0 \rangle}$

$JD_6 := Hebe^{\langle 2 \rangle}$

$DSun_6 := Hebe^{\langle 9 \rangle}$

$DL2_6 := Hebe^{\langle 11 \rangle}$

$\phi Sun_6 := Hebe^{\langle 14 \rangle}$

$TMS70_6 := Hebe^{\langle 21 \rangle}$

$TMS500_6 := Hebe^{\langle 26 \rangle}$

$Flora :=$

$pV_8 := 0.243$

$G_8 := 0.280$

$A_8 := (0.29 + 0.684 \cdot G_8) \cdot pV_8$

$A_8 = 0.117$

$Date_8 := Flora^{\langle 0 \rangle}$

$JD_8 := Flora^{\langle 2 \rangle}$

$DSun_8 := Flora^{\langle 9 \rangle}$

$DL2_8 := Flora^{\langle 11 \rangle}$

$\phi Sun_8 := Flora^{\langle 14 \rangle}$

$TMS70_8 := Flora^{\langle 21 \rangle}$

$TMS500_8 := Flora^{\langle 26 \rangle}$

$Fortuna :=$

$pV_{19} := 0.037$

$G_{19} := 0.100$

$A_{19} := (0.29 + 0.684 \cdot G_{19}) \cdot pV_{19}$

$A_{19} = 0.013$

$Date_{19} := Fortuna^{\langle 0 \rangle}$

$JD_{19} := Fortuna^{\langle 2 \rangle}$

$DSun_{19} := Fortuna^{\langle 9 \rangle}$

$DL2_{19} := Fortuna^{\langle 11 \rangle}$

$\phi Sun_{19} := Fortuna^{\langle 14 \rangle}$

$TMS70_{19} := Fortuna^{\langle 21 \rangle}$

$TMS500_{19} := Fortuna^{\langle 26 \rangle}$

$Euphrosyne :=$

$pV_{31} := 0.054$

$G_{31} := 0.150$

$A_{31} := (0.29 + 0.684 \cdot G_{31}) \cdot pV_{31}$

$A_{31} = 0.021$

$Date_{31} := Euphrosyne^{\langle 0 \rangle}$

$JD_{31} := Euphrosyne^{\langle 2 \rangle}$

$DSun_{31} := Euphrosyne^{\langle 9 \rangle}$

$DL2_{31} := Euphrosyne^{\langle 11 \rangle}$

$\phi Sun_{31} := Euphrosyne^{\langle 14 \rangle}$

$TMS70_{31} := Euphrosyne^{\langle 21 \rangle}$

$TMS500_{31} := Euphrosyne^{\langle 26 \rangle}$

$Europa :=$

$pV_{52} := 0.0578$

$G_{52} := 0.180$

$A_{52} := (0.29 + 0.684 \cdot G_{52}) \cdot pV_{52}$

$A_{52} = 0.024$

$Date_{52} := Europa^{\langle 0 \rangle}$

$JD_{52} := Europa^{\langle 2 \rangle}$

$DSun_{52} := Europa^{\langle 9 \rangle}$

$DL2_{52} := Europa^{\langle 11 \rangle}$

$\phi Sun_{52} := Europa^{\langle 14 \rangle}$

$TMS70_{52} := Europa^{\langle 21 \rangle}$

$TMS500_{52} := Europa^{\langle 26 \rangle}$

Calculate array index for selected JD

$jj := 0 .. rows(JD_1) - 1$

$JDind_{jj} := \left(if \left(\left| {JD_1}_{jj} - JD\_Selected \right| \le 0.1, jj, 0 \right) \right)$

$jd := max(JDind)$

$jd = 520$

Asteroid Standard Thermal Model

$JD_{1_{jd}} = 2455291.5$ $\quad Date_{1_{jd}} = $ "2010-Apr-05"

Astronomical unit: $AU := 1.4959787 \cdot 10^{11}$ **m** $\quad$ **Solar luminosity** $Lsun := 3.86 \cdot 10^{26}$ **W**

Solar constant (1 AU) $So := 1.367 \cdot 10^{3}$ **W m-2** $\quad$ **Phase angle factor** $\beta e := 0.01$ **Mag/deg**

	1 Ceres	**2 Pallas**
Radius (m):	$Rast_1 := 476.2 \cdot 10^3$	$Rast_2 := 266.0 \cdot 10^3$
Emissivity:	$\varepsilon_1 := 0.9$	$\varepsilon_2 := 0.9$
Bond albedo:	$A_1 = 0.032$	$A_2 = 0.052$
Beaming factor:	$\beta := 0.76$	$\beta := 0.76$

Parameters for observing date

Solar distance (AU):	$DSun_{1_{jd}} = 2.78273$	$DSun_{2_{jd}} = 2.72831$
L2 distance (AU):	$DL2_{1_{jd}} = 2.39216$	$DL2_{2_{jd}} = 1.96694$
Phase angle (deg):	$\phi Sun_{1_{jd}} = 20.8116$	$\phi Sun_{2_{jd}} = 16.4896$

Angular radius (rad.)

$$\theta ast_1 := \frac{Rast_1}{DL2_{1_{jd}} \cdot AU} \qquad \theta ast_1 = 1.331 \times 10^{-6} \qquad \theta ast_2 := \frac{Rast_2}{DL2_{2_{jd}} \cdot AU} \qquad \theta ast_2 = 9.03994 \times 10^{-7}$$

Angular radius ('')

$$rast_1 := \theta ast_1 \cdot \frac{360 \cdot 3600}{2 \cdot \pi} \qquad rast_1 = 0.274 \qquad rast_2 := \theta ast_2 \cdot \frac{360 \cdot 3600}{2 \cdot \pi} \qquad rast_2 = 0.186$$

Phase angle factor:

$$\Delta M_1 := \beta e \cdot \left| \phi Sun_{1_{jd}} \right| \qquad \Delta M_2 := \beta e \cdot \left| \phi Sun_{2_{jd}} \right|$$

$$Fcorr_1 := 10^{(-\Delta M_1 \cdot 0.4)} \qquad Fcorr_1 = 0.826 \qquad Fcorr_2 := 10^{(-\Delta M_2 \cdot 0.4)} \qquad Fcorr_2 = 0.859$$

Solar flux (W m-2)

$$S_1 := So \cdot \left(DSun_{1_{jd}}\right)^{-2} \qquad S_1 = 176.533 \qquad S_2 := So \cdot \left(DSun_{2_{jd}}\right)^{-2} \qquad S_2 = 183.646$$

Sub-solar temp. (K)

$$Tss_1 := \left[\frac{(1 - A_1) \cdot S_1}{\beta \cdot \varepsilon_1 \cdot \sigma}\right]^{0.25} \qquad Tss_1 = 257.65 \qquad Tss_2 := \left[\frac{(1 - A_2) \cdot S_2}{\beta \cdot \varepsilon_2 \cdot \sigma}\right]^{0.25} \qquad Tss_2 = 258.81$$

Temp. at radius r (K)

$$T_1(\theta) := \left[1 - \left(\frac{\theta}{\theta ast_1}\right)^2\right]^{0.125} \cdot Tss_1 \qquad T_2(\theta) := \left[1 - \left(\frac{\theta}{\theta ast_2}\right)^2\right]^{0.125} \cdot Tss_2$$

Surface brightness as f(radius):

$$Br_1(\theta, nu) := \frac{2 \cdot h \cdot nu^3}{c^2 \cdot \left(\exp\left(\frac{h \cdot nu}{kb \cdot T_1(\theta)}\right) - 1\right)} \qquad Br_2(\theta, nu) := \frac{2 \cdot h \cdot nu^3}{c^2 \cdot \left(\exp\left(\frac{h \cdot nu}{kb \cdot T_2(\theta)}\right) - 1\right)}$$

Observed spectrum:

$$Snu_1(nu) := \left(10^{26}\right) \cdot 2 \cdot \pi \cdot \varepsilon_1 \cdot Fcorr_1 \cdot \int_0^{\theta ast_1} Br_1(\theta, nu) \cdot \theta \, d\theta \qquad Snu_2(nu) := \left(10^{26}\right) \cdot 2 \cdot \pi \cdot \varepsilon_2 \cdot Fcorr_2 \cdot \int_0^{\theta ast_2} Br_2(\theta, nu) \cdot \theta \, d\theta$$

Flux density (Jy) vs. λ in µm:

$$Snu_{1\lambda}(lam) := Snu_1\left(\frac{c}{lam \cdot 10^{-6}}\right) \qquad Snu_{2\lambda}(lam) := Snu_2\left(\frac{c}{lam \cdot 10^{-6}}\right)$$

$Snu_{1\lambda}(150) = 93.57$ $\quad Snu_{1\lambda}(500) = 9.813$ $\quad Snu_{2\lambda}(70) = 159.53$ $\quad Snu_{2\lambda}(500) = 4.735$

TM $\quad TMS70_{1_{jd}} = 330.359$ $\quad TMS500_{1_{jd}} = 9.822$ $\quad TMS70_{2_{jd}} = 159.505$ $\quad TMS500_{2_{jd}} = 4.735$

3 Juno

$Rast_3 := 116.95 \cdot 10^3$

$\varepsilon_3 := 0.9$

$A_3 = 0.104$

$\beta := 0.76$

$DSun_{3_{jd}} = 1.99961$

$DL2_{3_{jd}} = 2.68963$

$\phi Sun_{3_{jd}} = 18.3118$

$\theta ast_3 := \dfrac{Rast_3}{DL2_{3_{jd}} \cdot AU}$ $\qquad \theta ast_3 = 2.907 \times 10^{-7}$

$rast_3 := \theta ast_3 \cdot \dfrac{360 \cdot 3600}{2 \cdot \pi}$ $\qquad rast_3 = 0.060$

$\Delta M_3 := \beta e \cdot \left| \phi Sun_{3_{jd}} \right|$

$Fcorr_3 := 10^{(-\Delta M_3 \cdot 0.4)}$ $\qquad Fcorr_3 = 0.845$

$S_3 := So \cdot \left(DSun_{3_{jd}} \right)^{-2}$ $\qquad S_3 = 341.882$

$Tss_3 := \left[\dfrac{(1 - A_3) \cdot S_3}{\beta \cdot \varepsilon_3 \cdot \sigma} \right]^{0.25}$ $\qquad Tss_3 = 298.12$

$$T_3(\theta) := \left[1 - \left(\frac{\theta}{\theta ast_3} \right)^2 \right]^{0.125} \cdot Tss_3$$

$$Br_3(\theta, nu) := \frac{2 \cdot h \cdot nu^3}{c^2 \cdot \left(\exp\left(\frac{h \cdot nu}{kb \cdot T_3(\theta)} \right) - 1 \right)}$$

$$Snu_3(nu) := \left(10^{26}\right) \cdot 2 \cdot \pi \cdot \varepsilon_3 \cdot Fcorr_3 \cdot \int_0^{\theta ast_3} Br_3(\theta, nu) \cdot \theta \, d\theta$$

$$Snu_{3\lambda}(lam) := Snu_3\left(\frac{c}{lam \cdot 10^{-6}} \right)$$

$Snu_{3\lambda}(70) = 19.97$ $\qquad Snu_{3\lambda}(500) = 0.559$

$TMS70_{3_{jd}} = 19.869$ $\qquad TMS500_{3_{jd}} = 0.557$

4 Vesta

$Rast_4 := 265.00 \cdot 10^3$

$\varepsilon_4 := 0.9$

$A_4 = 0.171$

$\beta := 0.76$

$DSun_{4_{jd}} = 2.35051$

$DL2_{4_{jd}} = 1.61281$

$\phi Sun_{4_{jd}} = 20.4173$

$\theta ast_4 := \dfrac{Rast_4}{DL2_{4_{jd}} \cdot AU}$ $\qquad \theta ast_4 = 1.098 \times 10^{-6}$

$rast_4 := \theta ast_4 \cdot \dfrac{360 \cdot 3600}{2 \cdot \pi}$ $\qquad rast_4 = 0.227$

$\Delta M_4 := \beta e \cdot \left| \phi Sun_{4_{jd}} \right|$

$Fcorr_4 := 10^{(-\Delta M_4 \cdot 0.4)}$ $\qquad Fcorr_4 = 0.829$

$S_4 := So \cdot \left(DSun_{4_{jd}} \right)^{-2}$ $\qquad S_4 = 247.426$

$Tss_4 := \left[\dfrac{(1 - A_4) \cdot S_4}{\beta \cdot \varepsilon_4 \cdot \sigma} \right]^{0.25}$ $\qquad Tss_4 = 269.64$

$$T_4(\theta) := \left[1 - \left(\frac{\theta}{\theta ast_4} \right)^2 \right]^{0.125} \cdot Tss_4$$

$$Br_4(\theta, nu) := \frac{2 \cdot h \cdot nu^3}{c^2 \cdot \left(\exp\left(\frac{h \cdot nu}{kb \cdot T_4(\theta)} \right) - 1 \right)}$$

$$Snu_4(nu) := \left(10^{26}\right) \cdot 2 \cdot \pi \cdot \varepsilon_4 \cdot Fcorr_4 \cdot \int_0^{\theta ast_4} Br_4(\theta, nu) \cdot \theta \, d\theta$$

$$Snu_{4\lambda}(lam) := Snu_4\left(\frac{c}{lam \cdot 10^{-6}} \right)$$

$Snu_{4\lambda}(70) = 241.51$ $\qquad Snu_{4\lambda}(500) = 7.042$

$TMS70_{4_{jd}} = 237.178$ $\qquad TMS500_{4_{jd}} = 6.952$

6 Hebe

$Rast_6 := 92.6\cdot 10^3$

$\varepsilon_6 := 0.9$

$A_6 = 0.122$

$\beta := 0.76$

$DSun6_{jd} = 2.23669$

$DL2_{6_{jd}} = 2.68280$

$\phi Sun_{6_{jd}} = 21.3271$

$\theta ast_6 := \dfrac{Rast_6}{DL2_{6_{jd}}\cdot AU}$ $\quad \theta ast_6 = 2.307\times 10^{-7}$

$rast_6 := \theta ast_6\cdot \dfrac{360\cdot 3600}{2\cdot\pi}$ $\quad rast_6 = 0.048$

$\Delta M_6 := \beta e\cdot \left|\phi Sun_{6_{jd}}\right|$

$Fcorr_6 := 10^{(-\Delta M_6\cdot 0.4)}$ $\quad Fcorr_6 = 0.822$

$S_6 := So\cdot\left(DSun_{6_{jd}}\right)^{-2}$ $\quad S_6 = 273.249$

$Tss_6 := \left[\dfrac{(1-A_6)\cdot S_6}{\beta\cdot\varepsilon_6\cdot\sigma}\right]^{0.25}$ $\quad Tss_6 = 280.47$

$T_6(\theta) := \left[1-\left(\dfrac{\theta}{\theta ast_6}\right)^2\right]^{0.125}\cdot Tss_6$

$Br_6(\theta,nu) := \dfrac{2\cdot h\cdot nu^3}{c^2\cdot\left(\exp\left(\dfrac{h\cdot nu}{kb\cdot T_6(\theta)}\right)-1\right)}$

$Snu_6(nu) := \left(10^{26}\right)\cdot 2\cdot\pi\cdot\varepsilon_6\cdot Fcorr_6\cdot\int_0^{\theta ast_6} Br_6(\theta,nu)\cdot\theta\, d\theta$

$Snu_{6\lambda}(lam) := Snu_6\left(\dfrac{c}{lam\cdot 10^{-6}}\right)$

$Snu_{6\lambda}(70) = 11.20$ $\quad Snu_{6\lambda}(500) = 0.321$

$TMS70_{6_{jd}} = 11.222$ $\quad TMS500_{6_{jd}} = 0.322$

8 Flora

$Rast_8 := 67.950\cdot 10^3$

$\varepsilon_8 := 0.9$

$A_8 = 0.117$

$\beta := 0.76$

$DSun_{8_{jd}} = 2.21719$

$DL2_{8_{jd}} = 2.58625$

$\phi Sun_{8_{jd}} = 22.6523$

$\theta ast_8 := \dfrac{Rast_8}{DL2_{8_{jd}}\cdot AU}$ $\quad \theta ast_8 = 1.756\times 10^{-7}$

$rast_8 := \theta ast_8\cdot \dfrac{360\cdot 3600}{2\cdot\pi}$ $\quad rast_8 = 0.036$

$\Delta M_8 := \beta e\cdot \left|\phi Sun_{8_{jd}}\right|$

$Fcorr_8 := 10^{(-\Delta M_8\cdot 0.4)}$ $\quad Fcorr_8 = 0.812$

$S_8 := So\cdot\left(DSun_{8_{jd}}\right)^{-2}$ $\quad S_8 = 278.075$

$Tss_8 := \left[\dfrac{(1-A_8)\cdot S_8}{\beta\cdot\varepsilon_8\cdot\sigma}\right]^{0.25}$ $\quad Tss_8 = 282.07$

$T_8(\theta) := \left[1-\left(\dfrac{\theta}{\theta ast_8}\right)^2\right]^{0.125}\cdot Tss_8$

$Br_8(\theta,nu) := \dfrac{2\cdot h\cdot nu^3}{c^2\cdot\left(\exp\left(\dfrac{h\cdot nu}{kb\cdot T_8(\theta)}\right)-1\right)}$

$Snu_8(nu) := \left(10^{26}\right)\cdot 2\cdot\pi\cdot\varepsilon_8\cdot Fcorr_8\cdot\int_0^{\theta ast_8} Br_8(\theta,nu)\cdot\theta\, d\theta$

$Snu_{8\lambda}(lam) := Snu_8\left(\dfrac{c}{lam\cdot 10^{-6}}\right)$

$Snu_{8\lambda}(70) = 6.47$ $\quad Snu_{8\lambda}(500) = 0.185$

$TMS70_{8_{jd}} = 6.478$ $\quad TMS500_{8_{jd}} = 0.185$

19 Fortuna

$Rast_{19} := 100.00 \cdot 10^{3}$

$\varepsilon_{19} := 0.9$

$A_{19} = 0.013$

$\beta := 0.76$

$DSun_{19_{jd}} = 2.31861$

$DL2_{19_{jd}} = 2.38949$

$\phi Sun_{19_{jd}} = 24.7228$

$\theta ast_{19} := \dfrac{Rast_{19}}{DL2_{19_{jd}} \cdot AU} \qquad \theta ast_{19} = 2.797 \times 10^{-7}$

$rast_{19} := \theta ast_{19} \cdot \dfrac{360 \cdot 3600}{2 \cdot \pi} \qquad rast_{19} = 0.058$

$\Delta M_{19} := \beta e \cdot \left| \phi Sun_{19_{jd}} \right|$

$Fcorr_{19} := 10^{\left(-\Delta M_{19} \cdot 0.4\right)} \qquad Fcorr_{19} = 0.796$

$S_{19} := So \cdot \left(DSun_{19_{jd}}\right)^{-2} \qquad S_{19} = 254.281$

$Tss_{19} := \left[\dfrac{\left(1 - A_{19}\right) \cdot S_{19}}{\beta \cdot \varepsilon_{19} \cdot \sigma}\right]^{0.25} \qquad Tss_{19} = 283.6$

$T_{19}(\theta) := \left[1 - \left(\dfrac{\theta}{\theta ast_{19}}\right)^{2}\right]^{0.125} \cdot Tss_{19}$

$Br_{19}(\theta, nu) := \dfrac{2 \cdot h \cdot nu^{3}}{c^{2} \cdot \left(\exp\left(\dfrac{h \cdot nu}{kb \cdot T_{19}(\theta)}\right) - 1\right)}$

$Snu_{19}(nu) := \left(10^{26}\right) \cdot 2 \cdot \pi \cdot \varepsilon_{19} \cdot Fcorr_{19} \cdot \int_{0}^{\theta ast_{19}} Br_{19}(\theta, nu) \cdot \theta \, d\theta$

$Snu_{19\lambda}(lam) := Snu_{19}\left(\dfrac{c}{lam \cdot 10^{-6}}\right)$

$Snu_{19\lambda}(70) = 16.22 \qquad Snu_{19\lambda}(500) = 0.463$

$TMS70_{19_{jd}} = 16.251 \qquad TMS500_{19_{jd}} = 0.464$

31 Euphrosyne

$Rast_{31} := 127.95 \cdot 10^{3}$

$\varepsilon_{31} := 0.9$

$A_{31} = 0.021$

$\beta := 0.76$

$DSun_{31_{jd}} = 3.71494$

$DL2_{31_{jd}} = 4.11350$

$\phi Sun_{31_{jd}} = 13.6401$

$\theta ast_{31} := \dfrac{Rast_{31}}{DL2_{31_{jd}} \cdot AU} \qquad \theta ast_{31} = 2.079 \times 10^{-7}$

$rast_{31} := \theta ast_{31} \cdot \dfrac{360 \cdot 3600}{2 \cdot \pi} \qquad rast_{31} = 0.043$

$\Delta M_{31} := \beta e \cdot \left| \phi Sun_{31_{jd}} \right|$

$Fcorr_{31} := 10^{\left(-\Delta M_{31} \cdot 0.4\right)} \qquad Fcorr_{31} = 0.882$

$S_{31} := So \cdot \left(DSun_{31_{jd}}\right)^{-2} \qquad S_{31} = 99.052$

$Tss_{31} := \left[\dfrac{\left(1 - A_{31}\right) \cdot S_{31}}{\beta \cdot \varepsilon_{31} \cdot \sigma}\right]^{0.25} \qquad Tss_{31} = 223.6$

$T_{31}(\theta) := \left[1 - \left(\dfrac{\theta}{\theta ast_{31}}\right)^{2}\right]^{0.125} \cdot Tss_{31}$

$Br_{31}(\theta, nu) := \dfrac{2 \cdot h \cdot nu^{3}}{c^{2} \cdot \left(\exp\left(\dfrac{h \cdot nu}{kb \cdot T_{31}(\theta)}\right) - 1\right)}$

$Snu_{31}(nu) := \left(10^{26}\right) \cdot 2 \cdot \pi \cdot \varepsilon_{31} \cdot Fcorr_{31} \cdot \int_{0}^{\theta ast_{31}} Br_{31}(\theta, nu) \cdot \theta \, d\theta$

$Snu_{31\lambda}(lam) := Snu_{31}\left(\dfrac{c}{lam \cdot 10^{-6}}\right)$

$Snu_{31\lambda}(70) = 6.90 \qquad Snu_{31\lambda}(500) = 0.220$

$TMS70_{31_{jd}} = 6.918 \qquad TMS500_{31_{jd}} = 0.220$

52 Europa

$$Rast_{52} := 151.25 \cdot 10^{3}$$

$$\varepsilon_{52} := 0.9$$

$$A_{52} = 0.024$$

$$\beta := 0.76$$

$$\begin{pmatrix} \dfrac{\nu}{10^{9}} & \dfrac{\nu}{100 \cdot c} & SNEP & TBNEP \end{pmatrix}$$

$$DSun_{52_{jd}} = 2.76745$$

$$DL2_{52_{jd}} = 2.85460$$

$$\phi Sun_{52_{jd}} = 20.6286$$

$$\theta ast_{52} := \frac{Rast_{52}}{DL2_{52_{jd}} \cdot AU} \qquad \theta ast_{52} = 3.542 \times 10^{-7}$$

$$rast_{52} := \theta ast_{52} \cdot \frac{360 \cdot 3600}{2 \cdot \pi} \qquad rast_{52} = 0.073$$

$$\Delta M_{52} := \beta e \cdot \left| \phi Sun_{52_{jd}} \right|$$

$$Fcorr_{52} := 10^{\left(-\Delta M_{52} \cdot 0.4\right)} \qquad Fcorr_{52} = 0.827$$

$$S_{52} := So \cdot \left(DSun_{52_{jd}}\right)^{-2} \qquad S_{52} = 178.487$$

$$Tss_{52} := \left[\frac{\left(1 - A_{52}\right) \cdot S_{52}}{\beta \cdot \varepsilon_{52} \cdot \sigma}\right]^{0.25} \qquad Tss_{52} = 258.89$$

$$T_{52}(\theta) := \left[1 - \left(\frac{\theta}{\theta ast_{52}}\right)^{2}\right]^{0.125} \cdot Tss_{52}$$

$$Br_{52}(\theta, nu) := \frac{2 \cdot h \cdot nu^{3}}{c^{2} \cdot \left(\exp\left(\frac{h \cdot nu}{kb \cdot T_{52}(\theta)}\right) - 1\right)}$$

$$Snu_{52}(nu) := \left(10^{26}\right) \cdot 2 \cdot \pi \cdot \varepsilon_{52} \cdot Fcorr_{52} \cdot \int_{0}^{\theta ast_{52}} Br_{52}(\theta, nu) \cdot \theta \, d\theta$$

$$Snu_{52\lambda}(lam) := Snu_{52}\left(\frac{c}{lam \cdot 10^{-6}}\right)$$

$$Snu_{52\lambda}(70) = 23.58 \qquad Snu_{52\lambda}(500) = 0.700$$

$$TMS70_{52_{jd}} = 23.632 \qquad TMS500_{52_{jd}} = 0.701$$

Asteroid monochromatic flux densities and spectra for selected date

$Snu_{1\lambda}(250) = 36.8$ $Snu_{1\lambda}(350) = 19.48$ $Snu_{1\lambda}(500) = 9.81$

$Snu_{2\lambda}(250) = 17.8$ $Snu_{2\lambda}(350) = 9.40$ $Snu_{2\lambda}(500) = 4.74$

$Snu_{3\lambda}(250) = 2.1$ $Snu_{3\lambda}(350) = 1.11$ $Snu_{3\lambda}(500) = 0.56$

$Snu_{4\lambda}(250) = 26.5$ $Snu_{4\lambda}(350) = 14.00$ $Snu_{4\lambda}(500) = 7.04$

$Snu_{6\lambda}(250) = 1.21$ $Snu_{6\lambda}(350) = 0.64$ $Snu_{6\lambda}(500) = 0.32$

$Snu_{8\lambda}(250) = 0.70$ $Snu_{8\lambda}(350) = 0.37$ $Snu_{8\lambda}(500) = 0.19$

$Snu_{19\lambda}(250) = 1.75$ $Snu_{19\lambda}(350) = 0.92$ $Snu_{19\lambda}(500) = 0.46$

$Snu_{31\lambda}(250) = 0.82$ $Snu_{31\lambda}(350) = 0.43$ $Snu_{31\lambda}(500) = 0.22$

$Snu_{52\lambda}(250) = 2.6$ $Snu_{52\lambda}(350) = 1.39$ $Snu_{52\lambda}(500) = 0.70$

$$\frac{Snu_{1\lambda}(250)}{Snu_{1\lambda}(500)} = 3.749$$

$$\frac{Snu_{31\lambda}(250)}{Snu_{31\lambda}(500)} = 3.711$$

$$\frac{Snu_{19\lambda}(250)}{Snu_{19\lambda}(500)} = 3.772$$

$$\frac{Snu_{52\lambda}(250)}{Snu_{52\lambda}(500)} = 3.751$$

Y = 2010 M = 4 D = 5 JD_Selected = 2455291.5 OD_Selected = 326

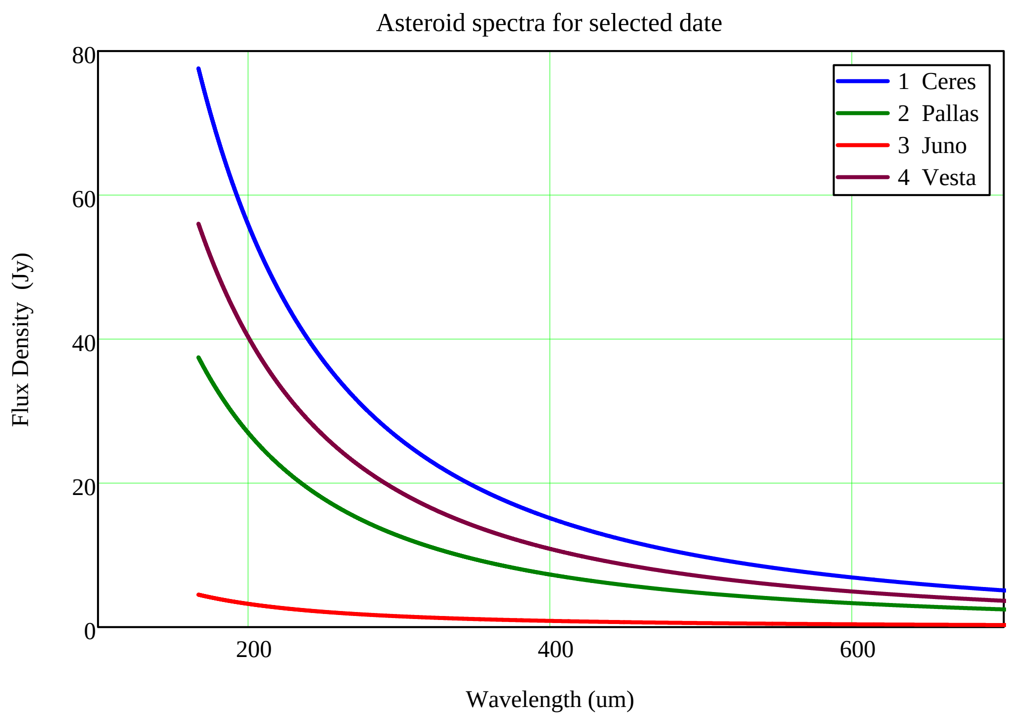

Ceres calibration flux densities (Jy) for selected date (no correction for beam dilution)

$$SCalib\_Cer_1 := \frac{\sum_{f=0}^{N-1}\left[\frac{Snu_1(\nu_{f+1}) + Snu_1(\nu_f)}{2}\cdot\frac{RP_1(\nu_{f+1}) + RP_1(\nu_f)}{2}\cdot(\nu_{f+1} - \nu_f)\right]}{\sum_{f=0}^{N-1}\left[\frac{RP_1(\nu_{f+1}) + RP_1(\nu_f)}{2}\cdot(\nu_{f+1} - \nu_f)\right]}$$

$$SCalib\_Cer_2 := \frac{\sum_{f=0}^{N-1}\left[\frac{Snu_1(\nu_{f+1}) + Snu_1(\nu_f)}{2}\cdot\frac{RP_2(\nu_{f+1}) + RP_2(\nu_f)}{2}\cdot(\nu_{f+1} - \nu_f)\right]}{\sum_{f=0}^{N-1}\left[\frac{RP_2(\nu_{f+1}) + RP_2(\nu_f)}{2}\cdot(\nu_{f+1} - \nu_f)\right]}$$

$$SCalib\_Cer_3 := \frac{\sum_{f=0}^{N-1}\left[\frac{Snu_1(\nu_{f+1}) + Snu_1(\nu_f)}{2}\cdot\frac{RP_3(\nu_{f+1}) + RP_3(\nu_f)}{2}\cdot(\nu_{f+1} - \nu_f)\right]}{\sum_{f=0}^{N-1}\left[\frac{RP_3(\nu_{f+1}) + RP_3(\nu_f)}{2}\cdot(\nu_{f+1} - \nu_f)\right]}$$

Ceres calibration flux densities for selected date (Jy):

$Y = 2010$ $M = 4$

$D = 5$ $OD\_Selected = 326$

$SCalib\_Cer_1 = 38.44$

$SCalib\_Cer_2 = 20.2$

$SCalib\_Cer_3 = 10.34$

Note that these values are not very different from the values at the nominal band frequencies

$Snu_1(\nu o_i) =$

36.79
19.48
9.81

Fortuna calibration flux densities (Jy) for selected date (no correction for beam dilution)

$$SCalib\_For_1 := \frac{\sum_{f=0}^{N-1}\left[\frac{Snu_{19}(\nu_{f+1}) + Snu_{19}(\nu_f)}{2}\cdot\frac{RP_1(\nu_{f+1}) + RP_1(\nu_f)}{2}\cdot(\nu_{f+1} - \nu_f)\right]}{\sum_{f=0}^{N-1}\left[\frac{RP_1(\nu_{f+1}) + RP_1(\nu_f)}{2}\cdot(\nu_{f+1} - \nu_f)\right]}$$

$$SCalib\_For_2 := \frac{\sum_{f=0}^{N-1}\left[\frac{Snu_{19}(\nu_{f+1}) + Snu_{19}(\nu_f)}{2}\cdot\frac{RP_2(\nu_{f+1}) + RP_2(\nu_f)}{2}\cdot(\nu_{f+1} - \nu_f)\right]}{\sum_{f=0}^{N-1}\left[\frac{RP_2(\nu_{f+1}) + RP_2(\nu_f)}{2}\cdot(\nu_{f+1} - \nu_f)\right]}$$

$$SCalib\_For_3 := \frac{\sum_{f=0}^{N-1}\left[\frac{Snu_{19}(\nu_{f+1}) + Snu_{19}(\nu_f)}{2}\cdot\frac{RP_3(\nu_{f+1}) + RP_3(\nu_f)}{2}\cdot(\nu_{f+1} - \nu_f)\right]}{\sum_{f=0}^{N-1}\left[\frac{RP_3(\nu_{f+1}) + RP_3(\nu_f)}{2}\cdot(\nu_{f+1} - \nu_f)\right]}$$

$SCalib\_For_1 = 1.83$ Jy

$SCalib\_For_2 = 0.95$

$SCalib\_For_3 = 0.49$

Note that these values are not very different from the values at the nominal band frequencies

$Snu_{19}(\nu o_i) =$

1.75
0.92
0.46

Vesta calibration flux densities (Jy) for selected date (no correction for beam dilution)

$$SCalib\_Ves_1 := \frac{\sum_{f=0}^{N-1}\left[\frac{Snu_4(\nu_{f+1}) + Snu_4(\nu_f)}{2}\cdot\frac{RP_1(\nu_{f+1}) + RP_1(\nu_f)}{2}\cdot(\nu_{f+1} - \nu_f)\right]}{\sum_{f=0}^{N-1}\left[\frac{RP_1(\nu_{f+1}) + RP_1(\nu_f)}{2}\cdot(\nu_{f+1} - \nu_f)\right]}$$

$$SCalib\_Ves_2 := \frac{\sum_{f=0}^{N-1}\left[\frac{Snu_4(\nu_{f+1}) + Snu_4(\nu_f)}{2}\cdot\frac{RP_2(\nu_{f+1}) + RP_2(\nu_f)}{2}\cdot(\nu_{f+1} - \nu_f)\right]}{\sum_{f=0}^{N-1}\left[\frac{RP_2(\nu_{f+1}) + RP_2(\nu_f)}{2}\cdot(\nu_{f+1} - \nu_f)\right]}$$

$$SCalib\_Ves_3 := \frac{\sum_{f=0}^{N-1}\left[\frac{Snu_4(\nu_{f+1}) + Snu_4(\nu_f)}{2}\cdot\frac{RP_3(\nu_{f+1}) + RP_3(\nu_f)}{2}\cdot(\nu_{f+1} - \nu_f)\right]}{\sum_{f=0}^{N-1}\left[\frac{RP_3(\nu_{f+1}) + RP_3(\nu_f)}{2}\cdot(\nu_{f+1} - \nu_f)\right]}$$

Vesta calibration flux densities for selected date (Jy):

$Y = 2010$ $M = 4$

$D = 5$ $OD\_Selected = 326$

$SCalib\_Ves_1 = 27.68$

$SCalib\_Ves_2 = 14.48$

$SCalib\_Ves_3 = 7.42$

Note that these values are not very different from the values at the nominal band frequencies

$Snu_4(\nu o_i) =$

26.48
14.00
7.04

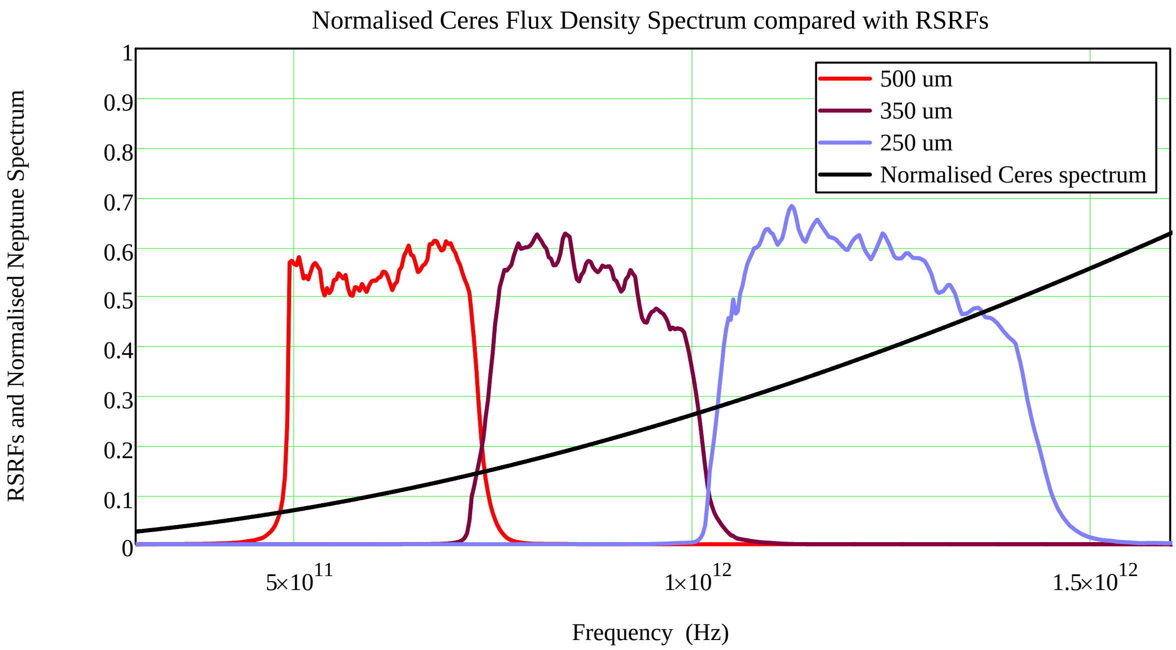

Juno calibration flux densities (Jy) for selected date (no correction for beam dilution)

$$SCalib\_Jun_1 := \frac{\sum_{f=0}^{N-1}\left[\frac{Snu_3(\nu_{f+1})+Snu_3(\nu_f)}{2}\cdot\frac{RP_1(\nu_{f+1})+RP_1(\nu_f)}{2}\cdot(\nu_{f+1}-\nu_f)\right]}{\sum_{f=0}^{N-1}\left[\frac{RP_1(\nu_{f+1})+RP_1(\nu_f)}{2}\cdot(\nu_{f+1}-\nu_f)\right]}$$

$$SCalib\_Jun_2 := \frac{\sum_{f=0}^{N-1}\left[\frac{Snu_3(\nu_{f+1})+Snu_3(\nu_f)}{2}\cdot\frac{RP_2(\nu_{f+1})+RP_2(\nu_f)}{2}\cdot(\nu_{f+1}-\nu_f)\right]}{\sum_{f=0}^{N-1}\left[\frac{RP_2(\nu_{f+1})+RP_2(\nu_f)}{2}\cdot(\nu_{f+1}-\nu_f)\right]}$$

$$SCalib\_Jun_3 := \frac{\sum_{f=0}^{N-1}\left[\frac{Snu_3(\nu_{f+1})+Snu_3(\nu_f)}{2}\cdot\frac{RP_3(\nu_{f+1})+RP_3(\nu_f)}{2}\cdot(\nu_{f+1}-\nu_f)\right]}{\sum_{f=0}^{N-1}\left[\frac{RP_3(\nu_{f+1})+RP_3(\nu_f)}{2}\cdot(\nu_{f+1}-\nu_f)\right]}$$

Juno calibration flux densities for selected date (Jy):

$Y = 2010$ $M = 4$

$D = 5$ $OD\_Selected = 326$

$SCalib\_Jun_1 = 2.21$

$SCalib\_Jun_2 = 1.2$

$SCalib\_Jun_3 = 0.59$

Note that these values are not very different from the values at the nominal band frequencies

$Snu_3(\nu o_i) =$

2.12
1.11
0.56

Stellar Models

Stellar flux densities from Leen Decin's HCalSG models:

$\lambda m := 1..8$

$\lambda_{\lambda m} :=$	$S_{\alpha Boo_{\lambda m}} :=$	$S_{\alpha Tau_{\lambda m}} :=$	$S_{\beta Peg_{\lambda m}} :=$	$S_{\beta And_{\lambda m}} :=$	$S_{\alpha Cet_{\lambda m}} :=$	$S_{\gamma Dra_{\lambda m}} :=$	$S_{Sirius_{\lambda m}} :=$	$S_{\beta Umi_{\lambda m}} :=$
10	750	640	375	250	220	147	147	124
50	30.34	27.51	16.68	10.93	9.52	6.42	5.86	5.36
100	7.506	6.90	4.20	2.736	2.40	1.60	1.425	1.33
150	3.296	3.048	1.861	1.210	1.05	0.708	0.622	0.585
198	1.874	1.74	1.064	0.691	0.6036	0.404	0.353	0.3341

Spectral indices (150 - 200 um)

$$\alpha_{\alpha Boo} := \frac{\ln\left(S_{\alpha Boo_5}\right) - \ln\left(S_{\alpha Boo_4}\right)}{\ln\left(\lambda_5\right) - \ln\left(\lambda_4\right)} \qquad \alpha_{\alpha Tau} := \frac{\ln\left(S_{\alpha Tau_5}\right) - \ln\left(S_{\alpha Tau_4}\right)}{\ln\left(\lambda_5\right) - \ln\left(\lambda_4\right)} \qquad \alpha_{\beta Peg} := \frac{\ln\left(S_{\beta Peg_5}\right) - \ln\left(S_{\beta Peg_4}\right)}{\ln\left(\lambda_5\right) - \ln\left(\lambda_4\right)}$$

$$\alpha_{\beta And} := \frac{\ln\left(S_{\beta And_5}\right) - \ln\left(S_{\beta And_4}\right)}{\ln\left(\lambda_5\right) - \ln\left(\lambda_4\right)} \qquad \alpha_{\alpha Cet} := \frac{\ln\left(S_{\alpha Cet_5}\right) - \ln\left(S_{\alpha Cet_4}\right)}{\ln\left(\lambda_5\right) - \ln\left(\lambda_4\right)} \qquad \alpha_{\gamma Dra} := \frac{\ln\left(S_{\gamma Dra_5}\right) - \ln\left(S_{\gamma Dra_4}\right)}{\ln\left(\lambda_5\right) - \ln\left(\lambda_4\right)}$$

$$\alpha_{Sirius} := \frac{\ln\left(S_{Sirius_5}\right) - \ln\left(S_{Sirius_4}\right)}{\ln\left(\lambda_5\right) - \ln\left(\lambda_4\right)} \qquad \alpha_{\beta Umi} := \frac{\ln\left(S_{\beta Umi_5}\right) - \ln\left(S_{\beta Umi_4}\right)}{\ln\left(\lambda_5\right) - \ln\left(\lambda_4\right)}$$

$\alpha_{\alpha Boo} = -2.03$ $\quad \alpha_{\alpha Tau} = -2.02$ $\quad \alpha_{\beta Peg} = -2.01$ $\quad \alpha_{\beta And} = -2.02$

$\alpha_{\alpha Cet} = -1.99$ $\quad \alpha_{\gamma Dra} = -2.02$ $\quad \alpha_{Sirius} = -2.04$ $\quad \alpha_{\beta Umi} = -2.02$

Comment: all very close to α = -2. Exact values are used in extrapolation to submm

Extrapolation to SPIRE wavelengths:

$\lambda s := 6..8$

$\lambda_{\lambda s} :=$
250
350
500

$$S_{\alpha Boo_{\lambda s}} := S_{\alpha Boo_5} \cdot \left(\frac{\lambda_{\lambda s}}{\lambda_5}\right)^{\alpha_{\alpha Boo}} \qquad S_{\alpha Tau_{\lambda s}} := S_{\alpha Tau_5} \cdot \left(\frac{\lambda_{\lambda s}}{\lambda_5}\right)^{\alpha_{\alpha Tau}} \qquad S_{\beta Peg_{\lambda s}} := S_{\beta Peg_5} \cdot \left(\frac{\lambda_{\lambda s}}{\lambda_5}\right)^{\alpha_{\beta Peg}}$$

$$S_{\beta And_{\lambda s}} := S_{\beta And_5} \cdot \left(\frac{\lambda_{\lambda s}}{\lambda_5}\right)^{\alpha_{\beta And}} \qquad S_{\alpha Cet_{\lambda s}} := S_{\alpha Cet_5} \cdot \left(\frac{\lambda_{\lambda s}}{\lambda_5}\right)^{\alpha_{\alpha Cet}} \qquad S_{\gamma Dra_{\lambda s}} := S_{\gamma Dra_5} \cdot \left(\frac{\lambda_{\lambda s}}{\lambda_5}\right)^{\alpha_{\gamma Dra}}$$

$$S_{Sirius_{\lambda s}} := S_{Sirius_5} \cdot \left(\frac{\lambda_{\lambda s}}{\lambda_5}\right)^{\alpha_{Sirius}} \qquad S_{\beta Umi_{\lambda s}} := S_{\beta Umi_5} \cdot \left(\frac{\lambda_{\lambda s}}{\lambda_5}\right)^{\alpha_{\beta Umi}}$$

Decin model spectra and extrapolations to SPIRE wavelengths

$l := 1 .. 5 \qquad e := 6 .. 8$

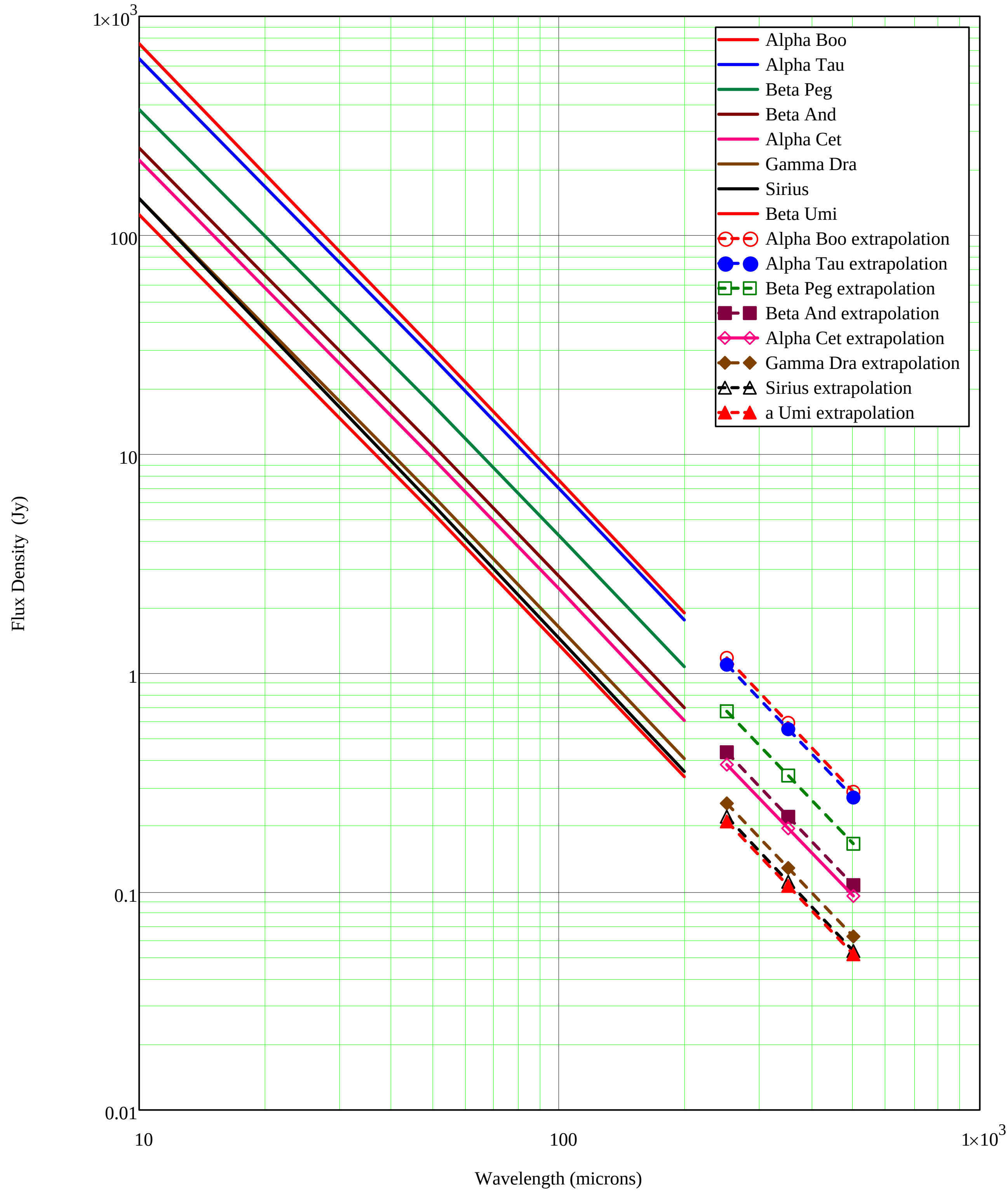

Extrapolated stellar flux densities (Jy) at SPIRE wavelengths (μm):

$\lambda_{\lambda s}$ =	$S_{\alpha Boo_{\lambda s}}$ =	$S_{\alpha Tau_{\lambda s}}$ =	$S_{\beta Peg_{\lambda s}}$ =	$S_{\beta And_{\lambda s}}$ =	$S_{\alpha Cet_{\lambda s}}$ =	$S_{\gamma Dra_{\lambda s}}$ =	$S_{Sirius_{\lambda s}}$ =	$S_{\beta Umi_{\lambda s}}$ =
250	1.166	1.087	0.665	0.432	0.3791	0.2522	0.2193	0.2087
350	0.588	0.551	0.338	0.219	0.1938	0.1278	0.1104	0.1059
500	0.285	0.268	0.165	0.107	0.0952	0.0621	0.0533	0.0515

Stellar calibration flux densities:

$$S\alpha Boo(\nu) := S_{\alpha Boo_5} \cdot \left(\frac{\nu}{c} \cdot \lambda_5 \cdot 10^{-6}\right)^{-\alpha_{\alpha Boo}}$$

Check: $S\alpha Boo\left(\frac{c}{500 \cdot 10^{-6}}\right) = 0.285$

$$S\alpha Tau(\nu) := S_{\alpha Tau_5} \cdot \left(\frac{\nu}{c} \cdot \lambda_5 \cdot 10^{-6}\right)^{-\alpha_{\alpha Tau}}$$

$S\alpha Tau\left(\frac{c}{500 \cdot 10^{-6}}\right) = 0.268$

$$S\beta Peg(\nu) := S_{\beta Peg_5} \cdot \left(\frac{\nu}{c} \cdot \lambda_5 \cdot 10^{-6}\right)^{-\alpha_{\beta Peg}}$$

$S\beta Peg\left(\frac{c}{500 \cdot 10^{-6}}\right) = 0.165$

$$S\beta And(\nu) := S_{\beta And_5} \cdot \left(\frac{\nu}{c} \cdot \lambda_5 \cdot 10^{-6}\right)^{-\alpha_{\beta And}}$$

$S\beta And\left(\frac{c}{500 \cdot 10^{-6}}\right) = 0.107$

$$S\alpha Cet(\nu) := S_{\alpha Cet_5} \cdot \left(\frac{\nu}{c} \cdot \lambda_5 \cdot 10^{-6}\right)^{-\alpha_{\alpha Cet}}$$

$S\alpha Cet\left(\frac{c}{500 \cdot 10^{-6}}\right) = 0.095$

$$S\gamma Dra(\nu) := S_{\gamma Dra_5} \cdot \left(\frac{\nu}{c} \cdot \lambda_5 \cdot 10^{-6}\right)^{-\alpha_{\gamma Dra}}$$

$S\gamma Dra\left(\frac{c}{500 \cdot 10^{-6}}\right) = 0.062$

$$SSirius(\nu) := S_{Sirius_5} \cdot \left(\frac{\nu}{c} \cdot \lambda_5 \cdot 10^{-6}\right)^{-\alpha_{Sirius}}$$

$SSirius\left(\frac{c}{500 \cdot 10^{-6}}\right) = 0.053$

$$S\beta Umi(\nu) := S_{\beta Umi_5} \cdot \left(\frac{\nu}{c} \cdot \lambda_5 \cdot 10^{-6}\right)^{-\alpha_{\beta And}}$$

$S\beta Umi\left(\frac{c}{500 \cdot 10^{-6}}\right) = 0.052$

α Boo calibration flux densities (Jy) for any date

$$SCalib\_\alpha Boo_1 := \frac{\sum_{f=0}^{N-1}\left[\frac{S\alpha Boo(\nu_{f+1}) + S\alpha Boo(\nu_f)}{2}\cdot\frac{RP_1(\nu_{f+1}) + RP_1(\nu_f)}{2}\cdot(\nu_{f+1}-\nu_f)\right]}{\sum_{f=0}^{N-1}\left[\frac{RP_1(\nu_{f+1}) + RP_1(\nu_f)}{2}\cdot(\nu_{f+1}-\nu_f)\right]}$$

$$SCalib\_\alpha Boo_2 := \frac{\sum_{f=0}^{N-1}\left[\frac{S\alpha Boo(\nu_{f+1}) + S\alpha Boo(\nu_f)}{2}\cdot\frac{RP_2(\nu_{f+1}) + RP_2(\nu_f)}{2}\cdot(\nu_{f+1}-\nu_f)\right]}{\sum_{f=0}^{N-1}\left[\frac{RP_2(\nu_{f+1}) + RP_2(\nu_f)}{2}\cdot(\nu_{f+1}-\nu_f)\right]}$$

$$SCalib\_\alpha Boo_3 := \frac{\sum_{f=0}^{N-1}\left[\frac{S\alpha Boo(\nu_{f+1}) + S\alpha Boo(\nu_f)}{2}\cdot\frac{RP_3(\nu_{f+1}) + RP_3(\nu_f)}{2}\cdot(\nu_{f+1}-\nu_f)\right]}{\sum_{f=0}^{N-1}\left[\frac{RP_3(\nu_{f+1}) + RP_3(\nu_f)}{2}\cdot(\nu_{f+1}-\nu_f)\right]}$$

α Boo calibration flux densities (Jy):

$SCalib\_\alpha Boo_1 = 1.226$

$SCalib\_\alpha Boo_2 = 0.611$

$SCalib\_\alpha Boo_3 = 0.302$

Flux densities at the nominal band frequencies (Jy):

$\nu o_i =$	$\lambda o_i \cdot 10^6 =$	$S\alpha Boo(\nu o_i) =$
$1.199\cdot10^{12}$	250	1.166
$8.565\cdot10^{11}$	350	0.588
$5.996\cdot10^{11}$	500	0.285

Flux densities (Jy that should be returned by the pipeline (i.e., still needing colour correction)

$SCalib\_\alpha Boo_1\cdot K4P_1(\alpha_{So}) = 1.240$

$SCalib\_\alpha Boo_2\cdot K4P_2(\alpha_{So}) = 0.615$

$SCalib\_\alpha Boo_3\cdot K4P_3(\alpha_{So}) = 0.304$

Check: Stars have given spectral index so multiplying Scalib x K4 x KC(-α_star) should yield the correct monochromatic flux density:

$\alpha_{\alpha Boo} = -2.034$ $\quad KPc_1(-\alpha_{\alpha Boo}) = 0.941$ $\quad KPc_2(-\alpha_{\alpha Boo}) = 0.957$ $\quad KPc_3(-\alpha_{\alpha Boo}) = 0.938$

$$\frac{SCalib\_\alpha Boo_1\cdot K4P_1(\alpha_{So})\cdot KPc_1(-\alpha_{\alpha Boo})}{S\alpha Boo(\nu o_1)} = 1.0000$$

$$\frac{SCalib\_\alpha Boo_3\cdot K4P_3(\alpha_{So})\cdot KPc_3(-\alpha_{\alpha Boo})}{S\alpha Boo(\nu o_3)} = 1.0000$$

$$\frac{SCalib\_\alpha Boo_2\cdot K4P_2(\alpha_{So})\cdot KPc_2(-\alpha_{\alpha Boo})}{S\alpha Boo(\nu o_2)} = 1.0000$$

α Tau calibration flux densities (Jy) for any date

$$SCalib\_\alpha Tau_1 := \frac{\sum_{f=0}^{N-1}\left[\frac{S\alpha Tau(\nu_{f+1})+S\alpha Tau(\nu_f)}{2}\cdot\frac{RP_1(\nu_{f+1})+RP_1(\nu_f)}{2}\cdot(\nu_{f+1}-\nu_f)\right]}{\sum_{f=0}^{N-1}\left[\frac{RP_1(\nu_{f+1})+RP_1(\nu_f)}{2}\cdot(\nu_{f+1}-\nu_f)\right]}$$

$$SCalib\_\alpha Tau_2 := \frac{\sum_{f=0}^{N-1}\left[\frac{S\alpha Tau(\nu_{f+1})+S\alpha Tau(\nu_f)}{2}\cdot\frac{RP_2(\nu_{f+1})+RP_2(\nu_f)}{2}\cdot(\nu_{f+1}-\nu_f)\right]}{\sum_{f=0}^{N-1}\left[\frac{RP_2(\nu_{f+1})+RP_2(\nu_f)}{2}\cdot(\nu_{f+1}-\nu_f)\right]}$$

$$SCalib\_\alpha Tau_3 := \frac{\sum_{f=0}^{N-1}\left[\frac{S\alpha Tau(\nu_{f+1})+S\alpha Tau(\nu_f)}{2}\cdot\frac{RP_3(\nu_{f+1})+RP_3(\nu_f)}{2}\cdot(\nu_{f+1}-\nu_f)\right]}{\sum_{f=0}^{N-1}\left[\frac{RP_3(\nu_{f+1})+RP_3(\nu_f)}{2}\cdot(\nu_{f+1}-\nu_f)\right]}$$

α Tau calibration flux densities (Jy):

$SCalib\_\alpha Tau_1 = 1.142$

$SCalib\_\alpha Tau_2 = 0.572$

$SCalib\_\alpha Tau_3 = 0.284$

Flux densities at the nominal band frequencies (Jy):

$\nu o_i =$	$\lambda o_i \cdot 10^6 =$	$S\alpha Tau(\nu o_i) =$
$1.199\cdot10^{12}$	250	1.087
$8.565\cdot10^{11}$	350	0.551
$5.996\cdot10^{11}$	500	0.268

Check: Stars have spectral index = +2 so multiplying Scalib x K4 x KC(-α_star) should yield the correct monochromatic flux density:

$$\frac{SCalib\_\alpha Tau_1\cdot K4P_1(\alpha_{So})\cdot KPc_1(-\alpha_{\alpha Tau})}{S\alpha Tau(\nu o_1)} = 1.0000 \qquad \frac{SCalib\_\alpha Tau_2\cdot K4P_2(\alpha_{So})\cdot KPc_2(-\alpha_{\alpha Tau})}{S\alpha Tau(\nu o_2)} = 1.0000$$

$$\frac{SCalib\_\alpha Tau_3\cdot K4P_3(\alpha_{So})\cdot KPc_3(-\alpha_{\alpha Tau})}{S\alpha Tau(\nu o_3)} = 1.0000$$

Flux densities that should be returned by the pipeline (i.e., still needing colour correction)

$SCalib\_\alpha Tau_1\cdot K4P_1(\alpha_{So}) = 1.155$

$SCalib\_\alpha Tau_2\cdot K4P_2(\alpha_{So}) = 0.575$

$SCalib\_\alpha Tau_3\cdot K4P_3(\alpha_{So}) = 0.286$

β Peg calibration flux densities (Jy) for any date

$$SCalib\_\beta Peg_1 := \frac{\sum_{f=0}^{N-1}\left[\frac{S\beta Peg(\nu_{f+1}) + S\beta Peg(\nu_f)}{2}\cdot\frac{RP_1(\nu_{f+1}) + RP_1(\nu_f)}{2}\cdot(\nu_{f+1} - \nu_f)\right]}{\sum_{f=0}^{N-1}\left[\frac{RP_1(\nu_{f+1}) + RP_1(\nu_f)}{2}\cdot(\nu_{f+1} - \nu_f)\right]}$$

$$SCalib\_\beta Peg_2 := \frac{\sum_{f=0}^{N-1}\left[\frac{S\beta Peg(\nu_{f+1}) + S\beta Peg(\nu_f)}{2}\cdot\frac{RP_2(\nu_{f+1}) + RP_2(\nu_f)}{2}\cdot(\nu_{f+1} - \nu_f)\right]}{\sum_{f=0}^{N-1}\left[\frac{RP_2(\nu_{f+1}) + RP_2(\nu_f)}{2}\cdot(\nu_{f+1} - \nu_f)\right]}$$

$$SCalib\_\beta Peg_3 := \frac{\sum_{f=0}^{N-1}\left[\frac{S\beta Peg(\nu_{f+1}) + S\beta Peg(\nu_f)}{2}\cdot\frac{RP_3(\nu_{f+1}) + RP_3(\nu_f)}{2}\cdot(\nu_{f+1} - \nu_f)\right]}{\sum_{f=0}^{N-1}\left[\frac{RP_3(\nu_{f+1}) + RP_3(\nu_f)}{2}\cdot(\nu_{f+1} - \nu_f)\right]}$$

β Peg calibration flux densities (Jy):

$SCalib\_\beta Peg_1 = 0.699$

$SCalib\_\beta Peg_2 = 0.351$

$SCalib\_\beta Peg_3 = 0.174$

Flux densities at the nominal band frequencies (Jy):

$\nu o_i =$	$\lambda o_i \cdot 10^6 =$	$S\beta Peg(\nu o_i) =$
$1.199\cdot10^{12}$	250	0.665
$8.565\cdot10^{11}$	350	0.338
$5.996\cdot10^{11}$	500	0.165

Check: Stars have spectral index = +2 so multiplying Scalib x K4 x KC(-α_star) should yield the correct monochromatic flux density:

$$\frac{SCalib\_\beta Peg_1\cdot K4P_1(\alpha_{So})\cdot KPc_1(-\alpha_{\beta Peg})}{S\beta Peg(\nu o_1)} = 1.0000 \qquad \frac{SCalib\_\beta Peg_2\cdot K4P_2(\alpha_{So})\cdot KPc_2(-\alpha_{\beta Peg})}{S\beta Peg(\nu o_2)} = 1.0000$$

$$\frac{SCalib\_\beta Peg_3\cdot K4P_3(\alpha_{So})\cdot KPc_3(-\alpha_{\beta Peg})}{S\beta Peg(\nu o_3)} = 1.0000$$

Flux densities that should be returned by the pipeline (i.e., still needing colour correction)

$SCalib\_\beta Peg_1\cdot K4P_1(\alpha_{So}) = 0.707$

$SCalib\_\beta Peg_2\cdot K4P_2(\alpha_{So}) = 0.353$

$SCalib\_\beta Peg_3\cdot K4P_3(\alpha_{So}) = 0.175$

β And calibration flux densities (Jy) for any date

$$SCalib\_\beta And_1 := \frac{\sum_{f=0}^{N-1}\left[\frac{S\beta And(\nu_{f+1})+S\beta And(\nu_f)}{2}\cdot\frac{RP_1(\nu_{f+1})+RP_1(\nu_f)}{2}\cdot(\nu_{f+1}-\nu_f)\right]}{\sum_{f=0}^{N-1}\left[\frac{RP_1(\nu_{f+1})+RP_1(\nu_f)}{2}\cdot(\nu_{f+1}-\nu_f)\right]}$$

$$SCalib\_\beta And_2 := \frac{\sum_{f=0}^{N-1}\left[\frac{S\beta And(\nu_{f+1})+S\beta And(\nu_f)}{2}\cdot\frac{RP_2(\nu_{f+1})+RP_2(\nu_f)}{2}\cdot(\nu_{f+1}-\nu_f)\right]}{\sum_{f=0}^{N-1}\left[\frac{RP_2(\nu_{f+1})+RP_2(\nu_f)}{2}\cdot(\nu_{f+1}-\nu_f)\right]}$$

$$SCalib\_\beta And_3 := \frac{\sum_{f=0}^{N-1}\left[\frac{S\beta And(\nu_{f+1})+S\beta And(\nu_f)}{2}\cdot\frac{RP_3(\nu_{f+1})+RP_3(\nu_f)}{2}\cdot(\nu_{f+1}-\nu_f)\right]}{\sum_{f=0}^{N-1}\left[\frac{RP_3(\nu_{f+1})+RP_3(\nu_f)}{2}\cdot(\nu_{f+1}-\nu_f)\right]}$$

β Peg calibration flux densities (Jy):

$SCalib\_\beta And_1 = 0.453$

$SCalib\_\beta And_2 = 0.227$

$SCalib\_\beta And_3 = 0.113$

Flux densities at the nominal band frequencies (Jy):

$\nu o_i =$	$\lambda o_i \cdot 10^6 =$	$S\beta And(\nu o_i) =$
$1.199\cdot10^{12}$	250	0.432
$8.565\cdot10^{11}$	350	0.219
$5.996\cdot10^{11}$	500	0.107

Check: Stars have spectral index = +2 so multiplying Scalib x K4 x KC(-α_star) should yield the correct monochromatic flux density:

$$\frac{SCalib\_\beta And_1\cdot K4P_1(\alpha_{So})\cdot KPc_1(-\alpha_{\beta And})}{S\beta And(\nu o_1)} = 1.0000 \qquad \frac{SCalib\_\beta And_2\cdot K4P_2(\alpha_{So})\cdot KPc_2(-\alpha_{\beta And})}{S\beta And(\nu o_2)} = 1.0000$$

$$\frac{SCalib\_\beta And_3\cdot K4P_3(\alpha_{So})\cdot KPc_3(-\alpha_{\beta And})}{S\beta And(\nu o_3)} = 1.0000$$

Flux densities that should be returned by the pipeline (i.e., still needing colour correction)

$SCalib\_\beta And_1\cdot K4P_1(\alpha_{So}) = 0.459$

$SCalib\_\beta And_2\cdot K4P_2(\alpha_{So}) = 0.229$

$SCalib\_\beta And_3\cdot K4P_3(\alpha_{So}) = 0.114$

α Cet calibration flux densities (Jy) for any date

$$\mathrm{SCalib\_\alpha Cet_1} := \frac{\sum_{f=0}^{N-1}\left[\frac{\mathrm{S\alpha Cet}(\nu_{f+1})+\mathrm{S\alpha Cet}(\nu_f)}{2}\cdot\frac{\mathrm{RP_1}(\nu_{f+1})+\mathrm{RP_1}(\nu_f)}{2}\cdot(\nu_{f+1}-\nu_f)\right]}{\sum_{f=0}^{N-1}\left[\frac{\mathrm{RP_1}(\nu_{f+1})+\mathrm{RP_1}(\nu_f)}{2}\cdot(\nu_{f+1}-\nu_f)\right]}$$

$$\mathrm{SCalib\_\alpha Cet_2} := \frac{\sum_{f=0}^{N-1}\left[\frac{\mathrm{S\alpha Cet}(\nu_{f+1})+\mathrm{S\alpha Cet}(\nu_f)}{2}\cdot\frac{\mathrm{RP_2}(\nu_{f+1})+\mathrm{RP_2}(\nu_f)}{2}\cdot(\nu_{f+1}-\nu_f)\right]}{\sum_{f=0}^{N-1}\left[\frac{\mathrm{RP_2}(\nu_{f+1})+\mathrm{RP_2}(\nu_f)}{2}\cdot(\nu_{f+1}-\nu_f)\right]}$$

$$\mathrm{SCalib\_\alpha Cet_3} := \frac{\sum_{f=0}^{N-1}\left[\frac{\mathrm{S\alpha Cet}(\nu_{f+1})+\mathrm{S\alpha Cet}(\nu_f)}{2}\cdot\frac{\mathrm{RP_3}(\nu_{f+1})+\mathrm{RP_3}(\nu_f)}{2}\cdot(\nu_{f+1}-\nu_f)\right]}{\sum_{f=0}^{N-1}\left[\frac{\mathrm{RP_3}(\nu_{f+1})+\mathrm{RP_3}(\nu_f)}{2}\cdot(\nu_{f+1}-\nu_f)\right]}$$

α Cet calibration flux densities (Jy):

$\mathrm{SCalib\_\alpha Cet_1} = 0.398$

$\mathrm{SCalib\_\alpha Cet_2} = 0.201$

$\mathrm{SCalib\_\alpha Cet_3} = 0.101$

Flux densities at the nominal band frequencies (Jy):

$\nu o_i =$	$\lambda o_i \cdot 10^6 =$	$\mathrm{S\alpha Cet}(\nu o_i) =$
$1.199\cdot10^{12}$	250	0.379
$8.565\cdot10^{11}$	350	0.194
$5.996\cdot10^{11}$	500	0.095

Check: Stars have spectral index = +2 so multiplying Scalib x K4 x KC(-α_star) should yield the correct monochromatic flux density:

$$\frac{\mathrm{SCalib\_\alpha Cet_1}\cdot \mathrm{K4P_1}(\alpha_{\mathrm{So}})\cdot \mathrm{KPc_1}(-\alpha_{\alpha\mathrm{Cet}})}{\mathrm{S\alpha Cet}(\nu o_1)} = 1.0000 \qquad \frac{\mathrm{SCalib\_\alpha Cet_2}\cdot \mathrm{K4P_2}(\alpha_{\mathrm{So}})\cdot \mathrm{KPc_2}(-\alpha_{\alpha\mathrm{Cet}})}{\mathrm{S\alpha Cet}(\nu o_2)} = 1.0000$$

$$\frac{\mathrm{SCalib\_\alpha Cet_3}\cdot \mathrm{K4P_3}(\alpha_{\mathrm{So}})\cdot \mathrm{KPc_3}(-\alpha_{\alpha\mathrm{Cet}})}{\mathrm{S\alpha Cet}(\nu o_3)} = 1.0000$$

Flux densities that should be returned by the pipeline (i.e., still needing colour correction)

$\mathrm{SCalib\_\alpha Cet_1}\cdot \mathrm{K4P_1}(\alpha_{\mathrm{So}}) = 0.403$

$\mathrm{SCalib\_\alpha Cet_2}\cdot \mathrm{K4P_2}(\alpha_{\mathrm{So}}) = 0.202$

$\mathrm{SCalib\_\alpha Cet_3}\cdot \mathrm{K4P_3}(\alpha_{\mathrm{So}}) = 0.101$

β Umi calibration flux densities (Jy) for any date

$$SCalib\_\beta Umi_1 := \frac{\sum_{f=0}^{N-1}\left[\frac{S\beta Umi(\nu_{f+1}) + S\beta Umi(\nu_f)}{2}\cdot\frac{RP_1(\nu_{f+1}) + RP_1(\nu_f)}{2}\cdot(\nu_{f+1} - \nu_f)\right]}{\sum_{f=0}^{N-1}\left[\frac{RP_1(\nu_{f+1}) + RP_1(\nu_f)}{2}\cdot(\nu_{f+1} - \nu_f)\right]}$$

$$SCalib\_\beta Umi_2 := \frac{\sum_{f=0}^{N-1}\left[\frac{S\beta Umi(\nu_{f+1}) + S\beta Umi(\nu_f)}{2}\cdot\frac{RP_2(\nu_{f+1}) + RP_2(\nu_f)}{2}\cdot(\nu_{f+1} - \nu_f)\right]}{\sum_{f=0}^{N-1}\left[\frac{RP_2(\nu_{f+1}) + RP_2(\nu_f)}{2}\cdot(\nu_{f+1} - \nu_f)\right]}$$

$$SCalib\_\beta Umi_3 := \frac{\sum_{f=0}^{N-1}\left[\frac{S\beta Umi(\nu_{f+1}) + S\beta Umi(\nu_f)}{2}\cdot\frac{RP_3(\nu_{f+1}) + RP_3(\nu_f)}{2}\cdot(\nu_{f+1} - \nu_f)\right]}{\sum_{f=0}^{N-1}\left[\frac{RP_3(\nu_{f+1}) + RP_3(\nu_f)}{2}\cdot(\nu_{f+1} - \nu_f)\right]}$$

β Umi calibration flux densities (Jy):

$SCalib\_\beta Umi_1 = 0.219$

$SCalib\_\beta Umi_2 = 0.110$

$SCalib\_\beta Umi_3 = 0.0545$

Flux densities at the nominal band frequencies (Jy):

$\nu o_i =$	$\lambda o_i \cdot 10^6 =$	$S\beta Umi(\nu o_i) =$
$1.199\cdot10^{12}$	250	0.209
$8.565\cdot10^{11}$	350	0.106
$5.996\cdot10^{11}$	500	0.052

Check: Stars have spectral index = +2 so multiplying Scalib x K4 x KC(-α_star) should yield the correct monochromatic flux density:

$$\frac{SCalib\_\beta Umi_1\cdot K4P_1(\alpha_{So})\cdot KPc_1(-\alpha_{\beta Umi})}{S\beta Umi(\nu o_1)} = 1.0000 \qquad \frac{SCalib\_\beta Umi_2\cdot K4P_2(\alpha_{So})\cdot KPc_2(-\alpha_{\beta Umi})}{S\beta Umi(\nu o_2)} = 1.0000$$

$$\frac{SCalib\_\beta Umi_3\cdot K4P_3(\alpha_{So})\cdot KPc_3(-\alpha_{\beta Umi})}{S\beta Umi(\nu o_3)} = 1.0000$$

Flux densities that should be returned by the pipeline (i.e., still needing colour correction)

$SCalib\_\beta Umi_1\cdot K4P_1(\alpha_{So}) = 0.222$

$SCalib\_\beta Umi_2\cdot K4P_2(\alpha_{So}) = 0.111$

$SCalib\_\beta Umi_3\cdot K4P_3(\alpha_{So}) = 0.0549$

γ Dra calibration flux densities (Jy) for any date

$$SCalib\_\gamma Dra_1 := \frac{\sum_{f=0}^{N-1}\left[\frac{S\gamma Dra(\nu_{f+1})+S\gamma Dra(\nu_f)}{2}\cdot\frac{RP_1(\nu_{f+1})+RP_1(\nu_f)}{2}\cdot(\nu_{f+1}-\nu_f)\right]}{\sum_{f=0}^{N-1}\left[\frac{RP_1(\nu_{f+1})+RP_1(\nu_f)}{2}\cdot(\nu_{f+1}-\nu_f)\right]}$$

$$SCalib\_\gamma Dra_2 := \frac{\sum_{f=0}^{N-1}\left[\frac{S\gamma Dra(\nu_{f+1})+S\gamma Dra(\nu_f)}{2}\cdot\frac{RP_2(\nu_{f+1})+RP_2(\nu_f)}{2}\cdot(\nu_{f+1}-\nu_f)\right]}{\sum_{f=0}^{N-1}\left[\frac{RP_2(\nu_{f+1})+RP_2(\nu_f)}{2}\cdot(\nu_{f+1}-\nu_f)\right]}$$

$$SCalib\_\gamma Dra_3 := \frac{\sum_{f=0}^{N-1}\left[\frac{S\gamma Dra(\nu_{f+1})+S\gamma Dra(\nu_f)}{2}\cdot\frac{RP_3(\nu_{f+1})+RP_3(\nu_f)}{2}\cdot(\nu_{f+1}-\nu_f)\right]}{\sum_{f=0}^{N-1}\left[\frac{RP_3(\nu_{f+1})+RP_3(\nu_f)}{2}\cdot(\nu_{f+1}-\nu_f)\right]}$$

γ Dra calibration flux densities (Jy):

$SCalib\_\gamma Dra_1 = 0.265$

$SCalib\_\gamma Dra_2 = 0.133$

$SCalib\_\gamma Dra_3 = 0.066$

Flux densities at the nominal band frequencies (Jy):

$\nu o_i =$	$\lambda o_i \cdot 10^6 =$	$S\gamma Dra(\nu o_i) =$
$1.199\cdot10^{12}$	250	0.252
$8.565\cdot10^{11}$	350	0.128
$5.996\cdot10^{11}$	500	0.062

Check: Stars have spectral index = +2 so multiplying Scalib x K4 x KC(-α_star) should yield the correct monochromatic flux density:

$$\frac{SCalib\_\gamma Dra_1\cdot K4P_1(\alpha_{So})\cdot KPc_1(-\alpha_{\gamma Dra})}{S\gamma Dra(\nu o_1)} = 1.0000 \qquad \frac{SCalib\_\gamma Dra_2\cdot K4P_2(\alpha_{So})\cdot KPc_2(-\alpha_{\gamma Dra})}{S\gamma Dra(\nu o_2)} = 1.0000$$

$$\frac{SCalib\_\gamma Dra_3\cdot K4P_3(\alpha_{So})\cdot KPc_3(-\alpha_{\gamma Dra})}{S\gamma Dra(\nu o_3)} = 1.0000$$

Flux densities that should be returned by the pipeline (i.e., still needing colour correction)

$SCalib\_\gamma Dra_1\cdot K4P_1(\alpha_{So}) = 0.268$

$SCalib\_\gamma Dra_2\cdot K4P_2(\alpha_{So}) = 0.133$

$SCalib\_\gamma Dra_3\cdot K4P_3(\alpha_{So}) = 0.0662$

Sirius calibration flux densities (Jy) for any date

$$SCalib\_Sirius_1 := \frac{\sum_{f=0}^{N-1}\left[\frac{SSirius(\nu_{f+1}) + SSirius(\nu_f)}{2}\cdot\frac{RP_1(\nu_{f+1}) + RP_1(\nu_f)}{2}\cdot(\nu_{f+1} - \nu_f)\right]}{\sum_{f=0}^{N-1}\left[\frac{RP_1(\nu_{f+1}) + RP_1(\nu_f)}{2}\cdot(\nu_{f+1} - \nu_f)\right]}$$

$$SCalib\_Sirius_2 := \frac{\sum_{f=0}^{N-1}\left[\frac{SSirius(\nu_{f+1}) + SSirius(\nu_f)}{2}\cdot\frac{RP_2(\nu_{f+1}) + RP_2(\nu_f)}{2}\cdot(\nu_{f+1} - \nu_f)\right]}{\sum_{f=0}^{N-1}\left[\frac{RP_2(\nu_{f+1}) + RP_2(\nu_f)}{2}\cdot(\nu_{f+1} - \nu_f)\right]}$$

$$SCalib\_Sirius_3 := \frac{\sum_{f=0}^{N-1}\left[\frac{SSirius(\nu_{f+1}) + SSirius(\nu_f)}{2}\cdot\frac{RP_3(\nu_{f+1}) + RP_3(\nu_f)}{2}\cdot(\nu_{f+1} - \nu_f)\right]}{\sum_{f=0}^{N-1}\left[\frac{RP_3(\nu_{f+1}) + RP_3(\nu_f)}{2}\cdot(\nu_{f+1} - \nu_f)\right]}$$

Sirius calibration flux densities (Jy):

$SCalib\_Sirius_1 = 0.231$

$SCalib\_Sirius_2 = 0.115$

$SCalib\_Sirius_3 = 0.056$

Flux densities at the nominal band frequencies (Jy):

$\nu o_i =$	$\lambda o_i \cdot 10^6 =$	$SSirius(\nu o_i) =$
$1.199\cdot10^{12}$	250	0.219
$8.565\cdot10^{11}$	350	0.110
$5.996\cdot10^{11}$	500	0.053

Check: Stars have spectral index = +2 so multiplying Scalib x K4 x KC(-α_star) should yield the correct monochromatic flux density:

$$\frac{SCalib\_Sirius_1\cdot K4P_1(\alpha_{So})\cdot KPc_1(-\alpha_{Sirius})}{SSirius(\nu o_1)} = 1.0000$$

$$\frac{SCalib\_Sirius_2\cdot K4P_2(\alpha_{So})\cdot KPc_2(-\alpha_{Sirius})}{SSirius(\nu o_2)} = 1.0000$$

$$\frac{SCalib\_Sirius_3\cdot K4P_3(\alpha_{So})\cdot KPc_3(-\alpha_{Sirius})}{SSirius(\nu o_3)} = 1.0000$$

Flux densities that should be returned by the pipeline (i.e., still needing colour correction)

$SCalib\_Sirius_1\cdot K4P_1(\alpha_{So}) = 0.233$

$SCalib\_Sirius_2\cdot K4P_2(\alpha_{So}) = 0.115$

$SCalib\_Sirius_3\cdot K4P_3(\alpha_{So}) = 0.0569$